2010

Quantum light for quantum technologies

William Nicholas Plick
Louisiana State University and Agricultural and Mechanical College, bplick@yahoo.com

QUANTUM LIGHT FOR QUANTUM TECHNOLOGIES

A Dissertation

Submitted to the Graduate Faculty of the
Louisiana State University and
Agricultural and Mechanical College
in partial fulfilment of the
requirements for the degree of
Doctor of Philosophy

in

The Department of
Physics and Astronomy

by
William Nicholas Plick
B.A., Connecticut College, 2004
May 2010

Acknowledgements

I would like to thank a few people without whom this work would not be possible. First on the list has to be my parents who always chose to support my interest in science and endlessly encouraged my academic progress. Without their profound love and dedication there is no way I would have made it this far in pursuit of difficult goals. I would also like to thank my family as a whole for their love and support. Many friends have also been invaluable, including my fellow grad-students who were there for all the rough spots of the PhD process. Specifically I would like to thank Ashley, Blane, Harold, Jeff, Jen, Ryan, Sai, and Sean. If I've left anyone out by accident I owe you a beer. Special thanks go to my wonderful girlfriend Karynne, my cheerleader and companion. Aside from my friends and family I have been unreasonably lucky to meet and be advised by exceptionally wonderful faculty and post-docs here, and elsewhere. Especially Drs. Agarwal, Anisimov, Cable, Lee, and Wildfeuer. Of course bearing special distinction is my advisor Dr. Jonathan Dowling, to whom I owe an incalculable amount. With a steady hand (when not shaking from a triple espresso) he has guided me to become the scientist I am today. He has done this with an uncommon kindness and skill.

Table of Contents

Abstract

In this thesis we will theoretically investigate three potentially useful physical systems, after first developing the theoretical framework necessary for studying them. First, we will study the multiphoton absorption properties of maximally path entangled number (N00N) states. This is directly relevant to quantum lithography, and beating the Rayleigh diffraction limit. Next, we will develop a new scheme for quantum interferometry: dubbed coherent-light boosted super-sensitive quantum interferometry, which has the potential to reach below the shot noise limit for high photon fluxes, and requires no esoteric detection protocol, or technological elements that have yet to be developed. Finally we propose a method to perform parity detection on the output modes of a Mach-Zehnder interferometer that has been fed with two-mode squeezed vacuum. This detection scheme relies on a double homodyning technique, that makes intensity correlation measurements at a series of chosen bias phases. Sub-Heisenberg sensitivity scaling is expected for this setup.

1 Introduction

It is my intention that the first two sections of this introduction be accessible to the layperson, with no advanced knowledge of physics or mathematics.

1.1 General Introduction

Out of all the sciences, physics is the most difficult to properly define. At its extremes it seems to infringe on the territory of other areas of study. At its most theoretical it becomes difficult to distinguish from abstract mathematics. As more complex atomic structures are considered it is more like chemistry. Analysis of emergent phenomena makes physics almost appear to be biology. It is so tied to astronomy that the two university curricula typically only differ by a few courses. Sometimes physics even encroaches on the domain of philosophy.

What makes physics so difficult to define is that it is fundamental. It lies at the root of our rational understanding of the world. The antiquated term for physics is natural philosophy, which fits well, as physics is Man's attempt to penetrate the secret order and law of the material universe.

When people only had access to the phenomena that they could see with their eyes or touch with their hands, the study of physics was more or less confined to a single discipline, what we now call classical mechanics. It was – and remains – the study of macroscopic forces and objects interacting in mathematically precise ways.

As we developed tools to expand our range of perception, our knowledge deepened, and the single discipline of natural philosophy fragmented into many different realms of study. As ever more minute objects and interactions (such as atoms and their relationship to light and each other) came under study, new theories needed to be created to describe the paradoxical behavior of these systems. Quantum Mechanics (quantum referring to small discrete objects) filled this need as the descriptor of the world of the very small. Study of the fundamental nature of light as a quantum object became known as Quantum Optics, and is the subject of this dissertation.

The first beachhead made in man's ongoing exploration of the quantum world occurred because of the observation of light. When many objects are heated to a sufficient temperature, they begin to emit light. First, as heat felt from the invisible infra red radiation, then a dull red glow transitioning to a bright orange, and eventually white. This pattern is called black-body radiation – because an idealized object called a black-body follows this pattern very well, as do stars. Theorists worked for years trying to describe this pattern mathematically, but failed. That was until 1900 when Max Planck was able to do so. His breakthrough was to assume that the light was emitted only in discrete packets of energy. A mathematical framework built on this idea correctly described the black-body radiation curve.

The idea that the world may be made of discrete pieces, in the early years of the 20^{th} century, led directly to all the following advances in the field of quantum mechanics.

Today quantum optics continues to be one of the pillars of the larger structure of quantum theory. Furthermore, the technological applications of quantum optics are becoming of greater interest. Quantum cryptographic networks [1], allowing completely secure communication over tens of miles, are already in limited production. Quantum imaging and

lithography [2] promise to create a plethora of technological improvements: smaller microchips, better microscopes, improved information storage, and more accurate imaging and ranging for radar-like devices. The study of meta-materials [3] may fulfil the science fiction dream of creating optically invisible objects. And, over the rest of this, looms the possibility of constructing a quantum computer [4], a device so powerful it could break previously unbreakable codes in a matter of hours or even minutes – among other impressive feats.

It is this interest in formidable technologies that drives much of the funding in quantum optics, but at its core the discipline is concerned with fundamental science. Quantum optics is driven by one, seemingly childish, yet eternally confounding question:

1.2 What Is Light?

At first the question seems harmless, even obvious. The simplest – modern – answer is that light is electromagnetic radiation.

In many ways this is an inadequate answer and says very little about one of the most complex, paradoxical, mysterious, important, and ever-present components of our world. It gives us life, warmth, and sight; but what is it? Let us begin by inspecting the history of Man's thoughts on light:

Many ancient philosophical traditions thought of light as being related to fire. This is not surprising as the most readily non-astronomical source of light in early man's experience was flame. Philosophers of India and Greece supposed that light was made of small particles of fire which operated with certain set laws. These particles interacted in various ways, producing radiant heat, and creating the sense of sight.

Euclid in *Optica* ($\sim$ 300BCE) demonstrated that light travelled in straight lines, and he also began to develop the modern discipline of geometrical optics by mathematically examining reflection. Ptolemy expanded on these concepts in *Optics* (sometime in the 2$^{\text{nd}}$ century CE) by studying refraction: the way light bends as it passes through different materials.

In 1021CE the great Middle Eastern scientist Alhazen completed *The Book of Optics*.[1] In this book he postulated that light was not a physical object, but a ray of particles with "no sensible quantities but energy" that came eerily close to the modern understanding of light as composed of photons. Alhazen was the first to form an image with a camera obscura (a pinhole camera capable of projecting an image from outside of a darkened room onto a screen in the room). Using the information about the geometry of light that the camera obscura revealed, he correctly stated that light was reflected in all directions from every point of an object, and that the eye formed an image from those rays. Alhazen further developed the science of geometrical optics by carrying out extensive experiments with mirrors, lenses, and

[1] "Alhazen" is the European name given to Abū 'Alī al-Ḥasan ibn al-Ḥasan ibn al-Haytham, one of the greatest scientists to ever have lived. It is a great shame that he is rarely – if ever – mentioned in the American scientific education system. He made large contributions to nearly every area of study, from anatomy to number theory. He is credited with developing the scientific method in a form that is very close to the modern definition. He has been called "The First (True) Scientist" by some modern physicists and historians of science. He wrote *The Book of Optics* under house arrest while feigning madness to avoid the ire of a capricious caliph.

other objects. He proved Euclid's hypothesis that light travels in straight lines in free space;[2] He was also the first person to split light into its constituent colors, and to magnify an object with a lens. He inferred that light travelled non-instantaneously and that refraction was due to light travelling at different speeds in different materials. Alberuni, a contemporary of Alhazen, and also a great Middle Eastern polymath, showed that the speed of light was indeed finite, yet much greater than the speed of sound.

In 1637, René Descartes published a paper in which he deviated from the tradition of thinking of light as a particle. Regarding it solely as a property of the object radiating the light, and thus he also concluded that light propagated as waves through a "plenum". Descartes reasoned that there was no such thing as vacuum, and that all space was filled with an invisible material capable of carrying waves. This began a schism in our understanding of the nature of light: between those who advocated the wave theory and those who maintained the particle theory. This split, in some sense, remains to this day.

Isaac Newton became the standard bearer for the opposing camp: what would become known as the corpuscular theory of light (a corpuscle being defined as a little particle). Newton argued in his *Opticks*, published in 1704, that the mechanics of light suggested it was composed of small particles, and not waves. Newton suggested that only a particle theory of light could explain the straight-line geometrical optics that had been developing for centuries. After all, sound, well known to be a wave, could be heard around a corner – whereas an image cannot be seen unless there is a direct line from the eye to the object. However, Newton's theory could not adequately explain some of the other behaviours of light, such as refraction and diffraction (the latter being – in this context – light's tendency to split into its component colors when passing through a transparent material). In order to compensate for these short-comings, Newton invented the concept of the *luminiferous aether*, ironically coining the preferred terminology of his rivals. To Newton's mind, the aether was a material that filled all space, like Descartes' plenum, capable of transmitting waves. However, unlike the supporters of the wave school of thought, Newton did not believe that vibrations in aether *were* light – but that they were *caused* by light particles as they travelled through the aether. These waves travelled faster than the light particles themselves, and then acted back on them at the boundaries of materials causing the phenomena of refraction and diffraction.

The battle between the two conceptions of light continued for centuries, with the weapons of theoretical arguments and painstaking experiments arrayed on either side.[3]

The next great leap came in 1864 when the Scottish mathematician and physicist James Clerk Maxwell published *A Dynamical Theory of the Electromagnetic Field*. Maxwell was concerned with studying the laws of electricity and magnetism. In this paper he laid out a series of equations (now known as Maxwell's Equations), which accurately described the behavior of electric and magnetic fields. He also discovered that these equations could be

[2]Actually, light does not travel in straight lines, but along "null geodesics", which are bent by gravity. However, the difference can only be noticed near very massive astronomical objects, and even then usually only with great care.

[3]A complete history of this debate could easily fill a separate doctoral thesis. The interested reader is referred to any one of dozens of books on the subject (for example *Newton to Einstein: The Trail of Light: An Excursion to the Wave-Particle Duality and the Special Theory of Relativity* by Ralph Baierlein), and to *Wikipedia*.

rearranged in such a way that they became wave equations.[4] These equations described an electric field and a complimentary magnetic field travelling at exactly the known speed of light! Maxwell correctly deduced that light must be an electromagnetic wave.[5]

In the modern era, it is a mater of general knowledge that light is an electromagnetic phenomenon. So, it is illuminating to point out that before Maxwell there was no reason to believe that there was a connection between the two concepts. Electromagnetism governed currents and compasses, light – apparently – had nothing to do with these types of things. The fact that the speed of light popped out of Maxwell's Equations was a surprise to everyone. It is this conceptual discontinuity that makes Maxwell's revelation so significant.

Maxwell considered electromagnetism and light to be two manifestations of the same, subtle, ever-present, continuous aether (or ether) – which both provided light with a medium through which to travel and allowed the electric and magnetic forces to act at a distance from their sources. Not long after Maxwell's discoveries, Heinrich Hertz experimentally demonstrated Maxwell's theory of light by transmitting and receiving radio waves for the first time (radio is simply light at a wavelength longer than what our eyes can detect).[6] Later, radio waves were seen to obey all the same laws of reflection and refraction that had been developed to describe visible light. Oddly, Hertz didn't see any use for radio-frequency light beyond proving Maxwell's theory. When asked what potential application his discovery might have had, he famously replied, "...nothing, I guess."

At that time, the particle theory of light fell into obscurity and physicists concentrated on developing evermore sophisticated models of how the ether behaved.

However, problems began to develop. It was reasoned that if there existed an all-encompassing ether then, as the Earth rotated, the ether would be perceived by observers on Earth to be moving. Following this line of thought, since light was apparently a kind of vibration moving through this material, light should be seen to move with different speeds depending on whether it was travelling upstream or downstream. Sophisticated devices were designed and built to search for this effect, but without success. The speed of light was measured to be the same no matter the direction.

This failure to detect traces of the ether did not deter the hypothesis' apologists. The mechanics of the ether became more and more elaborate in the minds of the physicists of the day, until this supposed ever present substance almost seemed to be conspiring to keep itself hidden.

While the majority of researchers were ministering to their ailing ether, other breakthroughs were being made that would eventually become a new system of more accurate theories: quantum mechanics and relativity.

Quantum mechanics began with the discoveries of Max Planck who, as previously mentioned, showed that the radiation field of a black body must be made of discrete pieces. Although Planck himself believed that this was a mere mathematical expediency, and not indicative of any deeper principle, this idea did plant the seeds that would grow into a whole new system of theories.[7] Not long after, the next breakthrough followed. Philipp Lenard first showed in 1902 that the amount of electric current a piece of metal would produce when light was shined on it was not only proportional to the intensity of the light (as was

[4]A wave equation is exactly what one would expect: An equation which describes how a wave moves. This can be anything from a vibrating guitar string, to water waves travelling across the surface of the ocean.

expected), but it also depended on the frequency of the light.[8] Furthermore, below a certain frequency threshold, no current would be produced at all – no matter the intensity. In 1905, Albert Einstein successfully explained this curious phenomenon when, taking Planck's "mathematical expediency" literally, he supposed that light, instead of being a continuous wave, was made of discrete pieces or quanta – photons.[9] Each photon carries with it a set amount of energy proportional to its frequency. Each photon then interacts with an electron bound to an atom in a one-to-one relationship. If the photon does not have enough energy to eject the electron from the atom, then additional photons of the same energy will not help the electron escape to create current.

Einstein also proposed a new theory of time and space – his theory of relativity – which asserted that the speed of light would be measured to be the same, regardless of the motion of the observer. In this formulation, light was the constant, and time and space were made relative. This theory successfully explained why no experiment was ever able to find two beams of light moving a different speeds (in the same material).

The particle theory, now called quantum theory, became resurgent. But physicists were still unable to reconcile the wave nature of light, which had been demonstrated time and time again, with the new necessity of calling it a particle as well. This conundrum was further compounded when, in 1924, Louis de Broglie proposed that *all matter*, not just light, was in truth composed of both particle and wave elements.[10] Not long after his hypothesis was confirmed when experiments showed electrons diffracting – behaving like waves – just as de Broglie predicted.

In quantum mechanics, every particle would be described by a wave equation (similar to Maxwell's wave equations for light), the famous Schrödinger equation.

Scientists now have to contend with the strange fact that all matter is both particle and wave at the same time. This is a paradox that remains today. The reason that we do not notice the wave nature of matter in our daily lives is because as the mass of the particle increases, its wave nature becomes less apparent, however the fact of wave-particle duality remains. Some scientists still grapple with this incongruity, trying to resolve it through somewhat convoluted means; others merely accept it.

But where does this leave us with respect to our question. "What is light?" Modern physicists typically treat the photon as a "wave packet," a self-contained rippling of electromagnetic waves that constitutes a discrete unit. Thus, it is a wave that does not wave *through* anything. It is a self sustaining swell of electromagnetic energy which travels through free space at 299,792,458 meters per second.

This answer is simple, direct, and sufficient for most purposes. There is more to the story though, and the study of photons can – and does – fill libraries where topics like photon statistics, gauge theories, information content, and entanglement are discussed. And the real complexity of light emerges when it begins to interact with matter. It can slow down, speed up, or even stop. It can split into different colors, bend, be reflected, be turned into other photons: light can be endlessly transmuted. Light is not just a particle and a wave at the same time, but also simultaneously simple and complex; at once an everyday presence, yet deeply mysterious.

The study of light is a richly rewarding enterprise. It provides us with a cornucopia of technologies that have become necessary for modern life. Equally importantly is the fact that the investigation of light has opened up whole new fields of science and changed the

way we think about space, time, and matter.

1.3 The Roots of Quantum Optics: Basic Theoretical Structure

In this section we will lay out the fundamental theoretical framework of quantum optics, with particular emphasis on those concepts and mathematical methods which will be needed in this thesis. At this point it becomes necessary to abandon the broad accessibility which was the goal of the previous two sections.

The notation and derivation of the equations in the following sections are based on my own class notes and several fine texts, most notably: *Introductory Quantum Optics* by C. C. Gerry and P. L. Knight. Specifically section 1.3.1 draws from chapter 2 of that text, section 1.3.2 and 1.3.4 from chapter 3, and section 1.3.5 from chapter 7. Section 1.3.6 draws from chapter 1 of the book *Nonlinear Optics* by Robert W. Boyd.

1.3.1 Maxwell and Schrödinger on a Ladder: The Quantum Light Field

The most natural place to begin is with Maxwell's equations

$$\begin{aligned}
\nabla \times \vec{B} &= \mu_o \vec{J} + \mu_o \epsilon_o \frac{\partial \vec{E}}{\partial t}, \\
\nabla \times \vec{E} &= -\frac{\partial \vec{B}}{\partial t}, \\
\nabla \cdot \vec{B} &= 0, \\
\nabla \cdot \vec{E} &= \frac{\rho}{\epsilon_o}.
\end{aligned}$$

Now assume that there are no charges or currents

$$\begin{aligned}
\nabla \times \vec{B} &= \mu_o \epsilon_o \frac{\partial \vec{E}}{\partial t}, && (1) \\
\nabla \times \vec{E} &= -\frac{\partial \vec{B}}{\partial t}, && (2) \\
\nabla \cdot \vec{B} &= 0, \\
\nabla \cdot \vec{E} &= 0.
\end{aligned}$$

Take the curl of the Eq.(1) and Eq.(2) and use the vector identity $\nabla \times (\nabla \times \vec{A}) = \nabla(\nabla \cdot \vec{A}) - \nabla^2 \vec{A}$ to obtain

$$\begin{aligned}
\nabla^2 \vec{B} &= -\mu_o \epsilon_o \frac{\partial}{\partial t} \nabla \times \vec{E}, \\
\nabla^2 \vec{E} &= \frac{\partial}{\partial t} \nabla \times \vec{B},
\end{aligned}$$

using the fact that the divergence of the electric and magnetic fields, in the absence of charges and currents, is zero. Now substituting the original expressions for the curl of $\vec{E}$ and $\vec{B}$ and rearranging

$$\begin{aligned} \frac{\partial^2 \vec{B}}{\partial t^2} - v_c^2 \nabla^2 \vec{B} &= 0, \\ \frac{\partial^2 \vec{E}}{\partial t^2} - v_c^2 \nabla^2 \vec{E} &= 0. \end{aligned} \tag{3}$$

We have arrived at two wave equations which describe electric and magnetic fields propagating through free space with a speed of $v_c = 1/\sqrt{\mu_o \epsilon_o} \simeq 3 \times 10^8 \text{m/s}$, reproducing Maxwell's revelation that light is an oscillating electromagnetic field.

Let's take a special case: A light field trapped inside two parallel planes of perfectly conducting material. We will assume that the electric field is defined along one dimension: x, parallel to the conducting planes. This introduces the concept of *polarization* which is defined to be the direction the electric field of a photon points along. The electric field must be zero at the surfaces of the conductor, creating a boundary value problem. First, assume the equation for the electric field is factorizable: $\vec{E} = \mathcal{E}(t)E(z)\vec{e}_x$, where $\vec{e}_x$ is the basis vector in the x direction.[5] The general solution for Eq. (3) for each part is then

$$E(z) = A_1 \sin(B_1 z) + C_1 \cos(D_1 z), \tag{4}$$

$$\mathcal{E}(t) = A_2 \sin(B_2 t) + C_2 \cos(D_2 t). \tag{5}$$

Imposing the boundary condition $E(0) = 0$ requires that $C_1 = 0$. The second boundary condition $E(L) = 0$ requires that $B_1 = \pi m/L$ where $m = 1, 2, 3...$ ignoring the trivial solution where $m = 0$. The fact that the standing electromagnetic wave equation can take only discrete values is sometimes called first quantization, and is purely a classical effect. The wave equation itself imposes the restrictions $B_2 = D_2 = v_c B_1$. We will collect and rename the overall factors which the boundary value problem does not constrain as E_o. And so we have

$$\vec{E} = E_o \sin(k_m z) \left\{ \sin(\omega_m t) + \cos(\omega_m t) \right\} \vec{e}_x, \tag{6}$$

where $\omega_m = v_c \pi m/L$, and $k_m = \omega_m / v_c$. Note that we have taken $A_2 = C_2$, though this is a valid solution, it is not the only one.

The interpretation of Eq. (6) is obvious. It is a standing electric wave with a frequency of ω_m, a wave-number of k_m, and and an amplitude of E_o. Since we have a field with one specific frequency, our equations thus far describe monochromatic light.

Maxwell's equations demand that, where ever there is an electric field that changes with time, there must be a magnetic field. Start with Eq.(2)[6]

[5] I will use basis vectors with the notation $\vec{e}_i$ instead of $\hat{i}$ in order to avoid confusion with quantum mechanical operators

[6] Strictly speaking to have my calculation flow from this statement I should use Eq.(1). However in order to do the calculation this way I would need to "uncurl" the magnetic field, which is much less direct. I have chosen the simplest conceptual explanation and matched it with the simplest calculation. This does create a slight incongruity, which the careful reader may have noticed.

$$\begin{aligned}
\frac{\partial \vec{B}}{\partial t} &= -\nabla \times \vec{E}, \\
&= -E_o \left\{\sin(\omega_m t) + \cos(\omega_m t)\right\} \frac{\partial}{\partial z} \sin(k_m z) \vec{e}_y, \\
\vec{B} &= -E_o k_m \cos(k_m z) \int dt \left\{\sin(\omega_m t) + \cos(\omega_m t)\right\} \vec{e}_y, \\
&= \frac{E_o k_m}{\omega_m} \cos(k_m z) \left\{\cos(\omega_m t) - \sin(\omega_m t)\right\} \vec{e}_y, \qquad (7)
\end{aligned}$$

which describes a companion magnetic field oscillating perpendicular to the electric field. The fields are self sustaining. In a sense they generate each other, forming a symbiotic relationship, trapping energy in a stable, ever-changing pattern.

To illustrate this we will examine the energy content of the light field, given by[7]

$$U \equiv \frac{1}{2} \int dV \left[\epsilon_o \vec{E} \cdot \vec{E} + \frac{1}{\mu_o} \vec{B} \cdot \vec{B} \right] = V \epsilon_o E_o^2,$$

where V is the volume between the conducting plates. As we expected, the energy content is independent of time. This also provides a normalization for the amplitude $E_o = \sqrt{U/V\epsilon_o}$.

Now let's take the electric field at a specific value of z, so we can examine the time dependent portion of the electric field by itself. We'll choose $\pi/(2k)$ so that $\sin(kz) = 1$ for the sake of simplicity. Equation (6) becomes

$$\vec{E}\left(t, \frac{\pi}{2k}\right) = \sqrt{\frac{U}{V\epsilon_o}} \left\{\sin(\omega_m t) + \cos(\omega_m t)\right\} \vec{e}_x.$$

This equation is familiar, it is the equation of motion of a classical harmonic oscillator: $x(t) = \sin(\omega t) + \cos(\omega t)$. So the electric field at each point along z is oscillating as an undampened simple harmonic oscillator (SHO). The magnetic field is behaving similarly but out of phase by $\pi/2$.

This should give us some inspiration for our task of deriving the quantum theory of the light field. The quantum theory of the harmonic oscillator is well known.

The object of deriving the quantum theory of anything, is to solve Schrödinger's equation for the physical system in question. Schrödinger's equation, given in its most general (one dimensional) form, for a single particle is

$$i\hbar \frac{\partial \Psi}{\partial t} = -\frac{\hbar^2}{2m} \frac{\partial^2 \Psi}{\partial x^2} + V\Psi, \qquad (8)$$

where $\hbar$ is Dirac's constant, m is the mass, Ψ is the total wave-function, x is the position, and V is the potential the particle experiences. As long as V is time independent we may

[7]See any text on electricity and magnetism. Griffiths' *Introduction to Electrodynamics* is recommended.

separate Eq. (8), a partial differential equation, into two ordinary differential equations[8]: $\Psi(x,t) = \psi(x)\phi(t)$. In its most convenient form, the solution is

$$\begin{aligned} U_Q\psi(x) &= -\frac{\hbar^2}{2m}\frac{d^2\psi(x)}{dx^2} + V\psi(x), \\ \Psi(x,t) &= \psi(x)e^{-iU_Qt/\hbar}. \end{aligned}$$

Where U_Q is a separation constant, which conveniently turns out to be the total energy of the system. Note that when we perform a measurement we only ever see $\int \Psi^*\hat{O}\Psi$ (where $\hat{O}$ is some observable), which is independent of time. So, while the wave-function is evolves with time, the expectation values of observable quantities do not, so separable wave-functions with time-constant potentials are called stationary.

The SHO has a simple time independent potential, so it is stationary. Since our light-field trapped in a cavity appears to be – on some level – behaving as a SHO we will write down its Schrödinger's equation

$$-\frac{\hbar^2}{2m}\frac{d^2\psi}{dx^2} + \frac{1}{2}m\omega^2x^2\psi = U_Q\psi, \tag{9}$$

Already we have problems with our attempt to build the quantum theory of a light field from the quantum theory of the SHO: the light field has no mass, and the particle in question has no defined position – spread out as it is throughout the cavity between the two plates.[9] It is clear we can not proceed entirely by direct analogy. *However*, what we do have is an object with a defined energy and a temporal component which behaves as the position variable of a SHO.

For now let's ignore the conceptual problems and focus on the mathematics of the situation. If the mathematical description of two things are the same, than mathematically they are the same. So let's call the time dependent part of the electric field the canonical position and define it as $\hat{\mathcal{E}}(t)$, sticking a hat (caret) on it to signify that it is now a quantum mechanical operator. We will associate it with x.

Now let's consider the first term of Eq. (9); $-i\hbar\partial_x$ is the momentum operator in quantum mechanics[10]: $\hat{p}$, this is because that first term $\hat{p}^2/2m$ is the kinetic energy. So if we've defined a mathematical object to be canonical position, we ought to be able to define a canonical momentum in a similar way. For a classical SHO the momentum is given by

$$p = mv = m\frac{dx}{dt} = m\omega\left\{\cos(\omega t) - \sin(\omega t)\right\}.$$

Again we are struck by a similarity, this time with the magnetic field given in Eq.(7). The momentum p has a mathematical description analogous to the temporal component of the

[8] I will skip the derivation as it proceededs fairly straightforwardly

[9] One might think, that because *no* quantum mechanical objects have a defined position until observation, that this point is not a problem. However, the light field does not have a set position even *classically*, so we must be more careful about drawing analogies.

[10] I will sometimes use the notation ∂_x to mean $\frac{\partial}{\partial x}$ in in-line equations, as a mechanism for saving space.

magnetic field, which we will now define as $\mathcal{B}(t) \equiv \omega_m[\cos(\omega_m t) - \sin(\omega_m t)]$. So now proceeding with our analogy we'll put a hat on $\mathcal{B}$, call it the canonical momentum, and make the identification $\hat{p} = m\hat{\mathcal{B}}(t)$. The normalization factor of ω_m in our definition of $\mathcal{B}$ comes from the fact that as canonical momenta and positions $\int dt\mathcal{B} = \mathcal{E}$ should be enforced. We have just completed the first step of second quantization: promoting classical variables to the status of quantum mechanical operators.

In light of all of this, let's substitute our canonical position and momentum (i.e. the temporal components of the electric and magnetic fields respectively) into the SHO wave-equation (9)

$$\frac{1}{2}m\left[\hat{\mathcal{B}}^2(t) + \omega_m\hat{\mathcal{E}}^2(t)\right]\psi = U_Q\psi. \tag{10}$$

Here we can see that the constant m (the mass for the SHO, an abstract mathematical object in our analogy) factors out of the left hand side of the equation. So we can treat it as an overall scale factor and subsume it into the energy which we will now relabel U'_Q.

We have successfully written down Schrödinger's equation for a light field trapped in a cavity. What remains is to solve it, and interpret our results in accordance with the knowledge, from Einstein, that light must come in discrete packets – photons.

Now it is convenient to switch to Dirac's linear algebra notation where wave functions are represented by state vectors in an abstract parameter space called Hilbert space: ψ becomes $|\psi\rangle$; and operators are represented by matrix transformations on these vectors. States which are eigenvectors of operators return the value of the physical quantity associated with that operator. For example, for a state of definite momentum p: $\hat{p}|\psi_p\rangle = p|\psi_p\rangle$.[11] In this notation Eq. (10) becomes

$$\frac{1}{2}\left[\hat{\mathcal{B}}^2(t) + \omega_m\hat{\mathcal{E}}^2(t)\right]|\psi\rangle = U'_Q.|\psi\rangle \tag{11}$$

It would be useful in solving this equation to be able to factor the left hand side. We "guess" the non-commuting objects

$$\hat{a}^\dagger = \frac{1}{\sqrt{2\hbar\omega_m}}\left[\omega_m\hat{\mathcal{E}}(t) - i\hat{\mathcal{B}}(t)\right], \tag{12}$$

$$\hat{a} = \frac{1}{\sqrt{2\hbar\omega_m}}\left[\omega_m\hat{\mathcal{E}}(t) + i\hat{\mathcal{B}}(t)\right]. \tag{13}$$

Note that though $\hat{a}$ and $\hat{a}^\dagger$ are time dependent we have dropped the parenthetical t, in order to avoid unnecessary clutter. In situations where there is some ambiguity we will write out the time dependence explicitly.

Using these two new operators, Eq.(11) becomes

[11] This is a wholly inadequate introduction to this rich and useful notation. The uninitiated reader is directed to one of the many very good books which deal with this subject. Recommended are Griffiths' *Introduction to Quantum Mechanics* and Sakurai's *Modern Quantum Mechanics*. By necessity I will proceed assuming the reader has a working knowledge of this topic.

$$\begin{aligned} \hbar\omega_m \left(\hat{a}^\dagger \hat{a} + \frac{1}{2}\right)|\psi\rangle &= U'_Q.|\psi\rangle \\ \hat{H}|\psi\rangle &= E|\psi\rangle \end{aligned} \tag{14}$$

This is not a complete factorization, though it is a more revealing form than we had previously. In the second line we have written the left side of the equation as $\hat{H}$ – the Hamiltonian – the operator which, has as its eigenstate, the total energy of the system. We have also renamed U'_Q as E.[12]

Since $\hat{a}$ and $\hat{a}^\dagger$ are composed of non-commuting operators we should work out their own commutation relations. Starting from the canonical commutation relation between position and momentum $[\hat{x}, \hat{p}] = i\hbar$ (and keeping in mind our mathematical analogy) it is straightforward to find that $[\hat{a}, \hat{a}^\dagger] = 1$.

But what is the significance of these two new operators? Lets us take $\hat{a}^\dagger$ and then $\hat{H}$ acting on a quantum state

$$\begin{aligned} \hat{H}\hat{a}^\dagger|\psi\rangle &= \hbar\omega_m \left(\hat{a}^\dagger\hat{a} + \frac{1}{2}\right)\hat{a}^\dagger|\psi\rangle, \\ &= \hbar\omega_m \left(\hat{a}^\dagger\hat{a}\hat{a}^\dagger + \frac{\hat{a}^\dagger}{2}\right)|\psi\rangle, \\ &= \hbar\omega_m \left(\hat{a}^\dagger(\hat{a}^\dagger\hat{a} + 1) + \frac{\hat{a}^\dagger}{2}\right)|\psi\rangle, \\ &= \hat{a}^\dagger\left(\hat{H} + \hbar\omega_m\right)|\psi\rangle, \\ &= \left(E + \hbar\omega_m\right)\hat{a}^\dagger|\psi\rangle. \end{aligned}$$

Where we have used the commutation relation from above. Examining the first and last lines we see that the state $\hat{a}^\dagger|\psi\rangle$ has an energy that is higher than $|\psi\rangle$ by $\hbar\omega_m$. A similar analysis shows that the state $\hat{a}|\psi\rangle$ has an energy which is lower than $|\psi\rangle$ by $\hbar\omega_m$. In the general case of a harmonic oscillator these operators are called ladder operators because they move the state up and down on an energy ladder, the rungs of which are separated by a distance of $\hbar\omega_m$. For our case, of a light field in a cavity there is a further interpretation. We know from Einstein's work on the photoelectric effect that a single packet of electromagnetic radiation (photon) has an energy of $\hbar\omega$. Thus $\hat{a}^\dagger$ represents the addition or *creation* of a photon in the light-field, and $\hat{a}$ represents the removal or *annihilation* of a photon. These two italicised words are most often used as the names of these operators.

Since we have operators that raise and lower the photon number of a field it is useful to create a basis which is defined by photon number.[13] This basis will be composed of states of

[12]Previously E was reserved for the electric field and U used for the energy to avoid confusion. Now, however, there will be little ambiguity between which of the two quantities is being spoken of. So, we return to the more natural notation of E as energy.

[13]I have not defined the concept of a basis. If someone without a strong background in quantum mechanics is still reading, then I again refer you to Griffiths' *Introduction to Quantum Mechanics* and Sakurai's *Modern Quantum Mechanics*. I will not make any further note of the use of undefined fundamental concepts and methods in quantum mechanics, focusing instead on the development of the theory of quantum optics.

definite photon number n and written in the Dirac notation as $|n\rangle$. The creation operator acting on this state will cause the photon number to be raised by one: $\hat{a}^\dagger|n\rangle = c_{n+1}|n+1\rangle$. Likewise the annihilation operator will raise the state by one: $\hat{a}|n\rangle = c_n|n-1\rangle$. The c's are normalization constants associated with the new state. Note that the index of c for the creation of a photon is written as the photon number of the new state, whereas for the annihilation of a photon it is the number of the old state. The reason for this convention is best seen by taking a simple example: We would like a state containing one photon after a single photon is added to be mathematically equivalent to a state containing one photon after a single photon has been removed – as these two states are physically the same. Thus we want (for instance)

$$\hat{a}^\dagger|0\rangle = \hat{a}|2\rangle,$$

which is maintained if we follow the above convention.

Much like a conventional ladder, the energy ladder must rest on a floor – a state below which there can be no further lowering. It is simple to see that one can not remove a photon from a field which contains no photons. Therefore the annihilation operator acting on the state with no photons in it (from here on called the *vacuum state*): $\hat{a}|0\rangle = c_0|0\rangle$ must have the normalization $c_0 = 0$, as the probability amplitude of this process must vanish. We wish to find the expression for the normalization constants in the general form. Towards this end take

$$\hat{a}\hat{a}^\dagger|0\rangle = (\hat{a}^\dagger\hat{a} + 1)|0\rangle = |0\rangle,$$

where the commutator has been used, and compare with $\hat{a}\hat{a}^\dagger|0\rangle = c_1^2$. Thus, by equating the two expressions we have $c_1 = 1$. Now let's take $\hat{a}\hat{a}^\dagger\hat{a}^\dagger|0\rangle$. Using the same procedure as above – continuously applying the commutator until we have an annihilation operator acting on the vacuum, and then comparing this with what we get when we apply the operators in their unaltered order – we obtain $c_2 = \sqrt{2}$. Applying this procedure recursively we can find in general that $c_n = \sqrt{n}$, yielding our final expressions for the creation and annihilation operators acting on a number state

$$\hat{a}^\dagger|n\rangle = \sqrt{n+1}|n+1\rangle, \tag{15}$$
$$\hat{a}|n\rangle = \sqrt{n}|n-1\rangle. \tag{16}$$

An arbitrary number state may therefore be written as

$$|n\rangle = \frac{(\hat{a}^\dagger)^n}{\sqrt{n!}}|0\rangle.$$

Taking the conjugate transpose of Eqs. (15 and 16) we see that a creation operator acting on a left hand state (bra) behaves as annihilation operator on that state, likewise an annihilation operator acting left behaves as a creation operator.

Now we wish to determine the value of the inner product $\langle m|n\rangle$, which given the above, we may write as

$$\langle 0|\frac{\hat{a}^m}{\sqrt{m!}}\frac{(\hat{a}^\dagger)^n}{\sqrt{n!}}|0\rangle.$$

Now note that if $m > n$, and we act the operators on the right-hand state (ket) there will be enough annihilation operators to remove all the photons from the state that the creation operators put there; with one or more left over to act on the vacuum state and cause the expression to evaluate to zero. Furthermore if $m < n$ we can act the operators on the left-hand state (bra) with the same result. The only case in which the expression does not evaluate to zero is when $m = n$ in which case the result is unity. Therefore $\langle m|n\rangle = \delta_{mn}$, the number states are orthonormal.

A monochromatic light field in a pure state may exist in a quantum mechanical superposition of containing different numbers of photons. Thus when a measurement is performed on the state it is found to have a specific number of photons. Mathematically this may be expressed, for some state $|\psi\rangle$, as

$$|\psi\rangle = \sum_{n=0}^{\infty} p_n|n\rangle,$$

where the p_n's are the probability amplitudes of the various definite photon number states. Since any quantum state may be decomposed in the number basis we can call it *complete*. Also, since orthonormality includes linear independence we can state that the the basis of definite number states (also called Fock states after Vladimir Fock, the Soviet Physicist) constituent a true and compete mathematical basis.

Now let's examine the expectation value of the product $\hat{a}^\dagger\hat{a}$ with respect to an arbitrary state

$$\langle\psi|\hat{a}^\dagger\hat{a}|\psi\rangle = \sum_{m=0}^{\infty}\sum_{n=0}^{\infty} p_m^* p_n\langle m|\hat{a}^\dagger\hat{a}|n\rangle = \sum_{m=0}^{\infty}\sum_{n=0}^{\infty} p_m^* p_n n\delta_{mn} = \sum_{n=0}^{\infty}|p_n|^2 n.$$

Which is simply the *average* number of photons in the light field. Thus we shall now rename the operator $\hat{a}^\dagger\hat{a}$ the "number operator" and write it as $\hat{n}$. It has as its eigenstates the number states. This sheds some further insight on Eq. (14) which we can now rewrite in its final form

$$\hbar\omega\left(\hat{n} + \frac{1}{2}\right)|\psi\rangle = E_n|\psi\rangle,$$

where the subscript m has been dropped from ω (in situations where there is some ambiguity in the frequency it will return). Unsurprisingly, the energy of the field is directly proportional to the number of photons. However what *is* surprising is that if there are no photons (i.e. $\hat{n}$ returns zero) the field still has energy! Put another way: the empty vacuum contains energy.

Not only that, but because this term exists in the Hamiltonian for every frequency, and there is no upper limit on the values frequency may take, the energy is infinite. This is called the vacuum energy or zero-point energy.

The obvious question is, "If the universe is pervaded by an omnipresent field with infinite energy, why don't we see it?" The answer is that it is precisely *because* of the fact that it is everywhere that we do not detect it. Imagine that we wanted to build an engine that ran off of the zero-point energy. In order to have this machine do work what we need is an energy *difference*. All engines take advantage of systems where there is an imbalance in energy content. A good example is a waterfall. There is a body of water above the waterfall and a body below. The higher reservoir has a larger potential energy than the lower one. As the water falls it may be used to turn a waterwheel, and do work. Note that the lower reservoir, as mass in a gravitational field, still contains potential energy, but if we can not find a lower place for the water to fall to we can not use it to do any work. This is exactly the same situation as the vacuum energy, since it is *everywhere* we can never find a "lower place", and set up an engine. This is why we usually don't notice it, because of its ubiquity.

There are ways we can observe its presence however. The most famous is the Casimir effect: If two parallel conducting plates are held very closely together (as in our model of the quantum light field) then a force of attraction will be observed between them. A somewhat involved calculation in quantum electrodynamics will show that this force is due to the vacuum energy.[14] But we can offer a good conceptual explanation by using our model. The zero-point energy exists in every frequency mode of the field. Due to the boundary conditions, however, the cavity can support no lower frequencies than the fundamental (first harmonic). However, the region outside the plates is not constrained in this way, and thus may have many more frequency modes of larger wavelength. The pressure of all these additional light modes can be seen as pushing the plates together.

Let's return to the time-dependent parts of the electric and magnetic fields (the canonical position and momentum). We had guessed Eqs. (12) and (13) in order to partially factor the Hamiltonian. If we invert these formulae we arrive at expressions for $\mathcal{E}$ and $\mathcal{B}$ in terms of the creation and annihilation operators,

$$\begin{aligned} \hat{\mathcal{E}}(t) &= \sqrt{\frac{\hbar}{2\omega}}[\hat{a}(t) + \hat{a}^\dagger(t)], \\ \hat{\mathcal{B}}(t) &= -i\sqrt{\frac{\hbar\omega}{2}}[\hat{a}(t) - \hat{a}^\dagger(t)], \end{aligned}$$

where the time dependence has been made explicit. We can solve for the time dependence of the annihilation operator by using the equation of motion for an operator

$$\frac{d\hat{a}}{dt} = \frac{i}{\hbar}[\hat{H}, \hat{a}],$$

[14]The situation is actually somewhat more complicated than this. This force may be equally well explained by radiation reaction (an electric self-force). It is currently unknown which of the two effects is a better description. The vacuum energy is usually preferred as the calculations are typically easier to perform.

$$
\begin{aligned}
&= \frac{i}{\hbar}\left[\hbar\omega\left(\hat{a}^\dagger\hat{a}+\frac{1}{2}\right),\hat{a}\right] \\
&= -i\omega\hat{a},
\end{aligned}
$$

which has the solution $\hat{a}(t) = \hat{a}(0)e^{-i\omega t}$. And taking the conjugate transpose we get the expression for the creation operator $\hat{a}^\dagger(t) = \hat{a}^\dagger(0)e^{i\omega t}$. This allows us to recast the electric (singly polarized) field as an operator

$$
\hat{E}(t,z) = E_0 \sin(kz)[\hat{a}e^{-i\omega t} + \hat{a}^\dagger e^{i\omega t}]. \tag{17}
$$

We can rewrite this in terms of two dimensionless quantities called quadrature operators defined as

$$
\hat{X}_1 = \frac{1}{2}(\hat{a}+\hat{a}^\dagger), \tag{18}
$$

$$
\hat{X}_2 = \frac{1}{2i}(\hat{a}-\hat{a}^\dagger). \tag{19}
$$

Inverting these equations and substituting into Eq. (17) yields

$$
\hat{E}(t,z) = 2E_0 \sin(kz)\left[\hat{X}_1\cos(\omega t) + \hat{X}_2\sin(\omega t)\right].
$$

From this it is clear that the two quadrature operators are always $\pi/2$ out of phase, and thus always in different quadratures (hence the name). These operators are related to $\hat{\mathcal{E}}$ and $\hat{\mathcal{B}}$ by constant factors.[15] It is standard to define an uncertainty relation using the generalized Heisenberg uncertainty principle for non-commuting operators $\Delta A\Delta B \geq \frac{1}{2}|\langle[\hat{A},\hat{B}]\rangle|$. This obtains

$$
\Delta\hat{X}_1\Delta\hat{X}_2 \geq \frac{1}{4}. \tag{20}
$$

The usefulness of this notation will be further developed in section 1.3.3.

We have extracted a rich quantity of information and insight from what is, physically, a very simple toy system. But, it should be pointed out that despite this there is much the model does *not* describe. Most prominently it does not describe *travelling* light – a realistic photonic wave packet. These can be modelled though by superimposing many (possibly infinity many) standing, or plane, waves with periodic boundary conditions. An example of this can be seen in section 2.4.3, when we define a realistic pulse of quantum light.

[15] I will use $\hat{X}_1$ and $\hat{X}_2$ interchangeably with $\hat{q}$ and $\hat{p}$ as the quadrature operators. This is not a good practice but it is common in the literature.

1.3.2 The Coherent State: The Friendliest State

In this section we will define a very user friendly quantum mechanical state of a light field. In order to derive this state let's start with the question of whether the annihilation operator has an eigenstate. Calling this hypothetical state $|\alpha\rangle$, we would have

$$\hat{a}|\alpha\rangle = \alpha|\alpha\rangle. \tag{21}$$

Since we know from the previous sections that the number states constitute a complete basis, and therefore any quantum state, may be expanded as a series of weighted number states we can write

$$|\alpha\rangle = \sum_{n=0}^{\infty} C_n|n\rangle. \tag{22}$$

If we can find a set of C_n's that cause Eq. (21) to be satisfied then it means that these states do exist. Combine Eq. (21) and Eq. (22) to obtain

$$\hat{a}|\alpha\rangle = \sum_{n=1}^{\infty} C_n\sqrt{n}|n-1\rangle = \alpha\sum_{n=0}^{\infty} C_n|n\rangle.$$

By taking the terms of equivalent photon number in the infinite sums we have the recursion relation $C_n\sqrt{n} = \alpha C_{n-1}$. Applying this in succession looks like

$$C_n = \frac{\alpha}{\sqrt{n}}C_{n-1} = \frac{\alpha^2}{\sqrt{n(n-1)}}C_{n-2} = ... = \frac{\alpha^n}{\sqrt{n!}}C_0,$$

until we reach the photon number ladder floor of C_0, which we can regard as a normalization constant of the state

$$|\alpha\rangle = C_0\sum_{n=0}^{\infty}\frac{\alpha^n}{\sqrt{n!}}|n\rangle.$$

We can find this normalization constant without too much difficulty

$$1 = \langle\alpha|\alpha\rangle = |C_0|^2\sum_{n=0}^{\infty}\sum_{m=0}^{\infty}\frac{\alpha^{*n}\alpha^m}{\sqrt{n!m!}}\langle n|m\rangle = |C_0|^2\sum_{n=0}^{\infty}\frac{|\alpha|^{2n}}{n!} = |C_0|^2 e^{|\alpha|^2}.$$

Now that we have shown that the state has a well-defined expansion and is normalizable we can write down the general expression

$$|\alpha\rangle = e^{-\frac{1}{2}|\alpha|^2}\sum_{n=0}^{\infty}\frac{\alpha^n}{\sqrt{n!}}|n\rangle. \tag{23}$$

This expression defines the *coherent state*. It should be noted that the creation operator does not have a left eigenstate (an attempt to define one will lead to an expression, which is not normalizable), it can only have a right eigenstate, which we can find by taking the conjugate transpose of Eq. (21),

$$\langle\alpha|\hat{a}^\dagger = \alpha^*\langle\alpha|. \tag{24}$$

Likewise the annihilation operator does not have a right eigenstate.

It is useful to determine some properties of the coherent state. Using Eqs. (21) and (24), we find that the number of photons in a coherent state is

$$\langle\alpha|\hat{n}|\alpha\rangle = \langle\alpha|\hat{a}^\dagger\hat{a}|\alpha\rangle = |\alpha|^2,$$

meaning that the absolute value of α is the the square root of the average number of photons in the field. One very useful property of the coherent state is that, when taking expectation values of operators, which may be very complicated functions of $\hat{a}$ and $\hat{a}^\dagger$, one only needs to normally order the function (place all the creation operators to the left of all the annihilation operators) for things to become simple to calculate.

Another property of the coherent state is that if we take two arbitrary states $|\alpha\rangle$ and $|\beta\rangle$ and calculate their inner product, we get,

$$\langle\beta|\alpha\rangle = e^{\frac{1}{2}\left[\beta^*\alpha - \beta\alpha^* - |\beta-\alpha|^2\right]}.$$

So the coherent states are not orthogonal, and as such are called over complete. Nonetheless they span the Hilbert space and thus may be used as a basis. Like any complete basis, we can use it to decompose unity. So for the coherent basis

$$\hat{1} = \frac{1}{\pi}\int\int d\mathrm{Re}(\alpha)d\mathrm{Im}(\alpha)|\alpha\rangle\langle\alpha|, \tag{25}$$

where the factor of $1/\pi$ compensates for the over-completeness of the basis. Since α is a continuous complex quantity we have a double integral instead of a single sum.

Before discussing another interesting property of coherent states, let's return to the vacuum state, discussed previously. It is useful to speak of the uncertainties of a state in its quadratures (recall that these are the dimensionless $\hat{\mathcal{E}}$ (or $\hat{q}$) and $\hat{\mathcal{B}}$ (or $\hat{p}$) operators) defined in Eqs. (18) and (19). For the vacuum state they are given by

$$\begin{aligned}
\Delta\hat{X}_1 &= \sqrt{\langle\hat{X}_1^2\rangle - \langle\hat{X}_1\rangle^2}, \\
&= \sqrt{\langle 0|\frac{1}{4}(\hat{a}^2 + \hat{a}\hat{a}^\dagger + \hat{a}^\dagger\hat{a} + \hat{a}^{\dagger 2})|0\rangle - \langle 0|\frac{1}{2}(\hat{a} + \hat{a}^\dagger)|0\rangle^2}, \\
&= \sqrt{\frac{1}{4} - 0} = \frac{1}{2},
\end{aligned}$$

$$\begin{aligned}\Delta\hat{X}_2 &= \sqrt{\langle 0| - \frac{1}{4}(\hat{a}^2 - \hat{a}\hat{a}^\dagger - \hat{a}^\dagger\hat{a} + \hat{a}^{\dagger 2})|0\rangle - \langle 0|\frac{1}{2i}(\hat{a} - \hat{a}^\dagger)|0\rangle^2}, \\ &= \sqrt{\frac{1}{4} - 0} = \frac{1}{2},\end{aligned}$$

where the commutator $[\hat{a}, \hat{a}^\dagger] = 1$ has been used. Which leads to

$$\Delta\hat{X}_1\Delta\hat{X}_2 = \frac{1}{4}.$$

Compare this to Eq. (20), the general expression for the quadrature uncertainty relation, and we see that vacuum states *minimize* the uncertainty relation. Vacuum states consequently receive the designation minimum uncertainty states.

We can compute the same relation for coherent states

$$\begin{aligned}\Delta\hat{X}_1 &= \sqrt{\langle\alpha|\frac{1}{4}(\hat{a}^2 + \hat{a}\hat{a}^\dagger + \hat{a}^\dagger\hat{a} + \hat{a}^{\dagger 2})|\alpha\rangle - \langle\alpha|\frac{1}{2}(\hat{a} + \hat{a}^\dagger)|\alpha\rangle^2}, \\ &= \sqrt{\frac{1}{4}(\alpha^2 + 2|\alpha|^2 + 1 + \alpha^{*2}) - \frac{1}{4}(\alpha + \alpha^*)^2}, \\ &= \frac{1}{2}, \\ \Delta\hat{X}_2 &= \sqrt{\langle\alpha| - \frac{1}{4}(\hat{a}^2 - \hat{a}\hat{a}^\dagger - \hat{a}^\dagger\hat{a} + \hat{a}^{\dagger 2})|\alpha\rangle - \langle\alpha|\frac{1}{2i}(\hat{a} - \hat{a}^\dagger)|\alpha\rangle^2}, \\ &= \sqrt{-\frac{1}{4}(\alpha^2 - 2|\alpha|^2 - 1 + \alpha^{*2}) + \frac{1}{4}(\alpha - \alpha^*)^2}, \\ &= \frac{1}{2}.\end{aligned}$$

Which again minimizes the uncertainty relation. So apparently coherent states are also minimum uncertainty states. This implies that the vacuum states are related to the coherent states on some level. In fact it is possible to mathematically generate the coherent states from the vacuum states. As it turns out this description is extremely useful, and will be expanded upon in the next section. To begin take Eq.(23) and rewrite in terms of the creation operators

$$|\alpha\rangle = e^{-\frac{1}{2}|\alpha|^2}\sum_{n=0}^{\infty}\frac{\alpha^n}{n!}(\hat{a}^\dagger)^n|0\rangle, \tag{26}$$

which can be recast as

$$\begin{aligned}|\alpha\rangle &= e^{-\frac{1}{2}|\alpha|^2}e^{\alpha\hat{a}^\dagger}|0\rangle, \\ &\equiv \hat{\mathcal{D}}|0\rangle,\end{aligned} \tag{27}$$

where we have defined $\hat{\mathcal{D}}$. Apparently we now have an operator which changes a vacuum state into a coherent state. We would like the conjugate transpose of this operator to change the coherent state back into the vacuum state (we would like it to be unitary) however the operation $\hat{\mathcal{D}}^\dagger|\alpha\rangle$ just generates a different coherent state. Unitary states have the property that $\hat{U}^\dagger\hat{U} = 1$.[16] Let's assume that there is some operator $\hat{\mathcal{D}}'$ which will make the combination $\hat{\mathcal{D}}'\hat{\mathcal{D}}$ unitary while still generating the same coherent state, i.e.:

$$(\hat{\mathcal{D}}'\hat{\mathcal{D}})^\dagger(\hat{\mathcal{D}}'\hat{\mathcal{D}}) = 1 \quad \text{and} \quad \hat{\mathcal{D}}'\hat{\mathcal{D}}|0\rangle = |\alpha\rangle.$$

We guess

$$\hat{\mathcal{D}}' = Ce^{-\alpha^*\hat{a}},$$

where C is some normalization constant. Now rewriting the first condition as,

$$\begin{aligned} 1 &= \hat{\mathcal{D}}^\dagger\hat{\mathcal{D}}'^\dagger\hat{\mathcal{D}}'\hat{\mathcal{D}}, \\ e^{|\alpha|^2} &= |C|^2 e^{\alpha^*\hat{a}} e^{-\alpha\hat{a}^\dagger} e^{-\alpha^*\hat{a}} e^{\alpha\hat{a}^\dagger}, \\ &= |C|^2 e^{\alpha^*\hat{a}} e^{-\alpha\hat{a}^\dagger} \times \text{h.c.} \end{aligned} \tag{28}$$

Where h.c. stands for the hermitian conjugate. Utilizing the disentangling theorem[17], which states that

$$e^{\hat{A}}e^{\hat{B}} = e^{\hat{A}+\hat{B}}e^{\frac{1}{2}[\hat{A},\hat{B}]},$$

as long as $\hat{A}$ and $\hat{B}$ both commute with their commutator, we obtain

$$e^{\alpha^*\hat{a}}e^{-\alpha\hat{a}^\dagger} = e^{\alpha^*\hat{a}-\alpha\hat{a}^\dagger}e^{-\frac{1}{2}|\alpha|^2}.$$

Plugging this back into Eq. (28), we get

$$e^{2|\alpha|^2} = |C|^2 e^{\alpha^*\hat{a}-\alpha\hat{a}^\dagger} e^{\alpha\hat{a}^\dagger-\alpha^*\hat{a}} = |C|^2,$$

where in the last equality we have again used the disentangling theorem. So evidently our choice of $\hat{\mathcal{D}}$ was correct as long as we define C to be $\exp(|\alpha|^2)$. Now we need to test the second condition

$$\begin{aligned} \hat{\mathcal{D}}'\hat{\mathcal{D}}|0\rangle &= e^{|\alpha|^2} e^{-\alpha^*\hat{a}} e^{-\frac{1}{2}|\alpha|^2} e^{\alpha\hat{a}^\dagger}|0\rangle, \\ &= e^{-\frac{1}{2}|\alpha|^2} e^{-\alpha\hat{a}^\dagger} e^{\alpha^*\hat{a}}|0\rangle, \\ &= e^{-\frac{1}{2}|\alpha|^2} e^{-\alpha\hat{a}^\dagger}|0\rangle, \\ &= |\alpha\rangle. \end{aligned}$$

[16] This is, in fact, the definition of unitary.

[17] Also called the the Campbell-Baker-Hausdorff theorem.

Where in the second line we have again used the (very useful) disentangling theorem. Note that when we expand the exponential of annihilation operators only the first term 1 survives, leaving the vacuum state unaltered for $\hat{\mathcal{D}}$ to act on. So we now have the mathematical operator which generates coherent states from vacuum states, it is called the displacement operator $\hat{D}(\alpha)$ (for reasons which will become apparent in the next section). Using the disentangling theorem *again* we can write it in its most common form

$$\hat{D}(\alpha) \equiv e^{(\alpha\hat{a}^\dagger - \alpha^*\hat{a})}. \tag{29}$$

Now we move along to another important property of the coherent states. Take the expectation value of the electric field operator with respect to a coherent state

$$\begin{aligned} \langle\alpha|\hat{E}(z,t)|\alpha\rangle &= \langle\alpha|E_0 \sin(kz)\left[\hat{a}e^{-i\omega t} + \hat{a}^\dagger e^{i\omega t}\right]|\alpha\rangle, \\ &= E_0 \sin(kz)\left[\alpha e^{-i\omega t} + \alpha^* e^{i\omega t}\right]. \end{aligned}$$

Any complex number may be decomposed into polar form as $\alpha = |\alpha|e^{i\theta}$; we shall do this for α and α^* in the above equation to get,

$$\begin{aligned} \langle\hat{E}(z,t)\rangle &= E_0|\alpha| \sin(kz)\left[e^{-i(\omega t+\theta)} + e^{i(\omega t+\theta)}\right], \\ &= 2E_0|\alpha| \sin(kz)\cos(\omega t + \theta). \end{aligned}$$

We had previously claimed that $|\alpha|$ (the radial part of the decomposition) was proportional to the intensity of the of the light – this is reinforced by seeing that it constitutes part of the amplitude of the electric field. We can now interpret the angular part of the decomposition θ as the phase of the electric field and thus of the coherent light. It is most important to note that this is the *classical* expression for the electric field. For this, and other reasons, coherent light is frequently called the most classical quantum state of a light field.[18] It behaves in a way that – sometimes – is very familiar to us from classical optics.

1.3.3 Quadrature Diagrams

We now move on to one of the most useful conceptual tools in quantum optics. We wish to define a two dimensional phase space spanned by the the expectation values of the quadrature operators $\langle\hat{X}_1\rangle$ and $\langle\hat{X}_2\rangle$. But first we should note that there is a key difference between a quantum phase space diagram and a classical phase space diagram, that is that variables may not be defined by exact quantities for conjugate observables. Thus states in our quantum-mechanical phase space will be defined by *areas* instead of *points*, these areas will be determined by finding the variances of the quadrature in question.

By way of example we'll take the most simple state we have found, the vacuum state, and plot it in quadrature space. The expectation value of both quadrature operators is zero for the vacuum state. Thus the centre of the vacuum state will be on the origin. We have

[18] Some of these other reasons will be discussed in section 4.1.

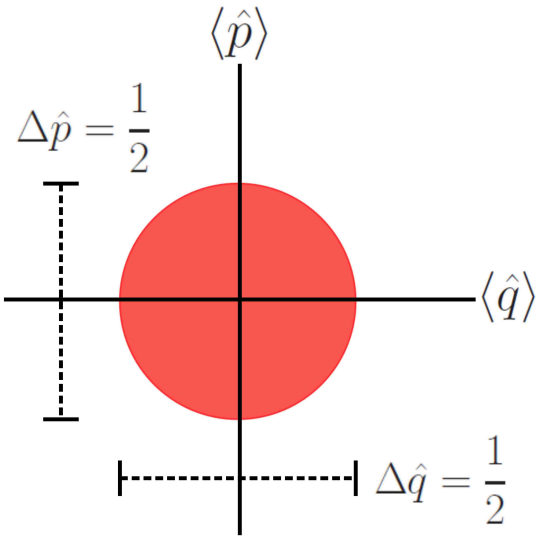

Figure 1: The quadrature-space diagram of the vacuum state. Its position at the origin represents that the expectation values in both quadratures is zero. The circular area represents is equal uncertainty (variance) with respect to $\hat{q}$ and $\hat{p}$. Note that we have switched from $\hat{X}_1$ and $\hat{X}_2$ to $\hat{q}$ and $\hat{p}$ to be more in line with the predominate convention. In my previous notation q and p were the canonical position and momentum, the difference is only a constant scale factor.

already calculated the uncertainties in both quadratures for a vacuum state: $\Delta\hat{X}_1 = 1/2$ and $\Delta\hat{X}_2 = 1/2$. So the shape of the state will be a circle. See Figure (1).

Note that we have switched from $\hat{X}_1$ and $\hat{X}_2$ to $\hat{q}$ and $\hat{p}$ to be more in line with the predominate convention. In my previous notation q and p were the canonical position and momentum, the difference is only a constant scale factor. I will use the X's in the text but use q and p in graphs.

Recall that for a coherent state the variances in quadrature are the same as for vacuum, since both are minimum uncertainty states. Now we'll calculate the average position in quadrature space

$$\begin{aligned}
\langle \hat{X}_1 \rangle &= \langle \alpha | \frac{1}{2} \left(\hat{a} + \hat{a}^\dagger \right) | \alpha \rangle, \\
&= \frac{1}{2}(\alpha + \alpha^*), \\
&= |\alpha| \cos(\theta). \\
\langle \hat{X}_2 \rangle &= \langle \alpha | \frac{1}{2i} \left(\hat{a} - \hat{a}^\dagger \right) | \alpha \rangle, \\
&= \frac{1}{2i}(\alpha - \alpha^*), \\
&= |\alpha| \sin(\theta).
\end{aligned}$$

These results are easily interpreted as transformations from linear to polar coordinates. The the coherent state's radial distance from the origin is $|\alpha|$ – the root of its intensity. The

polar coordinate is θ which, as we showed in the previous section, is the phase of the light field. The polar representation of the quadrature diagram is thus more useful. We can now interpret the displacement operator $\hat{D}(\alpha)$ as a physical displacement of the vacuum state in quadrature space into the coherent state. Coherent states are sometimes called displaced vacuum states. See Figure 2.

Another state that's useful to represent in quadrature space is the number state. Like the vacuum state the number state has no phase, and the expectation values of the quadratures is zero. However the number states have a definite non-zero photon number and are thus represented as *rings* in quadrature space. Their phase is undefined, but they have perfectly defined intensities. See Figure 3.

There are more sophisticated ways of visualizing the phase space behaviour of the quantum state of a light field. These methods provide a greater degree of mathematical rigor. These mathematical constructions will be the topic of the next section.

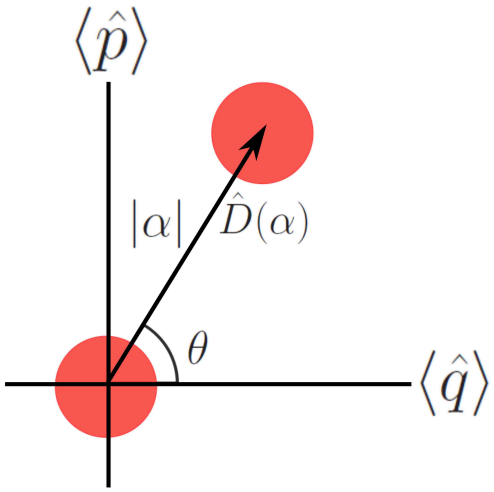

Figure 2: The displacement operator acting on a vacuum state to create a coherent state. The amplitude and phase of the light field are interpreted as the radial and polar coordinates, respectively, in phase space.

1.3.4 Quasi-Probability Distributions

In this section I will carefully develop the language of quantum quasi-probability distributions. But first I will review classical and quantum probabilities, and highlight the differences between them.

In classical mechanics it is frequently useful to define a probability distribution for a physical system. Probability distributions arise when, due to a lack of complete information about a system, we can not exactly determine the outcome of some physical process. A good example is a six-sided die. We know that when we roll the die we will get one of six different results: 1,2,3,4,5,6. We also know (for a fair die) that the probability of obtaining one of these results is equal to the probability of obtaining the others. We could say that the probability distribution is flat i.e. $P(x) = 1/6$, where P is the probability that we will get result x, where x is some integer number between one and six.

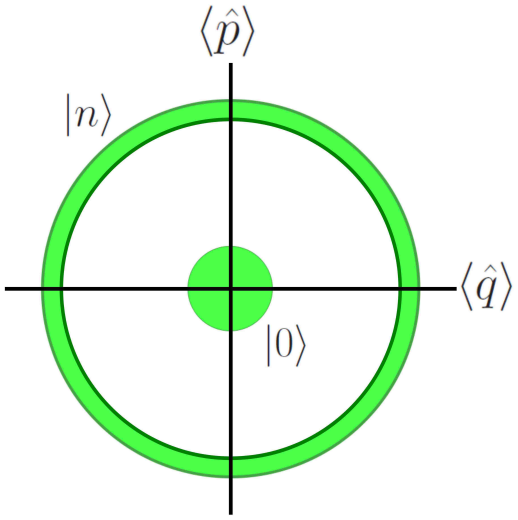

Figure 3: A vacuum state and a number state. The number state has completely definite photon number, but completely undefined phase.

Now let's make things a little more interesting. Suppose the die has spent some time in a microwave, six-side up.[19] Now the probability distribution might look like $P(6) = 1/4$, $P(2,3,4,5) = 1/6$, $P(1) = 1/12$; where the probability distribution has now been weighted (like the die).

The system of the die was very simple. But, it is possible to imagine much more elaborate systems, with a multitude of different outcomes, dependent on initial conditions in some complicated way. No matter the system though, some rules must be followed. All the probabilities must add up to one as *something* must happen (which could be violated for a total of less than one) and a process can not have two or more exclusive outcomes (which could be violated if the total was more than one).

Leaving behind classical mechanics we can consider a quantum die. The analogue of the probability distribution P in quantum mechanics is the *density matrix* $\hat{\rho}$, which is an operator which describes the quantum mechanical state of a system. We could write a density matrix for the above example of our die as

$$\hat{\rho}_{6-\text{side}} = \frac{1}{6}|1\rangle\langle 1| + \frac{1}{6}|2\rangle\langle 2| + \frac{1}{6}|3\rangle\langle 3| + \frac{1}{6}|4\rangle\langle 4| + \frac{1}{6}|5\rangle\langle 5| + \frac{1}{6}|6\rangle\langle 6|.$$

Which we could alternately represent in matrix form $\rho_{nm} = \langle n|\hat{\rho}_{6-\text{side}}|m\rangle$,

[19] This is a method used by unscrupulous individuals to change the internal density of a plastic die so that it is more likely to roll a six. As the interior melts slightly, gravity causes the bottom of the die to become more dense than the top.

$$\rho_{nm} = \frac{1}{6}\begin{bmatrix} 1 & 0 & 0 & 0 & 0 & 0 \\ 0 & 1 & 0 & 0 & 0 & 0 \\ 0 & 0 & 1 & 0 & 0 & 0 \\ 0 & 0 & 0 & 1 & 0 & 0 \\ 0 & 0 & 0 & 0 & 1 & 0 \\ 0 & 0 & 0 & 0 & 0 & 1 \end{bmatrix} \tag{30}$$

If we wish to extract the probability of a specific outcome from this we take the expectation value of that outcome, for example

$$\langle 2|\hat{\rho}_{6-\text{side}}|2\rangle = \frac{1}{6},$$

which is the probability of observing the die to have landed two-side up. However we can now consider a "quantum die", which may exist in a quantum mechanical superposition of existing in all six states simultaneously. The state vector for this die would be given as

$$|\psi_6\rangle = \frac{1}{\sqrt{6}}\left(|1\rangle + |2\rangle + |3\rangle + |4\rangle + |5\rangle + |6\rangle\right).$$

Which given the fact that for pure states[20] $\hat{\rho} = |\psi\rangle\langle\psi|$, in matrix form this becomes

$$\rho_{nm} = \frac{1}{6}\begin{bmatrix} 1 & 1 & 1 & 1 & 1 & 1 \\ 1 & 1 & 1 & 1 & 1 & 1 \\ 1 & 1 & 1 & 1 & 1 & 1 \\ 1 & 1 & 1 & 1 & 1 & 1 \\ 1 & 1 & 1 & 1 & 1 & 1 \\ 1 & 1 & 1 & 1 & 1 & 1 \end{bmatrix}. \tag{31}$$

This looks quite different from Eq. (30). What is the physical difference? For the die to be in a quantum mechanical superposition it must be *unobserved*. I will not get into the fascinating and sticky topic of what it means to observe an object. I will just say that the die must be completely isolated from the environment. Imagine the die is in a perfectly sealed box with some kind of automated (and fair) die-rolling robot. After the robot rolls the die, but before we open up the box to see inside, the die remains in the pure state described by the density matrix in Eq. (31). A die described by Eq. (30) would in truth be represented by a collection of die in a box, which is not well isolated from the surrounding environment. We could simply shake this box about and then reach in and pull out a die, which would have a one in six chance of having landed any particular side up. This kind of system is called a statistical mixture. On a fundamental level the difference is that before observation all the dice in the mixture are in defined states of having a single side up, whereas the quantum die in superposition has all sides up *simultaneously* until we look at it. These states may

[20]This term will be explained in a moment.

be completely defined by their state vectors (pure states). Systems in a statistical mixture must be described by a density matrix.

Mathematically the difference comes from the off-diagonal terms in the density matrix (also called coherence terms). The density matrix can represent not only pure states and mixtures but also physical systems which are between the two. Perhaps our little robot rolls the die, but the isolation of the box is not perfect and some of the coherence leaks out through the slightly porous walls. Another way to look at this, is that the outside environment is performing a partial measurement on the die. In this case the off diagonal terms of the matrix are reduced, but they do not become zero.

Another important property of the density matrix is that the trace (sum of diagonal terms) of the density matrix must add up to one. This is similar to the condition that the sum of probabilities must be one in the classical case.

A pernicious problem with the density matrix representation is the difficulty in visualizing what is going on. For our simple example of a six sided die we need a matrix of thirty six complex numbers. This may be very accurate and useful but it is not intuitive.

We can, however, extract from the density matrix a form of information which is more closely analogous to classical probability distributions. It will also lend itself, more directly, to visualization. Take a density matrix and multiply on both sides by Eq. (25)

$$\hat{\rho} = \int\int\int\int d\mathrm{Re}(\alpha) d\mathrm{Im}(\alpha) d\mathrm{Re}(\beta) d\mathrm{Im}(\beta) |\alpha\rangle\langle\alpha|\hat{\rho}|\beta\rangle\langle\beta|.$$

Making the definition $\langle\alpha|\hat{\rho}|\beta\rangle = P'(\alpha,\beta)$, and doing the integrals over β yields

$$\hat{\rho} = \int\int d\mathrm{Re}(\alpha) d\mathrm{Im}(\alpha) P(\alpha) |\alpha\rangle\langle\alpha|.$$

This shows that the density matrix may be completely represented by a single (complex) parameter function $P(\alpha)$ called the Glauber-Sudarshan P function. That is, as long as the density matrix represents only a single mode. The P function works in much the same way as a classical probability distribution, and if we define a space by $\mathrm{Re}(\alpha)$ and $\mathrm{Im}(\alpha)$ we can generate three dimensional plots of this quantity.

There are two other distributions, similar to P, that are used frequently in quantum optics: the Husimi-Bopp Q function, and the Wigner function. The Wigner function will be important in section 5.2. They differ in their derivation and uses, but share the ability to graphically represent quantum probability distributions.

The question of how to obtain these distributions in a direct manner is best addressed by recourse to the quantum characteristic functions, defined as

$$\begin{aligned} C_P(\lambda) &= \mathrm{Tr}\left[\hat{\rho} e^{\lambda\hat{a}^\dagger} e^{-\lambda^*\hat{a}}\right], \\ C_Q(\lambda) &= \mathrm{Tr}\left[\hat{\rho} e^{-\lambda^*\hat{a}^\dagger} e^{\lambda\hat{a}}\right], \\ C_W(\lambda) &= \mathrm{Tr}\left[\hat{\rho} e^{\lambda\hat{a}^\dagger - \lambda^*\hat{a}}\right]. \end{aligned}$$

The first is associated with the P function, the second with Q, and the last with Wigner. C_W can also be interpreted as the expectation value of the displacement operator $C_W =$

$\mathrm{Tr}\left[\hat{\rho}\hat{D}(\lambda)\right] = \langle\hat{D}(\lambda)\rangle$. These functions are connected to their related distributions via a Fourier transform, something I state without proof. For example the Wigner function is related to C_W by

$$W(\alpha) = \frac{1}{\pi^2}\int\int d\mathrm{Re}(\lambda)d\mathrm{Im}(\lambda)e^{\lambda^*\alpha-\lambda\alpha^*}C_W(\lambda).$$

It is more or less straightforward to calculate the Wigner distributions for a coherent state $|\beta\rangle$, and a number state $|n\rangle$

$$\begin{aligned} W_{|\beta\rangle}(\alpha) &= \frac{2}{\pi}e^{-2|\alpha-\beta|^2}, \\ W_{|n\rangle}(\alpha) &= \frac{2}{\pi}(-1)^n L_n(4|\alpha|^2)e^{-2|\alpha|^2}, \end{aligned}$$

where $L_n(x)$ is a Laguerre polynomial. $W_{|\beta\rangle}$ is a Gaussian, peaked at β, which is rather unsurprising. $W_{|n\rangle}$, however, displays some more interesting behaviour. First of all, it has negative values. This is part of the reason that the P, Q and Wigner functions are called *quasi*-probability distributions, because it is nonsensical to speak of an event having a negative probability. Furthermore some of these functions take on values at certain points, which are more singular than delta functions. The interpretation of these functions as probability distributions is therefore limited. Negatively, or singularly, valued quasi-probability distributions are a sign of non-classicality which will be further discussed in section 4.1.

The Wigner functions also relate back to the quadrature diagrams. If we take a planar slice through the Wigner distribution of a vacuum or coherent state, we get circles which correspond nicely with the quadrature diagrams for these states. Likewise, for the number states, we get a ring centred on the origin, at a distance corresponding to the root of photon number.

1.3.5 The Squeezed States

I will now move on to a very interesting and beneficial state: the squeezed state. We have seen in our discussion of the quadrature diagrams that there is some area of uncertainty for a quantum-mechanical light field. The minimum areas are determined by the appropriate Heisenberg uncertainty relations. However, only the *total area* must be maintained, the uncertainty relations make no demands on the *shape* the uncertainty may take in quadrature space. So, we may squeeze the uncertainty in one direction – more closely defining, say, the canonical momentum – at the cost of making the canonical position less certain. We can graphically represent this with the example of a squeezed vacuum state $|\xi\rangle$ in Figure 4.

I will write down, without proof or derivation, the operator that mathematically squeezes a quantum state

$$\hat{S}(\xi) = \exp\left[\frac{1}{2}\left(\xi^*\hat{a}^2 - \xi\hat{a}^{\dagger 2}\right)\right]. \tag{32}$$

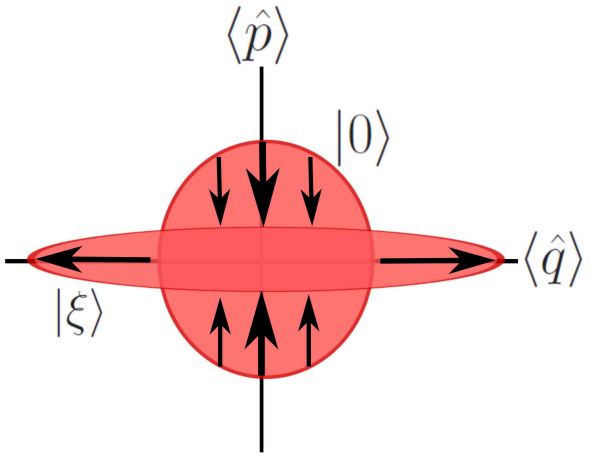

Figure 4: A squeezed vacuum state. We have increased our knowledge about the canonical momentum by decreasing our knowledge of the canonical position.

Where ξ is known as the squeezing parameter and quantifies the amount of squeezing. Acting on a mode operator this produces

$$\begin{aligned}\hat{S}^\dagger(\xi)\hat{a}\hat{S}(\xi) &= \hat{a}\cosh(r) - \hat{a}^\dagger e^{i\theta}\sinh(r),\\ \hat{S}^\dagger(\xi)\hat{a}^\dagger\hat{S}(\xi) &= \hat{a}^\dagger\cosh(r) - \hat{a}e^{-i\theta}\sinh(r),\end{aligned}$$

where we have used the polar decomposition $\xi = re^{i\theta}$. Equivalently we can have the squeezing operator acting on a state. Here the vacuum,

$$\hat{S}(\xi)|0\rangle \equiv |\xi\rangle = \frac{1}{\sqrt{\cosh(r)}}\sum_{n=0}^{\infty}(-1)^n\frac{\sqrt{(2n)!}}{2^n n!}e^{in\theta}[\tanh(r)]^n|2n\rangle.$$

Apparently squeezed vacuum states can only have an even number of photons. The reason for this will be explained in the next section. Figure 5 is a plot of a squeezed vacuum state in quadrature space.

This diagram demonstrates how a squeezing operator with a specific r and θ act on a vacuum state. The circular vacuum state is transformed into an ellipse, the major axis of which is rotated relative to the $\langle\hat{q}\rangle$ axis by θ. So squeezed vacuum states, unlike regular vacuum states, have definable phases. Recall that the uncertainties in the quadratures $\Delta\hat{X}_1$ and $\Delta\hat{X}_2$ for a vacuum state were calculated to be $1/2$ each. Now we find, for the squeezed vacuum, that these uncertainties have been multiplied by the factors e^r and e^{-r} respectively. Note that $\langle\hat{X}_1\rangle$ and $\langle\hat{X}_2\rangle$ are not the quadratures that define the diagram but the ones in the frame of reference of the squeezing. That is they constitute a coordinate system rotated from $\langle\hat{q}\rangle$ and $\langle\hat{p}\rangle$ by the angle θ.

There is another interesting revelation to be made about the squeezed vacuum. If we take the expectation value of the number operator with respect to the vacuum state

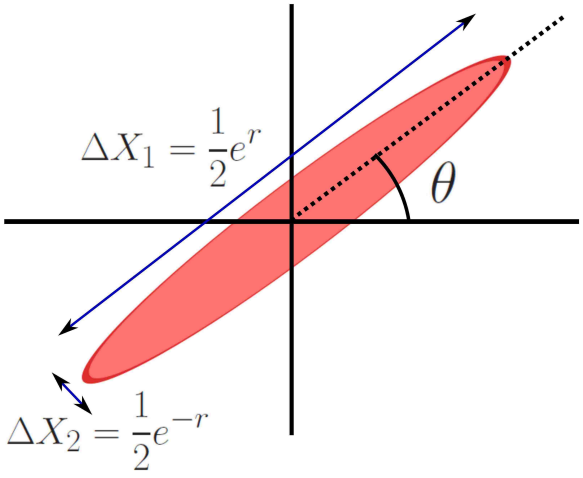

Figure 5: The circular vacuum state is transformed into an ellipse, the major axis of which is rotated relative to the $\langle\hat{q}\rangle$ axis by θ. The uncertainties in $\Delta\hat{X}_1$ and $\Delta\hat{X}_2$ have been multiplied by the factors e^r and e^{-r} respectively. Here $\langle\hat{X}_1\rangle$ and $\langle\hat{X}_2\rangle$ constitute a coordinate system rotated from $\langle\hat{q}\rangle$ and $\langle\hat{p}\rangle$ by the angle θ.

$$\begin{aligned}
\langle\xi|\hat{n}|\xi\rangle &= \langle 0|\hat{S}^\dagger(\xi)\hat{a}^\dagger\hat{a}\hat{S}(\xi)|0\rangle, \\
&= \langle 0|\hat{S}^\dagger(\xi)\hat{a}^\dagger\hat{S}(\xi)\hat{S}^\dagger(\xi)\hat{a}\hat{S}(\xi)|0\rangle, \\
&= \langle 0|\left\{\hat{a}^\dagger\cosh(r) - \hat{a}e^{-i\theta}\sinh(r)\right\}\left\{\hat{a}\cosh(r) - \hat{a}^\dagger e^{i\theta}\sinh(r)\right\}|0\rangle, \\
&= \sinh^2(r),
\end{aligned}$$

where in the second line we have used the fact (which I have not proven) that the squeezing operator is unitary, so we can insert $\hat{1}$ between $\hat{a}^\dagger$ and $\hat{a}$.[21] So not only does the squeezed vacuum state have phase but it also contains photons. Properly it should not be called a vacuum state at all, but it follows the same convention as calling the coherent state a displaced vacuum state.

Squeezed light apparently comes in packs of two. So far we have discussed the case of both photons of each pair existing in the same optical mode. It is possible to define a two-mode squeezed vacuum state where the photons exist in separate modes. The action of two-mode squeezing is represented by

$$\hat{S}_2(\xi) = \exp\left(\xi^*\hat{a}\hat{b} - \xi\hat{a}^\dagger\hat{b}^\dagger\right),$$

which transforms mode operators and the vacuum state by,

$$\hat{S}_2^\dagger(\xi)\hat{a}\hat{S}_2(\xi) = \hat{a}\cosh(r) - e^{i\theta}\hat{b}^\dagger\sinh(r),$$

[21] I chose to transform the operators instead of the states as working with the $|\xi\rangle$'s is usually incredibly onerous.

$$\begin{aligned}\hat{S}_2^\dagger(\xi)\hat{b}\hat{S}_2(\xi) &= \hat{b}\cosh(r) - e^{i\theta}\hat{a}^\dagger\sinh(r),\\ \hat{S}_2(\xi)|0,0\rangle \equiv |\xi_2\rangle &= \frac{1}{\cosh(r)}\sum_{n=0}^{\infty}(-1)^n e^{in\theta}[\tanh(r)]^n|n,n\rangle.\end{aligned}$$

Where $\hat{a}$ and $\hat{b}$ represent different (usually physical) modes, as do the two positions in the state vector.

The kind of squeezing we have discussed so far is known as quadrature squeezing. There exist other types of squeezing: such as number or phase. But, I will do no more than mention them in passing, as they have little bearing on this thesis. Furthermore it is possible to squeeze other states than the vacuum – most notably the coherent state. That particular kind of squeezed light will play a large part in this thesis and will be discussed at more length in section 4.2. Squeezed coherent states may be visualized in quadrature space as a vacuum state that has been first displaced than squeezed.[22] Mathematically, when dealing with this kind of light, it is most direct to squeeze the mode operators and take expectation values with respect to coherent states. Attempting to employ the equivalent description, of solving for the squeezed coherent states and using these to take expectation values, is the fever dream of a madman.

We have discussed at length the mathematical description of squeezing. The next section will be devoted to describing physically what squeezed light is, and the methods which are employed to generate it in a lab.

1.3.6 Generating Squeezed Light and Other States of Interest with Optical Nonlinearities

Linearity of light fields has been, up until this point, a tacit assumption. That is, when light fields spatially coincide their component electric (and magnetic) fields simply add as vectors. This is a fine assumption in free space, but inside of certain materials this condition is no longer met. Consider the expansion of the polarization of a general dielectric material

$$\frac{P_i}{\epsilon_o} = \sum_j \chi_{ij}^{(1)} E_j + \sum_{jk} \chi_{ijk}^{(2)} E_j E_k + \sum_{jkl} \chi_{ijkl}^{(3)} E_j E_k E_l + ...$$

The polarization P represents how a dielectric material reacts to the presence of electric fields. The index i runs over the three-dimensional vector components. The constant $\chi_{ij}^{(1)}$ is called the first order (or linear) susceptibility and it is a complex vector constant[23]; Likewise $\chi_{ijk}^{(2)}$ is the second order susceptibility (a tensor constant), and on and on in that manner. Most materials have only a non-negligible $\chi^{(1)}$. In this case as an electric field interacts with the material it induces an oscillating dipole moment, which in turn creates an oscillating electric field, and so on. Therefore the light propagates through the material with a dispersion and absorption determined by the real and imaginary parts of $\chi^{(1)}$, respectively.

[22] A state that has been first squeezed than displaced is not in general equivalent to one that has been first displaced than squeezed. Though they may be for specific cases.

[23] The vector nature of the constant takes into account that the material may not be symmetric, and that electric fields may propagate differently in different directions.

However, now consider the case where the other terms in this series are non-negligible. We will be interested in materials with a large $\chi^{(2)}$. Take an electric field that has two separate frequency components

$$E(t) = E_1 \left(e^{i\omega_1 t} + e^{-i\omega_1 t} \right) + E_2 \left(e^{i\omega_2 t} + e^{-i\omega_2 t} \right),$$

and input it into the second term of the polarization (ignoring the tensor nature of $\chi^{(2)}$)[24]

$$\begin{aligned} P^{(2)}(t) &= \epsilon_o \chi^{(2)} \left[E_1^2 \left(e^{2i\omega_1 t} + e^{-2i\omega_1 t} \right) + E_2^2 \left(e^{2i\omega_2 t} + e^{-2i\omega_2 t} \right) \right. \\ &\quad + 2E_1 E_2 \left(e^{i(\omega_1+\omega_2)t} + e^{-i(\omega_1+\omega_2 t)} \right) \\ &\quad \left. + 2E_1 E_2 \left(e^{i(\omega_1-\omega_2)t} + e^{-i(\omega_1-\omega_2 t)} \right) + 2E_1^2 + 2E_2^2 \right]. \end{aligned} \tag{33}$$

Where we have assumed that the electric amplitudes are real. Eq. (33) gives rise to several interesting phenomena, but we will be interested in the effect caused by the terms that oscillate as $\omega_1 - \omega_2$. This tells us that, given two light beams of different frequencies, a material with a large $\chi^{(2)}$ generates a new light beam at a frequency of $\omega_3 = \omega_1 - \omega_2$. This is called "difference frequency generation". Let's examine the level diagram for this process given in Figure 6.

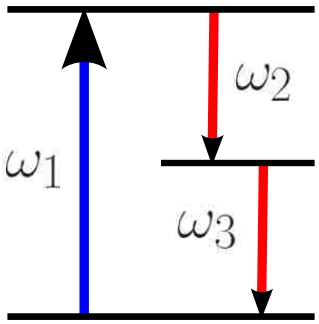

Figure 6: A level diagram for difference frequency generation for the case of $\omega_2 = \omega_3$. Some of the field at frequency ω_1 gets split into two fields at frequencies ω_2 and ω_3.

The graph is for the case of $\omega_2 = \omega_3$. Some of the field at frequency ω_1 gets split into two fields at frequencies ω_2 and ω_3.

Quantum mechanically the ω_2 mode need not be populated by photons (that is, it may be in the vacuum state) for the process to occur. In this case the interpretation is that a photon from a strong beam (called the pump) splits into two daughter photons inside the optical nonlinearity. If the two daughter photons are in the same spatial and spectral modes then we can write the interaction Hamiltonian for this process as

$$\hat{H}_I = i\hbar\chi^{(2)} \left(\hat{a}^2 \hat{b}^\dagger - \hat{a}^{\dagger 2} \hat{b} \right),$$

[24] i.e. assuming co-linearity.

where $\hat{b}$ represents the pump mode and $\hat{a}$ represents the mode of the daughter photons. The second term expresses one photon being transformed into two, the first term is present because the Hamiltonian must be Hermitian. Suppose the pump beam is in a coherent state (this is called the parametric approximation, meaning that the pump is *undepleted*: no photons are lost), then we can write for the daughter fields alone

$$\begin{aligned}\langle\beta|\hat{H}_I|\beta\rangle &= i\hbar\chi^{(2)}|\beta|\left(\hat{a}^2e^{i\omega_1 t}-\hat{a}^{\dagger 2}e^{-i\omega_1 t}\right),\\ &= i\hbar\chi^{(2)}|\beta|\left(\hat{a}^2e^{i(\omega_1-2\omega_2)t}-\hat{a}^{\dagger 2}e^{-i(\omega_1-2\omega_2)t}\right).\end{aligned}$$

Where in the second line the time dependence of $\hat{a}$ and $\hat{a}^\dagger$ has been made explicit. Recall though that we have chosen $\omega_1 = 2\omega_2$, so the Hamiltonian, is in fact time-independent and we can write the time evolution operator for the system simply as

$$\hat{U}(t) = e^{-i\hat{H}_I t/\hbar} = e^{\hbar\chi^{(2)}t|\beta|\left(\hat{a}^2-\hat{a}^{\dagger 2}\right)}.$$

Now compare this to Eq. (32) and we see that we have the single mode squeezing operator where $\xi = 2\hbar\chi^{(2)}t|\beta|$. Furthermore we could get two mode squeezing for the case where the daughter photons are not in the same modes. So we have a way to physically squeeze vacuum (and other) states.

Also, if we take $\hat{U}(t)$ acting on the vacuum and expand it as a power series

$$\hat{U}(t)|0\rangle = |0\rangle + \hbar\chi^{(2)}t|\beta||2\rangle + (\hbar\chi^{(2)}t|\beta|)^2|4\rangle + ...$$

For a coherent pump $|\beta|$ which is strong we can get several of these terms. In this case one pump photon can split into two (second term), two pump photons can combine and then split into four (third term) and so on. However if the pump is not very strong only the first two terms will be non-negligible. In this case we get spontaneous parametric down-conversion. Both of these processes are of great general use and will be discussed at length in this thesis.

The physical realization of a squeezed light source is a material with a large $\chi^{(2)}$ non-linearity, typically a noncentrosymmetric crystal, such as β-barium borate, pumped with a strong pulsed laser.

2 Quantum Lithography and Multiphoton Absorption

2.1 The Electric Brain and the World of Tomorrow

"Computers in the future may weigh no more than 1.5 tons."
-*Popular Mechanics* article from 1949

Computers have become such a ubiquitous and integrated part of daily life that it is unnecessary to extol their usefulness and power here. Sixty years ago, however, the coming information revolution was unforeseen. Rapid, disruptive advances in the ability to manufacture logic circuits made possible the information-steeped world we now live in.

The processing power of computers is proportional to the number of transistors that can be written on a chip. This quantity has been increasing exponentially in accordance with Moore's Law. This growth is facing a challenge though. It has been estimated by Intel^{TM} that by about 2018 the current program of increasing transistor density by continuing improvements in photolithography will no longer be tenable. This is due to the fact that the smallest feature that may be written on a chip is restricted by the Rayleigh diffraction limit. Which states that the smallest resolvable feature is on the order of the wavelength of the light used. As more and more energetic photons are used the optics become extremely difficult to make and operate. Eventually going to a yet higher energy regime will become intractable and progress will stall.

In order to avoid this it may be possible to fundamentally alter the method of lithography to work around the diffraction limit. We will discuss one such program: quantum lithography.

2.2 The Nature and Advantage of Quantum Lithography

With the technique of interferometric lithography the smallest feature size (s) which may be etched into a material is limited by the equation $s = \lambda/2$, where λ is the wavelength of the coherent (laser) light used.

The first attempt to circumvent this limit was the novel proposal by Yablonovitch and Vrijen who suggested that by taking advantage of two photon absorption in the photo-resist, and by using some optical techniques, the smallest feature size could be improved by a factor of two. [11]

Inspired both by this, and by the super-sensitive properties of entangled light, Boto et al. proposed a scheme in 2000 to use highly quantum mechanical[25] states of light to beat the Rayleigh diffraction limit. [2]

The premise is to use number states of the form

$$|\Psi\rangle_{ab} = \frac{|N\rangle_a|0\rangle_b + e^{iN\phi}|0\rangle_a|N\rangle_b}{\sqrt{2}},$$

where the subscripts a and b represent the two paths through the interferometer. This state is entangled because it can not be written as a product state such that $|\Psi\rangle_{ab} = |\psi\rangle_a|\psi\rangle_b$ and

[25] What it means to say that light is quantum vs. classical will be the topic of Section 4.1.

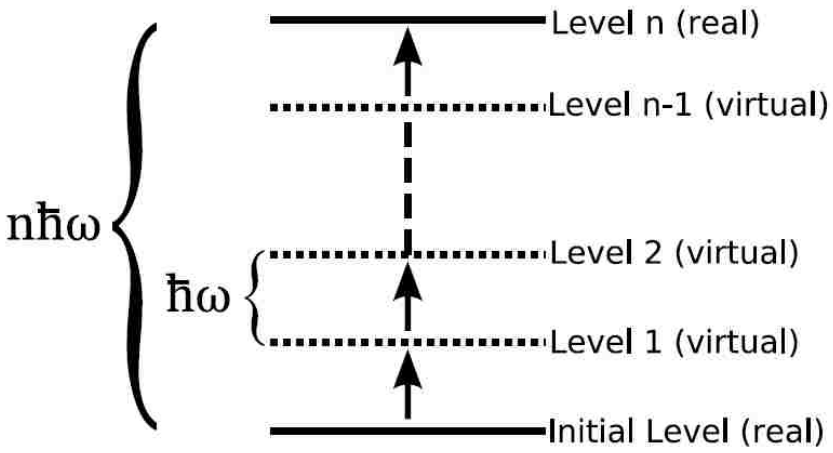

Figure 7: This diagram illustrates the general n-th order multiphoton absorption process.

also because they may be used to violate a Bell-inequality. [12] Not only is it entangled, but it is also maximally entangled. This terminology is applied when all the objects in the state are part of the entanglement, which is the case of the above state. $|\Psi\rangle$ is also commonly called a N00N state, after the way the state vector is written.

If these states were to be used in an interferometric-lithographic setup they would decrease the smallest resolvable object by a factor of N. Meaning that N^2 more features could be written on a chip, when compared to coherent light of the same wavelength.

2.3 Multiphoton Absorption and Its Relationship To Quantum Lithography

Critical to the quantum lithography scheme is that the photons from the N00N state arrive at the same place, at the same time, and be absorbed as one unit by the photo-resist. Quantitatively we would like the photons to have a high degree of both spatial and temporal correlation. Our objective in this chapter will be to study the multiphoton absorption properties of N00N states, but first a bit about the multiphoton absorption process itself.

A multiphoton absorption event is, in general, a n-th order process by which an atom (or other absorber) absorbs n photons while making only a single, real, level transition. Each photon posses a roughly proportionate fraction of the total energy required to make the full transition. The process is mediated by intermediate (or virtual) levels. See Fig.7. The physical interpretation of the virtual levels is that they are the levels in the atom (or other absorber) to which transitions would typically not be allowed. For example, in two photon absorption the electron first makes an energy non-conserving transition to a regularly inaccessible state, and then a second energy non-conserving transition to the final state. Although the individual transitions do not conserve energy the total process does. This behaviour is predicted by the second order term in the Dyson series, or in the general n-photon case the n-th order term in the Dyson series. For more detail see for example Ref.[21]. The n-th order quantum correlation function [13] arises from this formalism naturally as the main quantity of interest.

We do not consider the fact that multiphoton absorption events may be competing with lower order absorption. In the ideal case only the n-th order process will be resonant with a transition.

2.4 Characterizing and Improving the Multi-Photon Absorption Properties of Maximally Path Entangled Number States (N00N States)

In this section we investigate the multiphoton absorption probabilities of $N00N$ states: $|N :: 0\rangle \equiv (|N, 0\rangle + |0, N\rangle)/\sqrt{2}$. Again these states are of interest due to the fact that they greatly improve the resolution and sensitivity of interferometry for metrology. Also, as it has been shown, they would improve the resolution with which lithographic features may be written. We show that (monochromatic) N00N state absorption fares poorly as N increases, reinforcing through separate means a more sophisticated model presented in [14]. Thus when considering possible applications of these states, such as to quantum lithography [2, 15] or metrology [16, 17], we need to keep an eye towards maximizing these absorption rates by varying their spectral parameters. We do this knowing that it has been found that squeezed light can exhibit novel two photon absorption properties, such as linear growth of absorption rate with intensity and decreasing absorption, for increasing field [18, 19, 20].

We consider in detail the case of a $|2 :: 0\rangle$ state used in a quantum lithography or quantum metrology setup. We include spectral information and derive a general expression for the two-photon absorption probability. Then we numerically maximize the probability function and find the setup which maximizes the two-photon absorption. The absorption probability can be improved by several orders of magnitude by carefully adjusting the filter bandwidths, pump pulse length, and the length of the crystal. The absorption probability of $|2 :: 0\rangle$ is shown to be much better than analogous coherent light. Though the $|2 :: 0\rangle$ state would not be a desirable source for quantum lithography, our work shows that the absorption enhancement that the spectral properties of entangled light sources provide can compensate for their poor production rates. We go beyond most previous studies in that we obtain the two photon absorption probability directly, instead of only considering the second-order correlation function.

In section 2.4.1 we compare the absorption properties of ideal N00N states to other states of light. In section 2.4.2-2.4.7 we calculate the biphoton amplitude in the general case and then examine the absorption properties of this type of light in two regimes: the pulse-pumped, and the continuous-wave-pumped.

This chapter is based on my work with Drs. Anisimov, Dowling, and Wildfeuer.

2.4.1 Absorption Properties of Ideal N00N States

Initially one may consider the ideal N00N state: $|N :: 0\rangle$ [2]. This state contains no spectral information. It is an abstraction that can only exist in an optical cavity. Nonetheless it will provide some insight into how the absorption properties of N00N states compare to other sources.

Agarwal studied how multiphoton absorption rates are influenced by the specific properties of the incident light [22]. He found that the equation of motion for the field can be

written as

$$\frac{\partial\langle\hat{a}^\dagger\hat{a}\rangle}{\partial t} = -2n\lambda^{(n)}\langle\hat{a}^{\dagger n}\hat{a}^n\rangle.$$

Here, $\lambda^{(n)}$ is the absorption coefficient for the n-photon absorption process and contains information about the medium that is acting as the absorber, which is assumed to be much smaller spatially than the field (alternatively the field may be regarded as being spatially mode pure). Classically, n-photon absorption is proportional to n-th order intensity. Since we are comparing light sources of like intensities we make the substitution

$$\langle\hat{a}^{\dagger n}\hat{a}^n\rangle = r_n\langle\hat{a}^\dagger\hat{a}\rangle^n,$$

where r_n represents the degree to which the quantum statistical characteristics of the light affect the n-photon absorption. Now the rate of change of the field due to multiphoton absorption is equivalent to r_n and a factor of several constants. Collecting these constants into one factor κ and renaming r_n as the relative absorption rate R_n we arrive at

$$R_n = \kappa\frac{\langle\hat{a}^{\dagger n}\hat{a}^n\rangle}{\langle\hat{a}^\dagger\hat{a}\rangle^n},$$

where κ is some constant which we set to one in the interest of simplicity. We can use this information to produce a graph to see how the multi-photon absorption rate of N00N states scale with N, when compared to quantum states that are not path entangled such as thermal, number, and coherent.

Thermal states are described by the following density matrix

$$\hat{\rho}_{\text{thermal}} = \frac{1}{Z}\sum_{j=0}^{\infty} e^{-E_j/kT}|j\rangle\langle j|,$$
$$Z = \frac{e^{-\hbar\omega/2kT}}{1-e^{-\hbar\omega/kT}}, \quad E_j = \hbar\omega\left(j+\frac{1}{2}\right).$$

Obtaining the matrices for number, coherent, and N00N states is straightforward. For a two mode state the annihilation operator is given as $\hat{a} = 1/\sqrt{2}(\hat{a}_1 + \hat{a}_2)$ where one and two label the two paths the photon may take [2]. See Fig. 8. Thermal states clearly have the greatest rates of multiphoton absorption. This can be attributed to the fact that thermal states exhibit bunching. That is that photons from thermal radiation tend to be tightly correlated in time. Fock (number) states fare the worst. This feature of Fock states is connected to the fact that number states represent standing waves where the locations of the individual photons are evenly spaced out (or anti-bunched) in space and time with no definable phase. The multiphoton absorption properties of coherent states stay constant with respect to photon number. Since photons in coherent states are randomly dispersed in space and time the chance of two or more photons being correlated is simply proportional to

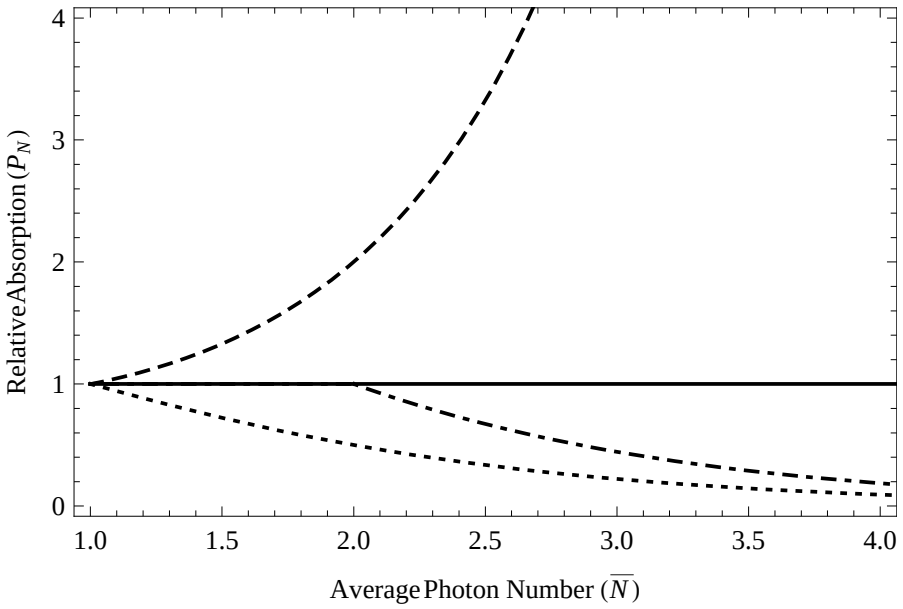

Figure 8: Multiphoton absorption rate of various sources as a function of the average number of photons in the field (N^{th} order absorption vs. $\bar{N}$ average photons). All rates normalized relative to coherent states (solid line). The dashed line is a thermal state. The dotted line is a Fock (number) state, and the dot-dashed line is a N00N state.

the intensity (average photon number). Since we are considering how n-photon absorption scales against average photon number, the graph is flat, providing a convenient measuring stick to gauge other fields.

For N00N states the multiphoton absorption behaves as

$$\begin{aligned} R_N &= 1 \qquad \text{for} \quad N = 1, \\ &= 2\frac{N!}{N^N} \quad \text{for} \quad N \geq 2, \end{aligned}$$

where κ has been set to one. N00N states fare a factor of two better than Fock states, although absorption rates are still far from optimal. The reason N00N sates have this factor of two is due to the path entanglement. Mathematically this two comes from the normalization constant that path entanglement requires.

These results seem to reinforce the findings of Tsang in Ref. [14]: generally the absorption properties of N00N states are poor. It should be re-emphasized that these states, containing no spectral or temporal information, are idealizations. Fig. 8 can only be seen as providing a rough idea of how absorption scales.

Quantum lithography or metrology will only be useful if the detector or material needs to be exposed to the field for a reasonable period of time. The above ideal-field results seem to make this unlikely. However, they show only that the quantum mechanical properties (i.e. the bare state vector) of N00N states lead to poor absorption rates. They say nothing about how the spectral properties of realistic N00N state pulses effect the multiphoton absorption probability. We thus examine in detail a specific well known case: the $|2::0\rangle$ state. Though

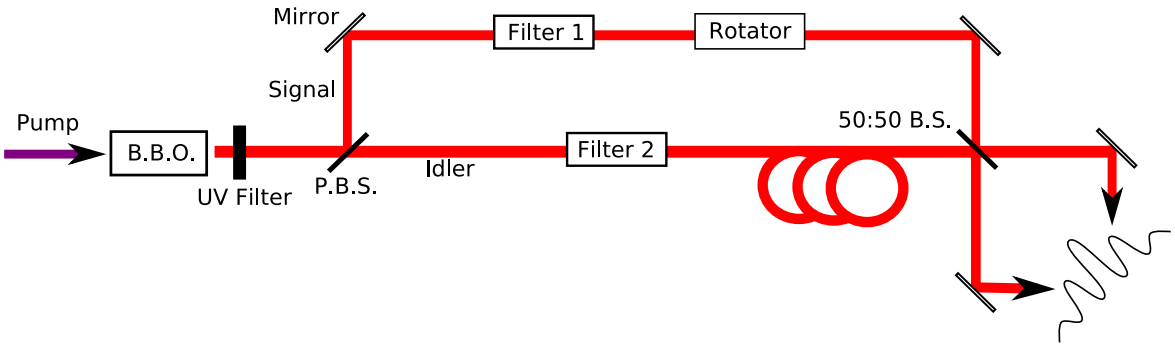

Figure 9: The basic setup. A nonlinear crystal (BBO in this case) creates a degenerate pair of photons. Each photon is subjected to a filter. A polarization rotator ensures that the two photons are indistinguishable. A beam splitter creates a $|2::0\rangle$ state that results in an interference pattern.

this state is not practical for metrology or lithography its optimization would provide a proof of principle that the absorption properties of higher N states could be improved in a similar manner.

2.4.2 Absorption Properties of Realistic $|2::0\rangle$ States

It is possible to write realistic states, which include the spectral information of the light of interest. Furthermore, after these states are used to obtain absorption rates, the arrangement of optical elements which optimizes absorption can be found.

Several works have examined how biphotons produced by parametric down conversion or electromagnetically induced transparency may be compressed or otherwise modified so that they exhibit tighter correlations [23, 24, 25, 26, 27, 28]. There is an excellent paper by Dayan which studies the properties of a semi-stationary, undepleted beam of squeezed light produced by a spectrally narrow pump [29]. Also worthy of particular note is a paper by O'Donnell and U'Ren which demonstrates experimentally the ultrafast nonclassical correlation between entangled photons [30].

We consider the case of a $|2::0\rangle$ state used in a quantum lithography [2, 15] or remote quantum metrology [16, 17] setup. The $|2::0\rangle$ state we investigate is produced by co-linear type II degenerate down conversion and a beam splitter (see Fig. 9). This setup is very simple, but by tuning these few basic optical elements we can see a large improvement in two photon absorption rates, without recourse to exotic techniques. We make no assumptions about stationarity or about the relative sizes of the field bandwidths (apart from one very broadly applicable assumption – that the field's bandwidth is narrower than the atomic transition frequencies; which will be discussed further).

2.4.3 The Type-II Biphoton

The output state of the crystal during type-II down conversion is described by Ref. [31]

$$|\Psi\rangle = C\sum_{kk'}\int_0^\infty d\omega_p \int_0^L dz e^{-\mathcal{D}\left(\frac{\omega_p-\Omega_p}{\sigma_p}\right)^2} e^{iz\Delta_{kk'}}\delta(\omega_{ok}+\omega_{ek'}-\omega_p)\hat{a}^\dagger_{ok}\hat{b}^\dagger_{ek'}|0\rangle_o|0\rangle_e \tag{34}$$

for a co-linear pump. The sum extends over all possible wavevector modes. A polarizing beam splitter separates the ordinary and extraordinary beams into different spatial modes. The operators $\hat{a}$ and $\hat{b}$ represent these modes. The object $\Delta_{kk'}$ is the phase mismatch, defined: $k_p - k - k'$, ω_p is the frequency of the pump laser, and the z integral extends over the length of the crystal. Also, Ω_p and σ_p are the central frequency and the spectral FWHM of the pump, respectively. Also, e and o label the extraordinary and ordinary beams. The factor $\mathcal{D}$ is defined as $4\ln(2)$. We are assuming the pump laser is Fourier-transform-limited.

This state corresponds to squeezing just above threshold, such that mainly $|0,0\rangle$ and $|1,1\rangle$ are produced. The $|0,0\rangle$ term is then dropped because it can not effect the two photon absorption process.

Since the two beams are distinguishable after the polarizing beam splitter, one of the beams must be subject to a polarization rotator in order for it to be made indistinguishable from the other. The beams must be indistinguishable so that the $|1,1\rangle$ states interfere destructively and produce $|2::0\rangle$ [32].

To study the two photon absorption probability of this state we utilize the well confirmed [33][34] Eqs. (2.15) and (2.16) from Mollow [35]

$$P_2 = \int\int d\omega' d\omega g^*(\omega') S^{(2)}(\omega_f - \omega', \omega'; \omega_f - \omega, \omega) g(\omega). \tag{35}$$

Where $g(\omega)$ is the atomic response function, ω_f is the frequency of the final state, and $S^{(2)}$ is the spectral correlation function (the Fourier transform of the temporal correlation function), which in our case is

$$S^{(2)}(\omega_1', \omega_2'; \omega_1, \omega_2) = \mathcal{Z}(\omega_1', \omega_2')^* \mathcal{Z}(\omega_1, \omega_2), \tag{36}$$

where,

$$\mathcal{Z}(\omega_1, \omega_2) \equiv \int\int dt_1^d dt_2^d e^{i\omega_1 t_1^d} e^{i\omega_2 t_2^d} A(t_1^d, t_2^d).$$

Here, ω_1' and ω_2' represent the negative frequency components of the field associated with ${t_1'}^d$ and ${t_2'}^d$. The factors ω_1 and ω_2 represent the positive frequency components of the field associated with ${t_1}^d$ and ${t_2}^d$. The above equation does not include the effects of natural linewidth, which will be discussed later. We should note that other equations, also derived by Mollow [35], assume that the field is stationary, something which is not true in general for our calculation here. A is the biphoton amplitude, defined below.

We start with the two-photon correlation function [13]

$$G^{(2)} = \langle\Psi|\hat{E}^{(-)}({t_1'}^d)\hat{E}^{(-)}({t_2'}^d)\hat{E}^{(+)}({t_1}^d)\hat{E}^{(+)}({t_2}^d)|\Psi\rangle. \tag{37}$$

The primed and unprimed time variables represent the possibility of the biphoton travelling via two different paths of different lengths, as is the case in an interferometric setup, and d labels the times as being detection times. $\hat{E}^{(+)}(t)$ is the positive-frequency electric field operator defined by

$$\hat{E}^{(+)}({t_j}^d) = i \sum_{s_j k_j} \left(\frac{\hbar \omega_{k_j}}{2\epsilon_0 V} \right)^{1/2} e^{-\mathcal{D}\left(\frac{\omega_{k_j} - \Omega_f}{\sigma_f}\right)^2} e^{-i\omega_{k_j} {t_j}^d} \hat{a}_{s_j k_j}(0). \tag{38}$$

Where the approximation $e^{\pm i\mathbf{k}\cdot\mathbf{r}} \approx 1$ has been made and s denotes either horizontal or vertical polarization. The time $t^d = 0$ is defined as the time the photon is created. Note that $\hat{E}^{(+)\dagger} = \hat{E}^{(-)}$. Also, Ω_f and σ_f are the central frequency and the FWHM of the filter in a specific arm, respectively.

Now, by inserting a complete set of number states in the correlation function, and observing that all but the $|0\rangle\langle 0|$ term will cancel, we can rewrite Eq. (37) as

$$G^{(2)} = \langle \Psi | \hat{E}^{(-)}({t_1'}^d) \hat{E}^{(-)}({t_2'}^d) |0\rangle\langle 0| \hat{E}^{(+)}({t_1}^d) \hat{E}^{(+)}({t_2}^d) | \Psi \rangle \equiv A({t_1'}^d, {t_2'}^d)^* A({t_1}^d, {t_2}^d).$$

The above equation defines the biphoton amplitude $A({t_1}^d, {t_2}^d)$. The expressions for A for SPDC were first calculated by Keller and Rubin in Ref. [36] and elaborated upon in Refs.[37, 38, 39]. We follow their calculations somewhat closely.

We start with a field at the detector, given by Eq. (38). Using the standard 50:50 beam splitter transformation we write out the electric field operator at the crystal

$$E^{(+)}(t^d) = \xi \sum_{k_1} \left(e^{-\mathcal{D}\frac{\omega_{k_1}^2}{\sigma_o^2}} \hat{a}_{k_1} + i e^{-\mathcal{D}\frac{\omega_{k_1}^2}{\sigma_e^2}} \hat{b}_{k_1} \right) \frac{e^{-i\omega_1 \tau}}{\sqrt{2}} + \xi \sum_{k_2} \left(i e^{-\mathcal{D}\frac{\omega_{k_2}^2}{\sigma_o^2}} \hat{a}_{k_2} + e^{-\mathcal{D}\frac{\omega_{k_2}^2}{\sigma_e^2}} \hat{b}_{k_2} \right) \frac{e^{-i\omega_2 \tau}}{\sqrt{2}},$$

where constants have been subsumed into the overall factor of ξ. The polynomials ω_{k_j} have been ignored because they vary slowly when compared to the exponential terms. The operators $\hat{a}$ and $\hat{b}$ are the annihilation operators acting on the first and second modes. The two mode annihilation operators are used to signify that the amplitude is dependent on the fields in both spatial modes. $\tau = t^d - l/c$ where l is the distance between the crystal and the detector. We only consider the case where the interferometer is path balanced. This implies we calculate the absorption properties of the central fringe. We assume that the absorption properties of the other fringes will behave similarly.

Now using the above and Eqs. (34, 37) we can find an expression for the biphoton amplitude of our setup

$$A({t_1}^d, {t_2}^d) = \mathcal{A}({t_1}^d, {t_2}^d) + \mathcal{A}({t_2}^d, {t_1}^d) \tag{39}$$

where $\mathcal{A}$ is the biphoton amplitude for just the output of BBO and filters

$$\mathcal{A}({t_1}^d, {t_2}^d) = iC\xi^2 \sum_{k_o k_e} e^{-\mathcal{D}\left(\frac{\omega_{k_o} - \Omega_o}{\sigma_o}\right)^2} e^{-i\omega_{k_o} {t_1}^d} e^{-\mathcal{D}\left(\frac{\omega_{k_e} - \Omega_e}{\sigma_e}\right)^2} e^{-i\omega_{k_e} {t_2}^d} \int_0^L dz e^{-\mathcal{D}\left(\frac{\omega_{k_o} + \omega_{k_e} - \Omega_p}{\sigma_p}\right)^2} e^{iz\Delta_{k_o k_e}}.$$

We have dropped the factor of $e^{-il/c}$ as it just introduces an overall phase. The central frequencies of the filters have been chosen to be the same as for the e and o rays.

Now, define the following variables,

$$\begin{aligned}\nu_o &\equiv \omega_o - \Omega_o,\\ \nu_e &\equiv \omega_e - \Omega_e,\\ \nu_p &\equiv \omega_p - \Omega_p.\end{aligned} \tag{40}$$

Due to the delta function in Eq. (34), $\Omega_o + \Omega_e = \Omega_p$ and $\nu_o + \nu_e = \nu_p$. Now, Taylor-series expand the wavevector out to second order

$$k(\nu_j) = k(\Omega_j) + \nu_j \left[\frac{dk(\nu_j)}{d\omega_j}\right]_{\omega_j=\Omega_j} = k(\Omega_j) + \frac{\nu_j}{U_j(\Omega_j)}.$$

Where $j = e, o, p$ and U is the group velocity, and $U = d\omega/dk$. Taking into account that $k_p(\Omega_p) = k_e(\Omega_e) + k_o(\Omega_o)$, the phase mismatch can now be rewritten as

$$\Delta_{k_o k_e} = \frac{\nu_p}{U_p(\Omega_p)} - \frac{\nu_o}{U_o(\Omega_o)} - \frac{\nu_e}{U_e(\Omega_e)} = \frac{\nu_o + \nu_e}{U_p(\Omega_p)} - \frac{\nu_o}{U_o(\Omega_o)} - \frac{\nu_e}{U_e(\Omega_e)}. \tag{41}$$

Taking the continuous limit of Eq. (39) and utilizing Eqs. (40) and (41) we obtain

$$\begin{aligned}\mathcal{A}({t_1}^d, {t_2}^d) &= iC\xi^2 \int dk_o \int dk_e \int_0^L dz e^{-\mathcal{D}\left(\frac{\nu_o}{\sigma_o}\right)^2} e^{-\mathcal{D}\left(\frac{\nu_e}{\sigma_e}\right)^2}\\ &\quad \times e^{-i(\nu_e+\Omega_e){t_2}^d} e^{-i(\nu_o+\Omega_o){t_1}^d} e^{-\mathcal{D}\left(\frac{\nu_o+\nu_e}{\sigma_p}\right)^2} e^{iz(u_e\nu_e + u_o\nu_o)}.\end{aligned}$$

Where $u_e = \frac{1}{U_p} - \frac{1}{U_e}$ and $u_o = \frac{1}{U_p} - \frac{1}{U_o}$. Note that $dk = \frac{dk}{d\omega}d\omega = \frac{1}{U}d\omega = \frac{1}{U}d\nu$, so that up to a constant we may switch integration variables between momentum and frequency. (Actually the U's are frequency dependent, however they do not vary significantly over the bandwidth of the field.) Here we diverge from Kim and Shih in that we integrate over ν_o and ν_e instead of $\nu_- \equiv \nu_o - \nu_e$, and ν_p and we do not take the filter bandwidths to be equivalent. Now

$$\begin{aligned}\mathcal{A}({t_1}^d, {t_2}^d) &= \frac{iC\xi^2}{U_e U_o} e^{-i(\Omega_o {t_1}^d + \Omega_e {t_2}^d)} \int d\nu_o \int d\nu_e \int_0^L dz e^{-\mathcal{D}\left(\frac{\nu_o}{\sigma_o}\right)^2} e^{-\mathcal{D}\left(\frac{\nu_e}{\sigma_e}\right)^2}\\ &\quad \times e^{-i\nu_e {t_2}^d} e^{-i\nu_o {t_1}^d} e^{-\mathcal{D}\left(\frac{\nu_o+\nu_e}{\sigma_p}\right)^2} e^{iz(u_e\nu_e + u_o\nu_o)}.\end{aligned}$$

We have the unitary Fourier transform over ν_o, ν_e (up to a factor of $\sqrt{2\pi}$), and the integral over z given by

$$\begin{aligned}\mathcal{A}({t_1}^d, {t_2}^d) &= \frac{2\pi iC\xi^2}{U_e U_o} e^{-i(\Omega_o {t_1}^d + \Omega_e {t_2}^d)} \int_0^L dz \hat{\mathcal{F}}(\nu_e \to {t_2}^d) \hat{\mathcal{F}}(\nu_o \to {t_1}^d) \Upsilon(\nu_o, \nu_e, z),\\ \Upsilon(\nu_o, \nu_e, z) &= e^{-\mathcal{D}\left[\left(\frac{\nu_o+\nu_e}{\sigma_p}\right)^2 + \left(\frac{\nu_o}{\sigma_o}\right)^2 + \left(\frac{\nu_e}{\sigma_e}\right)^2\right]} e^{iz(u_e\nu_e + u_o\nu_o)}.\end{aligned} \tag{42}$$

Where we have defined the biphoton kernel $\Upsilon(\nu_o, \nu_e, z)$. In the interest of clarity, the Fourier transforms have been written as operators

$$\hat{\mathcal{F}}(x \to y) \equiv \frac{1}{\sqrt{2\pi}} \int_{-\infty}^{\infty} dx e^{-ixy}$$

Using Mathematica$^{\text{TM}}$, we perform these operations in the above order. Note that another ordering will lead to the problem becoming intractable. The result is given by Eq.(43). For the sake of simplicity in most of our calculations we will take $\xi = 1$.

$$\mathcal{A}({t_1}^d, {t_2}^d) = e^{-i(\Omega_e {t_2}^d + \Omega_o {t_1}^d)} e^{-\frac{({t_1}^d O_U \sigma_o + {t_2}^d E_U \sigma_e)^2}{4\mathcal{D}U^2}} \frac{U_e U_o U_p \sigma_e \sigma_o \sigma_p}{U\sqrt{\mathcal{D}}} \left[\text{Erf}(\mathcal{T}) - \text{Erf}(\mathcal{T} + l)\right]. \quad (43)$$

Where

$$\begin{aligned} \mathcal{T} &= \frac{({t_1}^d - {t_2}^d) P_U \sigma_e \sigma_o + {t_1}^d E_U \sigma_o \sigma_p - {t_2}^d O_U \sigma_e \sigma_p}{2U\sqrt{\mathcal{D}({\sigma_e}^2 + {\sigma_o}^2 + {\sigma_p}^2)}} \\ l &= \frac{LU}{2U_e U_o U_p \sqrt{\mathcal{D}({\sigma_e}^2 + {\sigma_o}^2 + {\sigma_p}^2)}}. \end{aligned}$$

And

$$\begin{aligned} P_U = U_p(U_e - U_o)\sigma_e\sigma_o, \quad E_U = U_e(U_p - U_o)\sigma_p\sigma_o \\ O_U = U_o(U_e - U_p)\sigma_e\sigma_p, \quad U^2 = {P_U}^2 + {E_U}^2 + {O_U}^2. \end{aligned}$$

The error function is commonly defined as

$$\text{Erf}(x) = \frac{2}{\sqrt{\pi}} \int_0^x dy e^{-y^2}.$$

The terms U_e, U_o, and U_p represent the group velocities of the extraordinary, ordinary, and pump beams, respectively. The factors σ_e and σ_o are the bandwidths of the filters in the arms of the interferometer. The term σ_p is the bandwidth of the pump. The factors Ω_e and Ω_o are the central frequencies of the extraordinary and ordinary beams. For now the normalization constant has been left off for the sake of simplicity as it will only effect the height of the amplitude, not its overall shape.

Hence we give the general biphoton amplitude in its most general form, which is a new result.

In order to evaluate this expression we must find the group velocities of the pump, ordinary and extraordinary beams inside of the $\chi^{(2)}$ crystal. The index of refraction as a function of wavelength can be found using the Sellmeier equations. Below are the Sellmeier equations for β-Barium Borate (BBO) [40]

$$
\begin{aligned}
n_o(\lambda_o) &= \sqrt{2.7359 + \frac{0.01878}{\lambda_o^2 - 0.01822} - 0.0135\lambda_o^2}, \\
n_e(\lambda_e) &= \sqrt{2.3753 + \frac{0.01224}{\lambda_e^2 - 0.01667} - 0.01516\lambda_e^2},
\end{aligned}
$$

where the wavelength is given in micro-meters. In type-II down conversion in BBO the pump beam experiences the same index of refraction as the extraordinary beam. It is also important to consider the angle the beams form with respect to the optical axis of the crystal. Since we are investigating the degenerate co-linear case with planar phase matching the optical axis must be set to be 42.4° off the pump beam's direction of propagation for a 400nm pump (the ordinary and extraordinary beams are co-linear with the pump and selected with a pinhole downstream) [38]. For the pump and extraordinary beams we must use the effective index of refraction, given by

$$
n^{\text{eff}}(\lambda_e, \phi) = \left[\frac{\cos^2(\phi)}{n_o^2(\lambda)} + \frac{\sin^2(\phi)}{n_e^2(\lambda)} \right]^{-\frac{1}{2}},
$$

where ϕ is the angle between the beam and the optic axis of the crystal. We can now calculate the group velocity

$$
U_{e,o,p}(\lambda_{e,o,p}) = \left(\frac{n^{\text{eff}}_{e,o,e}(\lambda_{e,o,p})}{c} - \frac{\lambda_{e,o,p}}{c} \frac{\partial n^{\text{eff}}_{e,o,e}(\lambda_{e,o,p})}{\partial \lambda_{e,o,p}} \right)^{-1}.
$$

And $n_o^{\text{eff}} = n_o$. We then find for the degenerate case ($\Omega_o = \Omega_e$) for $\lambda_p = 400$nm that $U_o(\Omega_o) = 1.781 \times 10^8$m/s, $U_p(\Omega_p) = 1.756 \times 10^8$m/s and $U_e(\Omega_e) = 1.845 \times 10^8$m/s.

Fig. 10 contains a contour plot of the absolute value of the biphoton amplitude for our setup (A). This graph displays an interesting splitting which is symmetric about a line given by $t_1^d - t_2^d = 0$. Each point on this line represents a different average arrival time of the biphoton $(t_1^d + t_2^d)/2$, a line drawn perpendicular to this line of symmetry represents another axis. That axis defines an entanglement time (the temporal distance between the two photons) as $t_1^d - t_2^d$. The symmetric splitting represents the fact that two photons generated far away from the exit-surface of the crystal will drift apart in time. Thus, as the average arrival time increases (a delay being indicative of more time spent in the crystal) the photons drift apart. The symmetry is a result of the interferometer scrambling the information corresponding to which photon took which path. So for a set average arrival time there is an equal probability that the e photon will arrive first or that the o one will.

We can check Eq. (43) by taking limits and comparing to known formulae. Taking the limit of the biphoton amplitude as σ_o and σ_e go to infinity (the case of no filtering) and keeping in mind that one of the definitions of the Heaviside step function is,

$$
H(x) = \lim_{k \to \infty} \frac{1}{2} \left(1 + \text{Erf}(kx)\right). \tag{44}
$$

Figure 10: Contour plot of the absolute value of the biphoton amplitude for our setup $|A|$. $\sigma_e = \sigma_o = \sigma_p = 10^{13}$Hz and $L = 1.5$cm. t_1^d and t_2^d are in units of 10^{-13}sec

We are left with

$$\mathcal{A}({t_1}^d, {t_2}^d) \;=\; e^{-\sigma_p^2 J}\left[2H\left(A-\frac{B}{2}\right)-2H\left(A+\frac{B}{2}\right)\right],$$

where

$$\begin{aligned} A &= \frac{(t_1^d - t_2^d)U_eU_o + \frac{1}{2}L(U_e-U_o)}{2U_eU_o\sqrt{\mathcal{D}}}, \\ B &= \frac{L(U_e-U_o)}{2U_eU_o\sqrt{\mathcal{D}}}, \\ J &= \frac{\left[t_1^dU_o(U_e-U_p)+t_2^dU_e(U_p-U_o)\right]^2}{\sqrt{\mathcal{D}}(U_e-U_o)^2U_p^2}. \end{aligned}$$

Utilizing the identity

$$\text{Rect}\left(\frac{x}{\tau}\right) = H\left(x+\frac{\tau}{2}\right) - H\left(x-\frac{\tau}{2}\right),$$

where

$$\mathrm{Rect}(x) = \begin{cases} 0 & \text{if} \quad |x| > 0.5, \\ \frac{1}{2} & \text{if} \quad |x| = 0.5, \\ 1 & \text{if} \quad |x| < 0.5. \end{cases}$$

we obtain the expression

$$\mathcal{A}({t_1}^d, {t_2}^d) = -2e^{-\sigma_p^2 J}\mathrm{Rect}\left(\frac{A}{B}\right),$$

which is equivalent to the expression given by Kim, et al., in Ref. [38].

Eq. (35) given together with Eq. (42) gives all the necessary information for calculating the two-photon absorption probability for N00N states of $N = 2$. First note that Eq. (36) represents a unitary transform back from time space into frequency space we may write the $\mathcal{Z}$ function as

$$\mathcal{Z}(\omega_o, \omega_e) = 2\pi\hat{\mathcal{F}}({t_1}^d \to \omega_o)^*\hat{\mathcal{F}}({t_2}^d \to \omega_e)^* A({t_1}^d, {t_2}^d).$$

Therefore

$$\begin{aligned}
\mathcal{Z} &= 2\pi\hat{\mathcal{F}}({t_1}^d \to \omega_o)^*\hat{\mathcal{F}}({t_2}^d \to \omega_e)^* A({t_1}^d, {t_2}^d) \\
&= 2\pi\hat{\mathcal{F}}({t_1}^d \to \omega_o)^*\hat{\mathcal{F}}({t_2}^d \to \omega_e)^* \mathcal{A}({t_1}^d, {t_2}^d) + 2\pi\hat{\mathcal{F}}({t_1}^d \to \omega_o)^*\hat{\mathcal{F}}({t_2}^d \to \omega_e)^* \mathcal{A}({t_2}^d, {t_1}^d) \\
&= C'\hat{\mathcal{F}}({t_1}^d \to \omega_o)^*\hat{\mathcal{F}}({t_2}^d \to \omega_e)^* e^{-i(\Omega_o {t_1}^d + \Omega_e {t_2}^d)} \int_0^L dz \hat{\mathcal{F}}(\nu_e \to {t_2}^d)\hat{\mathcal{F}}(\nu_o \to {t_1}^d)\Upsilon(\nu_o, \nu_e, z) \\
&\quad + C'\hat{\mathcal{F}}({t_1}^d \to \omega_o)^*\hat{\mathcal{F}}({t_2}^d \to \omega_e)^* e^{-i(\Omega_o {t_2}^d + \Omega_e {t_1}^d)} \int_0^L dz \hat{\mathcal{F}}(\nu_e \to {t_1}^d)\hat{\mathcal{F}}(\nu_o \to {t_2}^d)\Upsilon(\nu_o, \nu_e, z) \\
&= C' \int_0^L dz \hat{\mathcal{F}}({t_2}^d \to \nu_e)^*\hat{\mathcal{F}}(\nu_e \to {t_2}^d)\hat{\mathcal{F}}({t_1}^d \to \nu_o)^*\hat{\mathcal{F}}(\nu_o \to {t_1}^d)\Upsilon(\nu_o, \nu_e, z) \\
&\quad + C' \int_0^L dz \hat{\mathcal{F}}({t_1}^d \to \nu_o)^*\hat{\mathcal{F}}(\nu_e \to {t_1}^d)\hat{\mathcal{F}}({t_2}^d \to \nu_e)^*\hat{\mathcal{F}}(\nu_o \to {t_2}^d)\Upsilon(\nu_o, \nu_e, z) \\
&= C' \int_0^L dz \Upsilon(\nu_o, \nu_e, z) + C' \int_0^L dz \Upsilon(\nu_e, \nu_o, z). \qquad (45)
\end{aligned}$$

In the second equality we have made a substitution using Eq. (39). In the third equality Eq.(42) was used. In the fourth equality the overall phases have combined with the Fourier transform operators to change their output variables. So the Fourier transforms from the biphoton amplitude exactly cancel with the Fourier transforms from the definition of the spectral correlation function, leaving a relatively simple result. Note that $\Upsilon(\nu_o, \nu_e, z) \neq \Upsilon(\nu_e, \nu_o, z)$. And

$$C' = 2\pi i(8\pi\mathcal{D})^{\frac{1}{4}}\sqrt{\frac{U_2}{L\sigma_p}},$$

where U_2 is as defined previously. Returning to Eq. (35) we make the assumption that $g(\omega) \approx g(\frac{1}{2}\Omega_p)$. To see why, we need to investigate the definition of the atomic response function, Eq. (3.8) from Mollow [35]

$$g(\omega) = \mu \sum_j p_{fj} p_{j0} \frac{1}{\omega - \omega_j + \frac{1}{2} i\kappa_j}.$$

Where μ is a constant representative of the absorber, j labels the possible intermediate (virtual) levels, p_{j0} and p_{fj} are the momentum matrix elements of the electron making a transition between the initial and jth states, and the jth and final states respectively. The constant κ_j is the linewidth of the intermediate level. Each term in the series represents the two-photon absorption process proceeding via a different intermediate level transition. We assume that the central frequency of the field is one half the resonant frequency of the final state. Note that each term of g is highly peaked around the characteristic frequency of the level, which will be far detuned from the central frequency of the field. Unless the bandwidth of the field is on the order of the transition frequency, the value of the atomic response function will not change much as ω is varied over the bandwidth of the incident light. Therefore our assumption is justified. Note that this is the *only* assumption we make about bandwidths in this paper. It is worth noting that there has been much work done towards engineering materials that have large two photon cross sections [43, 44], so as light sources are improving, so are absorbers.

So, using Eq. (45) and Eq. (35) we have

$$P_2 = \left| C' g\left(\frac{1}{2}\Omega_p\right) \int_{-\infty}^{\infty} d\nu \int_{-\infty}^{\infty} dz \left[\Upsilon(\nu_f - \nu, \nu, z) + \Upsilon(\nu, \nu_f - \nu, z)\right] \right|^2. \tag{46}$$

The importance of the atomic response function being separated from the integral should be noted. Essentially this means that the spectral properties of the light may be considered apart from the structure of the absorber. The remaining integral is not difficult to perform

$$\int_0^L dz \int_{-\infty}^{\infty} d\nu \Upsilon(\nu_f - \nu, \nu, z) = \frac{\pi}{U_2} e^{-\mathcal{D}{\nu_p}^2 \left(\frac{(u_e + U_2)^2}{\sigma_e^2 U_2^2} + \frac{u_e^2}{\sigma_o^2 U_2^2} + \frac{1}{\sigma_p^2} \right)} \left[\mathrm{Erf}\left(\mathcal{E}\nu_p\right) - \mathrm{Erf}\left(\mathcal{E}\nu_p - \mathcal{L}\right) \right].$$

Where U_2, u_e, $\mathcal{E}$, and $\mathcal{L}$ are defined in the main text in Eq. (48). The integral over $\Upsilon(\nu, \nu_f - \nu, z)$ differs only by a constant factor.

However, the utility of this expression is limited. It only describes the probability of a single frequency from the pump beam being absorbed. Furthermore it implies that this frequency will be on resonant with the final level. Realistically, all frequencies will have a chance to be absorbed, and only $\nu_f = 0$ will be resonant. To correct for this we can average the function over a Lorentzian line shape with its peak at $\nu_f = 0$ and a height of 1.

Furthermore we must solve for the normalization constant. Take again Eq.(34) where the integral over ω_p has been performed

$$|\Psi\rangle = C \sum_{k_e k_o} \int_0^L dz e^{-\mathcal{D}\left(\frac{\nu_e + \nu_o}{\sigma_p}\right)^2} e^{iz\Delta_{k_e k_o}} \hat{a}_e^\dagger \hat{a}_o^\dagger |0\rangle,$$

Now we take the inner product

$$\langle\Psi|\Psi\rangle = \frac{4C^2}{U_e^2U_o^2}\int_{-\infty}^{\infty}\int_{-\infty}^{\infty} d\nu_e d\nu_o e^{-2\mathcal{D}\left(\frac{\nu_s+\nu_i}{\sigma_p}\right)^2}\frac{\sin^2\left(\frac{L}{2}\left[\nu_e u_e+\nu_o u_o\right]\right)}{\left[\nu_e u_e+\nu_o u_o\right]^2}.$$

Where we have taken the continuous limit and switched integration variables. It is required that $\langle\Psi|\Psi\rangle = 1$. We make another change of variables: $p = \nu_e + \nu_o$ and $q = \nu_e u_e + \nu_o u_o$, as long as $U_e \neq U_o$ this is a well defined one-to-one transformation with a Jacobian $J = \frac{U_eU_o}{U_e-U_o}$. This allows us to separate the integral. Thus

$$\frac{4C^2}{U_eU_o(U_e-U_o)}\int_{-\infty}^{\infty} dp e^{-2\mathcal{D}\left(\frac{p}{\sigma_p}\right)^2}\int_{-\infty}^{\infty} dq\frac{\sin^2\left(\frac{L}{2}q\right)}{q^2} = \frac{2C^2}{U_eU_o(U_e-U_o)}\frac{\pi^{\frac{3}{2}}L\sigma_p}{\sqrt{2\mathcal{D}}}.$$

So

$$C = \left(\frac{\mathcal{D}}{2}\right)^{\frac{1}{4}}\frac{\sqrt{U_eU_o(U_e-U_o)}}{\pi^{\frac{3}{4}}\sqrt{L\sigma_p}}.$$

Now we can write the full equation

$$\widetilde{P}_2 = \frac{C''}{L\sigma_p}\int_{-\infty}^{\infty} d\nu_f e^{-2\mathcal{D}{\nu_f}^2\left(\frac{(u_e+U_2)^2}{\sigma_e^2U_2^2}+\frac{u_e^2}{\sigma_o^2U_2^2}+\frac{1}{\sigma_p^2}\right)}\frac{\left|\mathrm{Erf}\left(\mathcal{E}\nu_f\right)-\mathrm{Erf}\left(\mathcal{E}\nu_f-\mathcal{L}\right)\right|^2}{\left[1+4\left(\frac{\nu_f}{\kappa_f}\right)^2\right].} \tag{47}$$

Where

$$\begin{aligned}
u_e &= \frac{1}{U_p}-\frac{1}{U_e},\\
U_2 &= \frac{1}{U_o}-\frac{1}{U_e},\\
\mathcal{E} &= \frac{i\sqrt{\mathcal{D}}(U_2\sigma_o^2+u_e(\sigma_e^2+\sigma_o^2))}{U_2\sigma_e\sigma_o\sqrt{\sigma_e^2+\sigma_o^2}},\\
\mathcal{L} &= \frac{LU_2\sigma_e\sigma_o}{2\sqrt{\mathcal{D}(\sigma_e^2+\sigma_o^2)}},\\
C'' &= \frac{8}{U_2}(1+\sqrt{\pi})^2\sqrt{2\pi^7\mathcal{D}}
\end{aligned} \tag{48}$$

And κ_f is the FWHM of the final state. Unfortunately this integral is intractable analytically, we therefore perform the integration over ν_f numerically.

Figure 11: A plot of the scaled two-photon absorption probability for the realistic $|2 :: 0\rangle$ state as a function of the logs (base 10) of the bandwidths of the filters in the arms of the interferometer (in Hz). $L = 2.3$mm, $\sigma_p = 10^{12}$Hz, and $\kappa_f = 10^{14}$Hz.

2.4.4 Numerical Calculation of the Type-II Absorption Rate

We wish to use Eqs. (35,47,48) to calculate the relative absorption rate for type-II down conversion. After this is done, we can use the information to maximize absorption by adjusting the available spectral parameters.

2.4.5 Pulse-Pumped Case

We start with the case of a pulsed pump. Since the two-photon absorption probability is a complicated quantity with five adjustable parameters (σ_e, σ_o, σ_p, L, and κ_f), we present several graphs to help elucidate the structure of this mathematical object. All of the graphs are scaled so that the maximal absorption probability – within the parameters we consider – is set to one. Thus $\widetilde{P}_2 = 1$ does not represent an absorption probability of unity. The normalization is consistent across all the graphs so that they may be compared to one another on the same scale.

Fig. 11 is a plot of the two-photon absorption as a function of the base-ten logarithms of the filter bandwidths. We see that a wider filter is preferable. This is because if the spectrum of the light is wide then the temporal distribution will be narrow, increasing the probability that the photons will arrive close together, triggering a two-photon absorption event.

Fig. 12 is a plot of the two-photon absorption probability as a function of the logarithm base ten of the bandwidth of the pump for several different atomic linewidths. Clearly a broader atomic linewidth will result in better absorption, as this will allow a greater range of frequency pairs to be absorbed. For the pump beam a smaller bandwidth is preferable. Once the bandwidth of the pump approaches that of the filters, or the linewidth of the atom, the absorption drop off is dramatic. Furthermore a narrower pump bandwidth constrains the frequencies of the daughter photons, increasing the probability that the sum of their

Figure 12: A plot of the scaled two photon absorption probability for the realistic $|2::0\rangle$ state as a function of the log (base 10) of the bandwidth of the pump (in Hz) for three separate settings of the width of the final state of the absorber (in Hz). $L = 2.3$mm and $\sigma_e = \sigma_o = 10^{13}$Hz.

energies will be resonant.

Fig. 13 is a plot of the two-photon absorption probability of a $|2::0\rangle$ pulse as a function of crystal length for two separate cases. This is perhaps the most interesting of the representations of Eq. (47). The plot indicates the feature that for each setting of σ_o, σ_e, σ_p, and κ_f there is an optimal crystal length that maximizes the probability of two-photon absorption.

As light travels through the crystal the dispersive nature of the medium causes the two photons to drift apart in time. This effect results in a drop off in absorption as length increases. Conversely, if the crystal length is very short, the spectrum of the light will be very broad, and the filters will strongly limit the amount of light that can reach the absorber. For broad filters, any deviation from the optimal length causes a dramatic drop off in absorption. Information of this type would be useful when we design a two-photon quantum lithography experiment. A crystal cut to a specific length, for a given setup, would have the potential to enhance the two-photon absorption properties of the generated light.

For example, take the case we have defined to be $\widetilde{P}_2 = 1$: Here we have chosen, $\sigma_e = \sigma_o = 10^{13}$Hz, $\sigma_p = 10^9$Hz, $L = 2.3$ mm, and $\kappa_f = 10^{14}$Hz. For the same absorber (κ_f the same), $\sigma_e = \sigma_o = 10^{11}$Hz, $\sigma_p = 10^{13}$Hz, and $L = 2$ cm, the absorption probability is is $\widetilde{P}_2 = 2.07 \times 10^{-5}$.

We may obtain completely analytical results for the case where there are no filters in the arms of the interferometer. Using Eq. (44), Eq. (47) becomes

$$\lim_{\sigma_e,\sigma_o\to\infty} \widetilde{P}_2 = \frac{C''\kappa_f e^{\frac{\mathcal{D}\kappa_f^2}{8\sigma_p^2}}}{2L\sigma_p} K_0\left(\frac{\mathcal{D}\kappa_f^2}{8\sigma_p^2}\right), \tag{49}$$

so long as $L \neq 0$. The function K_n is the modified Bessel function of the second kind.

Figure 13: A plot of the scaled two photon absorption probability for the realistic $|2::0\rangle$ state as a function of the length of the crystal for two different settings of the filters (in Hz). $\sigma_p = 10^{12}$Hz and $\kappa_f = 10^{14}$Hz

Features of this function include a simple dependence on L and a modified σ_p dependence, as shown in Fig. 14. Interestingly, for absorbers with very wide final states, the two photon absorption probability becomes almost independent of the bandwidth of the pump.

In all cases, given a particular κ_f, a balance must be struck between the related quantities of temporal and spectral correlation. Tight temporal correlation increases the probability of absorption. However this necessitates broad spectral distributions which have a lower probability of matching the correct energy for transition.

2.4.6 Comparison to Coherent Light

We can now tell how varying the spectral properties of $|2::0\rangle$ states will effect the absorption probability. However we have discovered nothing about how $|2::0\rangle$ light's absorption properties compare to other, more familiar, states of light. We would like to say whether $|2::0\rangle$ has any benefits or disadvantages when compared to, for example, coherent light. Coherent light has the advantage of being relatively well understood (or at least very extensively studied). Thus we shall attempt to find a state of coherent light which will serve as a fair comparison to $|2::0\rangle$, as produced in the fashion presented in this paper. We would like this fair state to have the same spectral profile as $|2::0\rangle$, but to lack the unique properties that the N00N state possesses: momentum entanglement and a high degree of temporal correlation.

In order to do this begin, again, with our $|2::0\rangle$ state is produced from a photon pair from a type II spontaneous parametric down conversion event, incident on two filters and a symmetric beam splitter. We can examine $|\Psi\rangle$, Eq. (34), and see that – given our previous assumptions – this state has a spectral profile (the relative probability amplitude of the photons having frequencies ν_e and ν_o) given by

Figure 14: A plot of the scaled two-photon absorption probability for the $|2::0\rangle$ state (in the limit of no filtering) as a function of the bandwidth of the pump. We indicate three separate settings of the width of the absorber. We also set $L = 1$ mm. The scaling is the same as on the other pulse pumped plots.

$$F_{|2::0\rangle}(\nu_e, \nu_o) = C \int_0^L dz e^{-\mathcal{D}\left(\frac{\nu_e+\nu_o}{\sigma_p}\right)^2} e^{iz\left(\frac{\nu_e+\nu_o}{U_p}-\frac{\nu_e}{U_e}-\frac{\nu_o}{U_o}\right)},$$

where $|\Psi\rangle$ represents two entangled down conversion modes. To remove the non-classical nature of this light we project out one of the modes. We arbitrarily choose the ordinary mode. The remaining state will have the spectral profile we desire for one mode of our fair coherent state (F_α), that is,

$$\begin{aligned}\int_{-\infty}^{\infty} d\nu_o \langle 1_{\nu_o}|\Psi\rangle &= \sqrt{\frac{\pi\sigma_p^2}{\mathcal{D}}} \sum_{k'} F_{\alpha,z}(\nu_e)\hat{a}^\dagger_{ek'}|0\rangle_e, \\ F_\alpha(\nu_e) &= \int_0^L dz e^{-iz\nu_e(u_o-u_e)} e^{-\frac{u_o^2 z^2 \sigma_p^2}{4\mathcal{D}}},\end{aligned}$$

where $u_e = 1/U_p - 1/U_e$ and $u_o = 1/U_p - 1/U_o$. This will represent one mode of the fair comparison coherent light. The normalization will be discussed shortly. The other mode will have a separate, but identical, spectral profile. Both modes will be mixed with a symmetric beam splitter.

In order to assimilate this spectral information into a coherent state we identify the spectral profile with α thus: $\alpha_k = F_{\alpha_k}(\nu_k)$.

The beam splitter transformation operating on the displacement operators which create the two mode coherent state, $|\alpha\rangle_1|\beta\rangle_2$ produces an output of $|\frac{\alpha+i\beta}{\sqrt{2}}\rangle_3|\frac{i\alpha+\beta}{\sqrt{2}}\rangle_4$, where 1 and 2 label the input modes and 3 and 4 label the output modes.

So now we can write the temporal correlation function for the fair coherent state

$$
\begin{aligned}
G_\alpha^{(2)} \quad & (t'^d_1, t'^d_2, t^d_1, t^d_2) \\
= \quad & \xi^4 \bigotimes_\nu \left\langle \frac{\alpha+i\beta}{\sqrt{2}}\gamma_3 \right|_{3\nu} \left\langle \frac{i\alpha+\beta}{\sqrt{2}}\gamma_4 \right|_{4\nu} \sum_{\nu_a} \hat{a}^\dagger_{3\nu_a} e^{i(\nu_a+\Omega)t'^d_1} e^{-\mathcal{D}\left(\frac{\nu_a}{\sigma'}\right)^2} \sum_{\nu_b} \hat{a}^\dagger_{4\nu_b} e^{i(\nu_b+\Omega)t'^d_2} e^{-\mathcal{D}\left(\frac{\nu_b}{\sigma'}\right)^2} \\
& \times \sum_{\nu_c} \hat{a}_{3\nu_c} e^{-i(\nu_c+\Omega)t^d_1} e^{-\mathcal{D}\left(\frac{\nu_c}{\sigma'}\right)^2} \sum_{\nu_d} \hat{a}_{4\nu_d} e^{-i(\nu_d+\Omega)t^d_2} e^{-\mathcal{D}\left(\frac{\nu_d}{\sigma'}\right)^2} \bigotimes_\nu \left| \frac{\alpha+i\beta}{\sqrt{2}}\gamma_3 \right\rangle_{3\nu} \left| \frac{i\alpha+\beta}{\sqrt{2}}\gamma_4 \right\rangle_{4\nu} \\
= \quad & \xi^4 \pi^2 |\gamma_3|^2 |\gamma_4|^2 e^{i\Omega(t'^d_1 + t'^d_2 - t^d_1 - t^d_2)} \hat{\mathcal{F}}(\nu_a \to t'^d_1)^* \hat{\mathcal{F}}(\nu_b \to t'^d_2)^* \hat{\mathcal{F}}(\nu_c \to t^d_1) \hat{\mathcal{F}}(\nu_d \to t^d_2) \\
& \times \left[F^*_\alpha(\nu_a) - iF^*_\beta(\nu_a) \right] \left[-iF^*_\alpha(\nu_b) + F^*_\beta(\nu_b) \right] \left[F_\alpha(\nu_c) + iF_\beta(\nu_c) \right] \left[iF_\alpha(\nu_d) + F_\beta(\nu_d) \right].
\end{aligned}
$$

The factors γ are the normalizations in the indexed modes. The central frequencies (Ω) have been taken to be the same. The filters in the arms $\sigma_e = \sigma_o$ have been removed in order to make the calculation which follows mathematically tractable. The frequencies have been labelled a,b,c, and d. As before ξ represents the constants associated with the electric field operators. We shall eventually take the two, two-photon absorption probabilities in ratio, the ξ's will cancel exactly. In light of this we simply set $\xi = 1$. We need to normalize such that the information about the intensity of the coherent light in each arm is contained in the γ's

$$
\begin{aligned}
I \quad &= \quad \int_{-\infty}^{\infty} dt \bigotimes_\omega \langle \gamma\alpha_\omega | \sum_{\omega'} \hat{a}^\dagger_{\omega'} e^{i\omega' t} \sum_{\omega''} \hat{a}_{\omega''} e^{-i\omega'' t} \bigotimes_\omega |\gamma\alpha_\omega\rangle \\
&= \quad |\gamma|^2 \int_{-\infty}^{\infty} d\omega' \int_{-\infty}^{\infty} d\omega'' \delta(\omega' - \omega'') F^*_\alpha(\omega') F_\alpha(\omega'') \\
&= \quad |\gamma|^2 \int_{-\infty}^{\infty} d\omega' |F_\alpha(\omega')|^2 \\
&= \quad |\gamma|^2 \int_{-\infty}^{\infty} d\nu' \int_0^L dz_1 \int_0^L dz_2 e^{i(z_1 - z_2)\nu'(u_o - u_e)} e^{-\frac{u_o^2 \sigma_p^2}{4\mathcal{D}}(z_1^2 + z_2^2)} \\
&= \quad \frac{|\gamma|^2 \sqrt{2\pi}}{u_o - u_e} \int_0^L dz_1 \int_0^L dz_2 \delta(z_1 - z_2) e^{-\frac{u_o^2 \sigma_p^2}{4\mathcal{D}}(z_1^2 + z_2^2)}.
\end{aligned}
$$

The double integral is tractable, yielding the result,

$$
\gamma = \left(\frac{I^2 (u_o - u_e)^2 u_o^2 \sigma_p^2}{\mathcal{D}\pi^2} \right)^{\frac{1}{4}} \mathrm{Erf}\left(\frac{L u_o \sigma_p}{\sqrt{2\mathcal{D}}} \right)^{-\frac{1}{2}}.
$$

Using the same procedure as in Eq. (45), we obtain the spectral correlation function

$$
\begin{aligned}
S^{(2)} \quad &= \quad 2\pi^2 |\gamma_3|^2 |\gamma_4|^2 \left[F^*_\alpha(\nu'_1) - iF^*_\beta(\nu'_1) \right] \left[F_\alpha(\nu_1) + iF_\beta(\nu_1) \right] \\
&\quad \times \left[iF_\alpha(\nu_2) + F_\beta(\nu_2) \right] \left[F^*_\beta(\nu'_2) - iF^*_\alpha(\nu'_2) \right].
\end{aligned}
$$

Now we can write the two-photon absorption probability Eq. (35) as

$$
\begin{aligned}
P_2^\alpha &= \pi^2|\gamma|^4\left|\int_{-\infty}^{\infty} d\nu F_\alpha(\nu_f-\nu)F_\alpha(\nu)\right|^2 \\
&= \pi^2|\gamma|^4\left|\int_{-\infty}^{\infty}\frac{d\nu_u}{u_o-u_e}\int_0^L dz_1\int_0^L dz_2 e^{-iz_2\nu_f(u_o-u_e)}e^{-i(z_1-z_2)\nu_u}e^{\frac{u_o^2\sigma_p^2}{4\mathcal{D}}(z_1+z_2)}\right|^2 \\
&= \frac{\pi^2|\gamma|^4}{(u_o-u_e)^2}\left|\int_0^L dz_1\int_0^L dz_2 e^{-iz_2\nu_f(u_o-u_e)}\delta(z_1-z_2)e^{\frac{u_o^2\sigma_p^2}{4\mathcal{D}}(z_1+z_2)}\right|^2 \\
&= \frac{\pi^3\mathcal{D}|\gamma|^4}{2u_o^2\sigma_p^2(u_o-u_e)^2}e^{-\frac{\mathcal{D}(u_o-u_e)^2\nu_f^2}{u_o^2\sigma_p^2}}|\mathrm{Erf}(\mathcal{E}_\alpha\nu_f)-\mathrm{Erf}(\mathcal{E}_\alpha\nu_f+\mathcal{L}_\alpha)|^2.
\end{aligned}
$$

Where $\mathcal{E}_\alpha$ and $\mathcal{L}_\alpha$ are defined as previously. In the interest of simplicity the initial coherent states have been taken to be equivalent. As in our previous derivation of the two-photon absorption we must now take the integral of the above expression, times a Lorentzian line shape, over ν_f. This new function, $\widetilde{P}_2^\alpha$, is given in the main text by

$$
\widetilde{P}_2^\alpha = \pi I^2\mathrm{Erf}\left(\frac{Lu_o\sigma_p}{\sqrt{2\mathcal{D}}}\right)^{-2}\int_{-\infty}^{\infty}d\nu_f e^{-\frac{\mathcal{D}(u_o-u_e)^2\nu_f^2}{u_o^2\sigma_p^2}}\frac{|\mathrm{Erf}(\mathcal{E}_\alpha\nu_f)-\mathrm{Erf}(\mathcal{E}_\alpha\nu_f+\mathcal{L}_\alpha)|^2}{\left[1+4\left(\frac{\nu_f}{\kappa_f}\right)^2\right]}. \tag{50}
$$

Where

$$
\begin{aligned}
\mathcal{E}_\alpha &= \frac{i\sqrt{\mathcal{D}}(u_o-u_e)}{\sqrt{2}u_o\sigma_p}, \\
\mathcal{L}_\alpha &= \frac{Lu_o\sigma_p}{\sqrt{2\mathcal{D}}}.
\end{aligned} \tag{51}
$$

and $u_e = \frac{1}{U_p}-\frac{1}{U_e}$ and $u_o = \frac{1}{U_p}-\frac{1}{U_o}$. Again, I is the intensity of the light in each arm of the interferometer (i.e. $2I$ would be the total amount of light in the device).

This fair-comparison light can be though of as a very spectrally broad coherent source incident on a magic "filter", which imposes on it the same spectral profile as the $|2::0\rangle$ state. Two spatial modes of this light are then used as the input into an interferometer without filters in the arms. The two-photon absorber is placed at the far end.

The error functions in the the above coherent-state expression diverge much more rapidly than for the $|2::0\rangle$ case. Thus it is only possible to compute P_2^α for relatively narrow arguments of the integral over ν_f, so we must consider a non-maximal setup as a test case. So for $\sigma_p = 10^9$Hz, $\kappa_f = 10^{10}$Hz, and $L = 1$ cm we have

$$
\widetilde{P}_2^\alpha = 5.65\times10^{-6}\widetilde{P}_2 I^2,
$$

where $\widetilde{P}_2$ has been calculated using Eq. (49).

If the intensities of the two kinds of light are set to be equal ($I = 1$ in the above equation) then $|2 :: 0\rangle$ is absorbed with a much higher probability than coherent light. This is directly a result of the frequency entanglement. Maximal absorption probability occurs when the photon energies add, such that the total is the same as the centre of the final level. For SPDC it is insured that this condition will be closely met (exactly met in the case of a cw pump and a very thin crystal). However for the coherent analogue there is no such requirement, in fact the probability of two randomly chosen photons from the coherent pulses adding up to the resonance energy is minuscule. Even so, the above equation may be overly *optimistic* about the absorption properties of coherent light. Recall that we were forced to consider narrow-band fields to make the calculation numerically tractable. The effect that causes coherent light to have a poor two-photon absorption probability will be worsened when the bandwidth is broader; a regime in which the $|2 :: 0\rangle$ states' absorption probability improves.

These positive results for the multiphoton absorption of entangled light is in seeming contradiction to the results of section II, which shows that coherent states should fair better than $|N :: 0\rangle$ states, where N-photon absorption is concerned. However that treatment does not take into account the spectral properties of highly quantum-mechanical states of light, which are likely to have high degrees of temporal correlation.

In a paper by Tsang [14], it was shown that the *spatial* properties of N00N states cause them to have poor N-photon absorption rates. The relationship found in that paper is that N00N states have absorption rates that are lower than a classical analogue (in his case a monochromatic Fock state incident on a beam splitter) by a factor of $1/2^{N-1}$, due to spatial considerations independent of temporal correlations. He leaves open the question of whether time-domain effects can compensate for this effect. Given our above results it seems likely that the answer to this question is yes.

However, the advantage entangled light enjoys is offset by the fact that SPDC has an extremely small intensity. Even relatively high production efficiencies are only approximately one pair per 10^{12} incident photons (see for example Ref. [41]). Furthermore it has been shown that correlated two photon absorption (absorption from two photons of the same pair as opposed to absorption from two photons of different pairs) from entangled light dominates only when the intensity is small [42]. This makes it even more important to improve absorption rates.

It could also be pointed out that $|2 :: 0\rangle$ light is not a good candidate for lithography or metrology due to the fact that the pump light could just be used at double the frequency to achieve the same enhancement. This paper does not suggest, however, that it would be. Instead the purpose of our analysis is to take a simple case of the $|N :: 0\rangle$ state ($N = 2$) and show that the phenomenon of frequency entanglement prevalent in quantum mechanical states of light boosts multiphoton absorption to a degree which may counteract, or at least partially mitigate, small production rates. In this light our work may be viewed as a proof of principle. When $|N :: 0\rangle$ states of large N become available it is highly likely that an analysis similar to the one presented in this section may be utilized to enhance the N-photon absorption rate. One might even conjecture – from the above discussion – that for higher N the temporal advantage of using entangled light may be more pronounced, since for classical light the problem of arranging for N photons to arrive at the same time is compounded as N increases.

2.4.7 Continuous-Wave-Pumped Case

Let us now investigate the case of a continuous-wave pump. The expressions derived in the previous section only make sense when considering a biphoton *pulse*. They give the absorption probability of a biphoton of finite extent being absorbed as it passes an atom or other absorber. Note that since the pulses are Gaussian-like they are not strictly finite, but they are so closely temporally correlated that we may treat them as such. However the continuous wave case is stationary. We must now speak of a two photon absorption *rate*.

First we recalculate the biphoton amplitude. Take Eq. (39), for a cw pump we set $\sigma_p = 0$ and $\omega_{k_o} + \omega_{k_e} = \Omega_p$. We can then rewrite this equation as

$$\begin{aligned}
\mathcal{A}({t_1}^d, {t_2}^d)_{\text{cw}} &= \sum_{k_o k_e} e^{-\mathcal{D}\left(\frac{\omega_{k_o}-\Omega_o}{\sigma_o}\right)^2} e^{-i\omega_{k_o}{t_1}^d} e^{-\mathcal{D}\left(\frac{\omega_{k_e}-\Omega_e}{\sigma_e}\right)^2} e^{-i\omega_{k_e}{t_2}^d} \int_0^L dz e^{iz\Delta_{k_o k_e}} \delta(\omega_{k_o} + \omega_{k_e} - \Omega_p) \\
&= \frac{e^{-i(\Omega_o {t_1}^d + \Omega_e {t_2}^d)}}{U_e U_o} \int_{-\infty}^{\infty} d\nu \int_0^L dz e^{-\mathcal{D}\left(\frac{\nu}{\sigma}\right)^2} e^{-i\nu({t_2}^d - {t_1}^d)} e^{iz\Delta_{k_o k_e}},
\end{aligned}$$

where

$$\sigma = \frac{\sigma_e \sigma_o}{\sqrt{\sigma_e^2 + \sigma_o^2}}.$$

In the second equality we have taken the continuous limit, changed variables from momentum to frequency, performed one of these integrals to eliminate the delta function, and then changed variables again to $|\nu_e| = |\nu_o| \equiv \nu$. We are able to do this due to conservation of energy for a cw pump: once the momentum of one photon is chosen the momentum of the other one is determined. Also the phase mismatch becomes

$$\Delta_{k_e k_o} = \nu \left(\frac{U_e - U_o}{U_e U_o} \right) \equiv u\nu.$$

We now write in analogy to Eq. (42)

$$\begin{aligned}
\mathcal{A}({t_1}^d, {t_2}^d)_{\text{cw}} &= \frac{e^{-i(\Omega_o {t_1}^d + \Omega_e {t_2}^d)}}{U_e U_o} \int_0^L dz \hat{\mathcal{F}}(\nu \to [{t_2}^d - {t_1}^d]) Y(\nu) \\
Y(\nu) &= e^{-\mathcal{D}\left(\frac{\nu}{\sigma}\right)^2} e^{izu\nu}.
\end{aligned}$$

The solution for A is easily found

$$\mathcal{A}({t_1}^d, {t_2}^d)_{\text{cw}} = \frac{e^{-i(\Omega_o {t_1}^d + \Omega_e {t_2}^d)}}{U_e - U_o} \left[\text{Erf}\left(\sigma \frac{({t_1}^d - {t_2}^d)}{2\sqrt{\mathcal{D}}} \right) - \text{Erf}\left(\sigma \frac{({t_1}^d - {t_2}^d) - Lu}{2\sqrt{\mathcal{D}}} \right) \right].$$

The absorption rate for stationary states is given by Eq. (3.17a) in Ref. [35]

$$w_2 = 2\left|g\left(\frac{1}{2}\Omega_p\right)\right|^2 \int_{-\infty}^{\infty} dt e^{2i\Omega_p t - \kappa_f|t|} G^{(2)}(-t,-t;t,t),$$

where κ_f is the width of the final state of the absorber. We have for the second-order correlation function,

$$G^{(2)}(-t,-t;t,t) = \frac{2e^{-2i\Omega_p t}}{(U_e - U_o)^2}\left|\mathrm{Erf}\left(\frac{Lu\sigma}{2\sqrt{\mathcal{D}}}\right)\right|^2,$$

and thus

$$w_2 = \frac{2\left|g\left(\frac{1}{2}\Omega_p\right)\right|^2}{(U_e - U_o)^2}\left|\mathrm{Erf}\left(\frac{Lu\sigma}{2\sqrt{\mathcal{D}}}\right)\right|^2 \int_{-\infty}^{\infty} dt e^{-\kappa_f|t|}.$$

The modulus squared of the error function is the only part that is dependent on the spectral properties of the field, so we fold the overall constants into the atomic response function, which we will then ignore. We then obtain the relatively simple result

$$\widetilde{w}_2 = \frac{1}{L}\left|\mathrm{Erf}\left(\frac{Lu\sigma}{2\sqrt{\mathcal{D}}}\right)\right|^2, \tag{52}$$

where the factor of $1/L$ comes from the state normalization. Unlike for the general case, the cw expression is fully analytical. Figs. 15 and 16 are plots of the absorption rate as a function of crystal length and filter bandwidths. The graphs have been normalized such that the greatest absorption rate for the range of parameters we consider is set to $\widetilde{w}_2 = 1$.

So for a cw pump we have generally the same results as in the pulse-pumped case, with absorption improving as bandwidth increases. We also again observe that the graph of $\widetilde{w}_2$ as a function of L displays peak values.

2.4.8 Conclusion

First, we analysed the multiphoton absorption probability of states of the form $|N :: 0\rangle$ in the ideal case (with no spectral information). We found that the absorption probability scales poorly with N when compared to coherent states, but well when compared to Fock states. Thus we reinforced the original findings of Ref. [14] through less sophisticated means.

Second, we considered the case of a realistic $|2 :: 0\rangle$ state produced by type-II spontaneous parametric down conversion, a polarization rotator and a beam splitter. We found that generally the two photon absorption properties of this states are highly dependent on the specific optical setup used. Using numerical methods it is possible to analyse the absorption probability as a function of the realistic parameters of the experiment. We can then adjust the optical setup of our model, including the length of the crystal, the bandwidths of the filters in the extraordinary and ordinary beams, and the pulse length of the pump. Running a

Figure 15: Plot of the two-photon absorption rate from a cw pumped crystal, as a function of crystal length, for four separate settings of the filters (in Hz).

Figure 16: Plot of the two-photon absorption rate from a cw-pumped crystal, as a function of the bandwidths of the filters in the ordinary and extraordinary arms. Here $L = 6$ mm.

maximization procedure over these variables it is possible to find the setup, which optimizes two-photon absorption. The difference between the optimal setup and a slight deviation may be dramatic.

This research constitutes a proof of principle of the idea that the poor production rates and detrimental spatial effects of highly quantum mechanical states of light may be mitigated by improving the absorption rates through spectral means. Though we consider in detail only the $|2 :: 0\rangle$ case, it is likely that once methods of developing N00N states of higher N are developed, similar methods may be applied to improve their N photon absorption properties as well.

It's also encouraging to note that advances are continually being made in creating resists that have greater multi-photon cross sections. See for example Ref. [43] and Ref. [44].

Also, in a broader sense, similar techniques may be applied to increase the multiphoton absorption properties of any desirable state of light. All that is required is the quantum mechanical state vector.

3 Optical Interferometers and Measures of Sensitivity

"There is nothing new to be discovered in physics now; All that remains is more and more precise measurement."
-Lord Kelvin 1900

We'll now change topics by a half-step and move to the related field of interferometry. Lithographic interference fringes on a multiphoton resist will be replaced with photodetectors and measurement protocols. Optical interferometers can be used to detect path differences for accurate distance measurements, they can be employed to detect very small magnetic fields, even to detect gravitational radiation, among a plethora of other uses. Making improving their sensitivity potentially very rewarding. The focus of the remaining chapters will be on techniques in quantum optical interferometry. With the goal being improving the sensitivity of measuring devices. Before we do that though, it will be useful to review, briefly, the field of optical interferometry as a whole, and develop the mathematical methods we will need to gauge the sensitivity of specific optical sensors.

3.1 Optical Interferometers: From Young to the Present

The techniques of optical interferometry arose from the battles between the wave, and corpuscular camps in the 1800s and early 1900s. In the introduction to this thesis we briefly discussed the conflict between these two paradigms, and the uneasy truce that resulted when it became apparent that light was *both* a particle and a wave. But before this revelation the odds heavily favoured the wavests[26]. One large piece of evidence in their employ, was the discovery by Maxwell of the electromagnetic wave equation – which was discussed in detail in the introduction. But another big feather in their communal cap was the result of Young's interference experiment...

3.1.1 Young's Interference

It was reasoned that if light were a wave it would behave in much the same way a water-wave would. One property being the phenomena of constructive and destructive interference.

Imagine a jetty that runs parallel to a beach, the jetty has a small gap in it where waves from the ocean may come through. Standing on the beach we would see waves radiate out from this point and lap the shore. Imagine now that there is a second gap in the jetty some distance from the first. The waves from both gaps are made up of alternating series of high points and low points: swells and troughs. As two waves move into each other, and merge, there will be points where one wave has a swell where the other has a trough. When this happens the two cancel[27] and the water stays still, this is called *destructive interference*. On the other hand there will be points where the swells and troughs coincide, and here the waves will be twice as strong, this is called *constructive interference*. Standing on the shore

[26] This is probably not a word, but I like it.

[27] As long as both waves have swells and troughs of the same heights and depths. That is that they have the same amplitude.

we see points along the beach that are lapped by strong waves, blending into and alternating with, points where the water is still.

But will we see this effect with light? This is a question which was asked over two-hundred years ago, and that Thomas Young sought to answer. In a paper published in 1803 titled *Experiments and Calculations Relative to Physical Optics* Young described an experiment he performed.[28] An incoherent source such as a candle, or sunlight, is attenuated and filtered (in original experiments with a series of prisms and pinholes, now a strong coherent source – such as a laser – is simply used) until it is coherent. This light is then shown on two small slits placed close together. The light beams interfere and produce a pattern of bright and dark fringes on a screen. See Figure 17. Young noted that if one of the beams is blocked then the interference pattern disappears, insuring that this was indeed an effect generated by the interaction of the two sources of light.

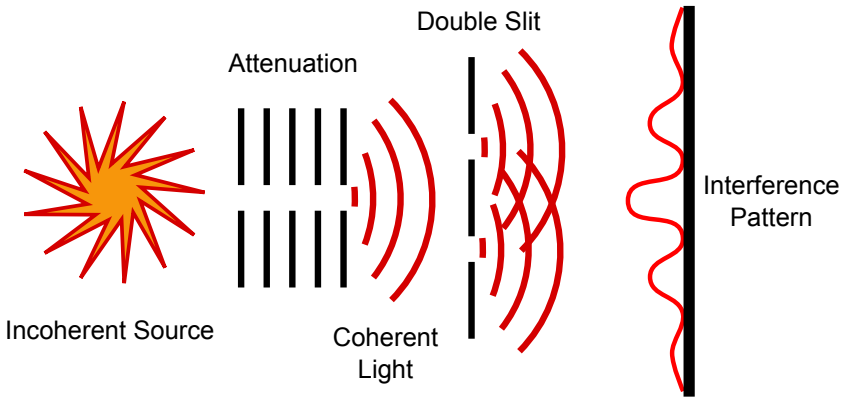

Figure 17: The Young interference experiment. An incoherent source such as a candle or sunlight is attenuated and filtered until coherent. This light is then shown on two small slits placed close together. The light beams interfere and produce a pattern of bright and dark fringes on a screen.

At the time this was taken to be further proof of the wave nature of light. In the modern era this experiment takes on a new level of interpretation. Since we know that light is both a particle and a wave, it is understood that what is happening is a quantum-mechanical superposition. Each photon takes both paths simultaneously, and it is the probability amplitudes of these two possibilities that interfere on the screen.

Though Young did not intend his device to probe any specific quantity, it did kick-start the field of interferometric measurement.

3.1.2 Michelson, Morley, and the Ether

In 1851 the French physicist Hippolyte Fizeau carried out an interference experiment where the two light beams propagated through moving water [45]. He measured that light moving against the flow of water propagated with a smaller velocity than light moving with the flow

[28]There is some controversy as to whether Young actually performed the experiment himself. See *Everything's Relative and Other Fables from Science and Technology* by Tony Rothman.

of water.[29]

This served as an inspiration for Albert Michelson, who reasoned he could use the same idea to detect the presence of the Ether as the Earth moved through it. All that he required was a sufficiently sensitive interferometer. The device he designed – today known as the Michelson interferometer – took light (which by hook or crook was made coherent) and shined it on a partially silvered mirror, that split the beams into two paths. The transmitted light travelled some distance before reflecting off a mirror (fully silvered this time) which sent it back to the beam splitter. A similar thing happened to the reflected light. The mirrors and beam splitters were carefully aligned such that the reflected part of the initially transmitted beam lined up exactly with the transmitted part of the initially reflected beam. The light that was transmitted twice was discarded, along with the light that was reflected twice. This setup is graphically represented in Figure 18.

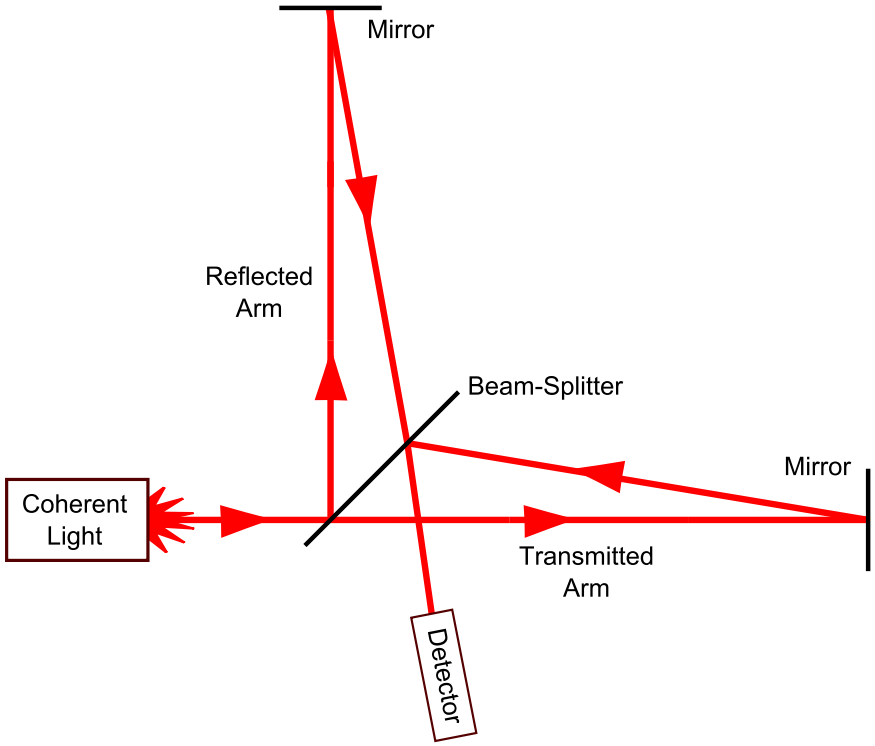

Figure 18: The Michelson Interferometer.

Detection was done on this output beam. For Michelson this was a simple eyepiece, through which he watched the interference fringes. His plan was to rotate the interferometer while taking measurements and thus detect the light in one of the arms moving against the "ether wind" while the other remained perpendicular to it. His initial attempt was a failure but he reasoned that this was because the sensitivity of the device was bellow the theoretically expected results. So he teamed up with Edward Morley, and constructed a larger and much more sensitive version of the device in 1887. Despite their extended efforts, and the estimated

[29]This is now understood in the context of special relativity, and follows from the composition law for velocities.

sensitivity of the device being above the calculated threshold, they never saw any evidence of the Ether. This is still perhaps the most famous null result in physics.

3.1.3 The Mach-Zehnder Interferometer

The most common description of a general interferometer, and the one I will make extensive use of in this thesis, is the Mach-Zehnder interferometer (MZI). Named after the German physicists Ernst Mach and Ludwig Zehnder who pioneered use of the device in 1891-1892. Such a device is represented in Figure 19.

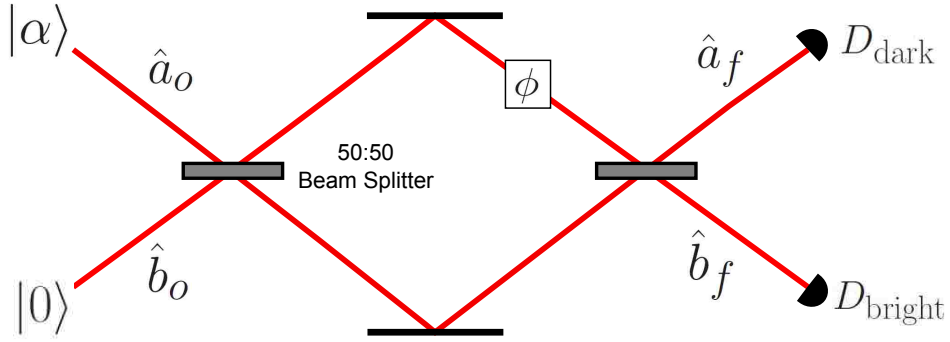

Figure 19: A Mach-Zehnder Interferometer. A light beam is divided at a beam splitter (each photon taking both paths simultaneously), one arm interacts with an abstract phase, and then both arms are mixed again, at another beam splitter, before detection.

In the MZI a coherent beam of light is incident on a 50:50 beam splitter.

Classically this is understood as one input mode being split into two output modes. Quantum mechanically, however, this needs to be recast as a two input port device. There is the coherent input, which spatially lines up with the transmitted exit mode, but the output mode which contains the reflected coherent light also needs to be lined up with a transmitted input mode. In this case it is the vacuum. In the classical description there is no point to saying that there is an empty input mode. But quantum mechanically, though the vacuum contains no photons, it *does* contain fluctuations in the field which add noise to the device.

After the first beam splitter each photon in the MZI is now taking both paths simultaneously in a superposition. One of the paths interacts with an abstract phase shift ϕ. The abstract phase may represent any number of physical processes that can cause the phase of one arm to change, relative to the phase of the other. Some examples are a path length difference, which would allow the interferometer to measure very small changes in length and size. It could be induced by the presence of a magnetic field if the light was transmitted through an optically active medium (OAM).[30] It could also be caused by an acceleration, a gravity wave, or several other things. For many cases the actual mechanism of phase shift may be ignored, and we can examine the device independent of what physical quantity it is probing.

After the phase shift, the beams are mixed again at a second 50:50 beam splitter, which allows the photons to constructively and destructively interfere. Detection is then done at

[30] An OAM is a material that has an index of refraction which is a function of magnetic field.

the two outputs of this beam splitter. This type of interferometer is typically balanced such that the abstract phase is zero in the absence of external perturbation. This causes one of the output ports to be dark (all photon probability amplitudes destructively interfere) while the other is bright (all photon probability amplitudes constructively interfere). This allows very sensitive photo-detectors (which would otherwise be burnt out from the bright light) to be used at the dark port as any small change in the phase caused by the probed physical process will result in some light exiting from the dark port. Typically detection is done by taking the intensity difference between the two ports. This allows fluctuations in the device that are present in both beams to be subtracted out.

The MZI has become the standard in both experiment and theory. Experimentally it is a broadly usefully and highly sensitive measuring tool. Theoretically it is a system that is relatively easy to represent mathematically, yet contains a lot of depth and subtlety.

3.1.4 The Hong-Ou-Mandel Quantum Device

A modification of the MZI can be made if, instead of classical light, we input a single number state into each input port. This situation was first studied by Hong, Ou, and Mandel. [32] What they found was that if the photons lined up very precisely in time they "bunched" after the beam splitter, and always both took the same path. This is a fundamentally quantum effect which we will explain by applying the beam splitter transformation to the input state

$$\begin{aligned} |1\rangle_a|1\rangle_b &= \hat{a}^\dagger_{\text{in}}\hat{b}^\dagger_{\text{in}}|0,0\rangle = \frac{1}{\sqrt{2}}(\hat{a}^\dagger_{\text{out}} + i\hat{b}^\dagger_{\text{out}})\frac{1}{\sqrt{2}}(\hat{b}^\dagger_{\text{out}} + i\hat{a}^\dagger_{\text{out}})|0,0\rangle \\ &= \frac{1}{2}(i\hat{a}^{\dagger 2}_{\text{out}} + \hat{a}^\dagger_{\text{out}}\hat{b}^\dagger_{\text{out}} - \hat{b}^\dagger_{\text{out}}\hat{a}^\dagger_{\text{out}} + i\hat{b}^{\dagger 2}_{\text{out}})|0,0\rangle \\ &= \frac{i}{\sqrt{2}}\left(|2,0\rangle + |0,2\rangle\right). \end{aligned}$$

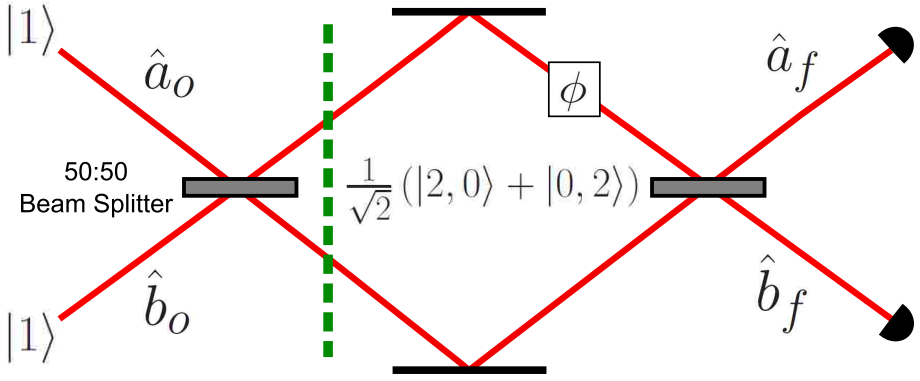

Figure 20: A diagrammatic representation of the Hong-Ou-Mandel Interferometer. The probability amplitudes of both photons being transmitted cancels exactly with the probability that they are both reflected, resulting in photon-bunching where both photons take one path or the other.

Also see Figure 20. The probability amplitudes of both photons being transmitted cancels exactly with the probability that they are both reflected. This is because the beam splitter induces a $\pi/2$ phase shift on reflected light. The resultant state is entangled, meaning the two paths of the quantum state can not be separated mathematically or conceptually. The two photons along, with the two paths they simultaneously take must be regarded as a single object a biphoton. This was extensively discussed in section 2.4.2.

3.1.5 Beyond the Optical: All Things Are Waves

Though the subject of this thesis is optical interferometry it is worthwhile pointing out that interferometry is done with matter as well. The impetus for this started with Louis de Broglie, who hypothesized in his 1924 PhD thesis that matter had a wave nature, like light.[31] According to this theory, the wavelength of a particle of matter would be inversely proportional to its momentum. This hypothesis was confirmed in 1927 when diffraction (fundamentally an interference effect) was seen for electrons shot at low velocities through a crystal. [46] Matter-wave interferometry has since blossomed into a vibrant field. Recently interference experiments have even been done with large molecules, including buckyballs (C_{60}). [47]

3.2 Characterizing Sensitivity

We have established that optical interferometers are very useful and sensitive measuring tools. But *how* sensitive are they? How do we characterize sensitivity? In this section I'll present an outline of some of the various methods that are employed to gauge sensitivity.

3.2.1 The Shot Noise Limit

The shot noise limit is one half of what is known as the standard quantum limit. The standard quantum limit encapsulates two sources of noise, both a result of the quantum nature of light.

The first is the radiation-pressure noise, which is a result of the light beam imparting a fluctuating amount of momentum into the mirror. Obviously, the imparted momentum causes "jitter", fowling up the very sensitive phase measurements an interferometer might otherwise perform. This noise increases as the power of the light increases. Conversely it decreases as the mass of the mirror increases. Much of the research into reducing radiation pressure noise is concerned with mirror stabilization.

The second is shot noise, which is a result of the photon number fluctuations from "shot to shot". Shot noise decreases as the intensity increases. This is the noise source we will focus on characterizing and reducing throughout the rest of this thesis. In principle the mass of the mirrors in an interferometer may be made very large, such that radiation pressure becomes small when compared to the shot noise. Though in practice this may be very difficult, there are a number of systems where the dominant source of noise is indeed the shot noise.

As such I will now present a more detailed, but still conceptually intuitive derivation of the shot noise limit.

[31] In the process setting standards far to high for Doctoral Theses.

Before we start, however, it should be stated that the shot noise limit, though a "quantum" limit only applies to the most classical form of light: coherent light. What it means to say that light is "quantum" or "classical" and why coherent states (despite being a perfectly well defined quantum states) fall mostly into the classical category will be discussed in the next chapter. For now it is sufficient to point out that practical interferometry is almost exclusively done with laser light, which is excellently described by coherent states.

First recall the description of the quadrature diagrams given in the introduction. We shall now utilize the square of one of these diagrams (that is instead of the axes being $\langle q \rangle$ and $\langle p \rangle$ they will be $\langle q \rangle^2$ and $\langle p \rangle^2$). In a space defined thusly we shall plot some light fields. See Figure 21.

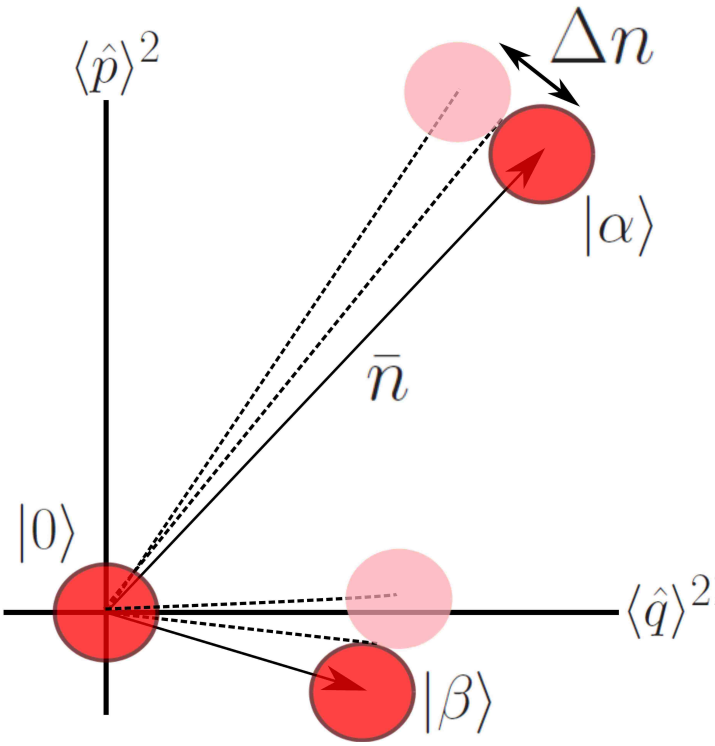

Figure 21: A square-quadrature diagram with several states and their uncertainties plotted: The vacuum state at the origin, and two displaced coherent states (red) $|\alpha\rangle$ and $|\beta\rangle$, each paired with a partner (pink) which is the same, except phase shifted by the smallest amount that is possible, while still being distinguishable.

We have the vacuum state at the origin. The area of the state represents our uncertainty about the state in both quadratures. As discussed in the introduction this is a minimum uncertainty state. Also as discussed in the introduction, the way to mathematically generate coherent states is to act the displacement operator ($\hat{D}_\alpha$), on the vacuum state. This (mathematical) action is represented in the plot by the solid arrows. The polar decomposition of α into $|\alpha|e^{i\theta}$ has a nice interpretation in square quadrature space. The radial distance that the state is displaced is the total intensity (average photon number) $\bar{n}$ of the newly generated coherent state (whereas in "regular" quadrature space it is the square root of the intensity). The polar direction of the displacement is the angle θ, which is the phase of the light field.

The coherent state, like the vacuum state, is a minimum uncertainty state.

In order for two coherent states of different phases (represented by the two sets of red and pink states) to be distinguishable, they must be outside of each other's areas of uncertainty. In Figure 21 the pink states are as close as they can be to the red states without overlapping. The angle formed between the line drawn from the origin to a red state, and from the origin to its pink state partner, is the minimum detectable phase shift ($\Delta\phi_{\min}$). Compare this angle for $|\alpha\rangle$ and for $|\beta\rangle$. Qualitatively we can see that the angle is smaller for $|\alpha\rangle$, thus the minimum detectable shift shrinks for increasing photon number. This relationship can be made quantitative without too much difficulty. First note that, since the coherent states are circles, the uncertainty along the radial direction – Δn – is equivalent to the uncertainty perpendicular to the radial. Also note that, since the red and pink states are described by circles of the same radius, the distance between their centres is also Δn. The line $\bar{n}$ and the line Δn constitute the two sides of a triangle. This is sufficient to solve for the angle we are interested in: $\Delta\phi_{\min}$ in the small angle limit (this is a good approximation since for realistic coherent states $\bar{n}$ is very large[32])

$$\Delta\phi_{\min} = \frac{\Delta n}{\bar{n}}. \tag{53}$$

It is straightforward to solve for the variance of n, for a coherent state. Employing the relation $\Delta\hat{O} = \sqrt{\langle\hat{O}^2\rangle - \langle\hat{O}\rangle^2}$, for any observable $\hat{O}$, we have

$$\begin{aligned}
\Delta n &= \sqrt{\langle\hat{n}^2\rangle - \langle\hat{n}\rangle^2}, \\
&= \sqrt{\langle\alpha|\hat{a}^\dagger\hat{a}\hat{a}^\dagger\hat{a}|\alpha\rangle - \langle\alpha|\hat{a}^\dagger\hat{a}|\alpha\rangle^2}, \\
&= \sqrt{\langle\alpha|\hat{a}^\dagger\hat{a}^\dagger\hat{a}\hat{a}|\alpha\rangle + \langle\alpha|\hat{a}^\dagger\hat{a}|\alpha\rangle - \langle\alpha|\hat{a}^\dagger\hat{a}|\alpha\rangle^2}, \\
&= \sqrt{|\alpha|^4 + |\alpha|^2 - |\alpha|^4}, \\
&= \sqrt{|\alpha|^2}, \\
&= \bar{n}^{1/2}.
\end{aligned}$$

This combined with Eq. (53) yields

$$\Delta\phi_{\min} = \frac{1}{\sqrt{\bar{n}}}, \tag{54}$$

which is the shot noise limit on the minimum detectable phase shift. Which is the best we can do classically. But what if we begin to employ quantum tricks and non-coherent light? Might we be able to do better than this? And, is there a more fundamental limit on phase sensitivity?

[32]The average laser pointer outputs about 10^{16}photons/sec.

3.2.2 The Heisenberg Limit

The Heisenberg limit presumes to be the absolute limit on the phases sensitivity of an interferometer. Unlike the shot noise limit, it makes no assumptions about the specific kind of light being used. Instead the Heisenberg limit draws upon the fundamental laws of quantum mechanics to place a bound on how accurately we may measure a light field's (or matter wave's) phase.

I will present a quick and direct derivation of the Heisenberg limit. I will then show how this proof is flawed, and briefly discuss the implications of this on the nature of phase sensitivity.

To begin we return to the line of thought we followed in the introduction where we sought to "put hats" on variables to turn them into quantum mechanical observables.[33] Likewise it would be favourable if the operators in quantum optics could be associated with quantities we are familiar with from classical optics. Specifically, take the annihilation operator acting on a coherent state

$$\hat{a}|\alpha\rangle = \alpha|\alpha\rangle = e^{i\phi}|\alpha||\alpha\rangle = e^{i\phi}\sqrt{\bar{n}}|\alpha\rangle.$$

The annihilation operator is a purely quantum mechanical object with no classical analogue. However, it can be decomposed into quantities that *are* familiar in classical optics: the intensity and the phase of a beam of light. It was Dirac [48] who first took this to mean that the creation and annihilation operators could be factored into Hermitian observables as

$$\begin{aligned} \hat{a} &= e^{i\hat{\phi}}\sqrt{\hat{n}} \\ \hat{a}^\dagger &= \sqrt{\hat{n}}e^{-i\hat{\phi}}, \end{aligned}$$

where the second equation is obtained by simply taking the conjugate transpose of the first. We have thus defined the phase operator $\hat{\phi}$. This combined with the commutation relation $[\hat{a}, \hat{a}^\dagger] = 1$ yields

$$[\hat{n}, \hat{\phi}] = i. \tag{55}$$

So photon number and phase are conjugate observables, in order to become more certain about one, we must become less certain about the other. This relationship can be made quantitative by employing the generalized Heisenberg uncertainty principle for non-commuting operators: $\Delta A \Delta B \geq \frac{1}{2}|\langle[\hat{A}, \hat{B}]\rangle|$. Using this we have $\Delta n \Delta\phi \geq 1/2$. So in order to know as much as we can about the phase, we must reduce by as much as possible, our knowledge of the number of photons in the field. Since we are concerned with fundamental limits we will take the case where photon number is as uncertain as possible: when $\Delta n = \bar{n}/2$. The uncertainty can not be made any larger than this because then there would be a non-zero probability of detecting a negative number of photons in the field (which would be silly). Which brings us the Heisenberg limit

[33] The fancy word for this, is again, "second quantization".

$$\Delta\phi_{\min} = \frac{1}{\bar{n}}. \tag{56}$$

However there is a flaw in this argument. The problem arose when we defined the phase operator. If we want to have a Hermitian operator representing an observable then that operator should have eigenstates. However if we attempt to write down an eigenstate for the phase operator then trouble arises. This is most easily seen by looking at the quadrature diagram in Figure 22.

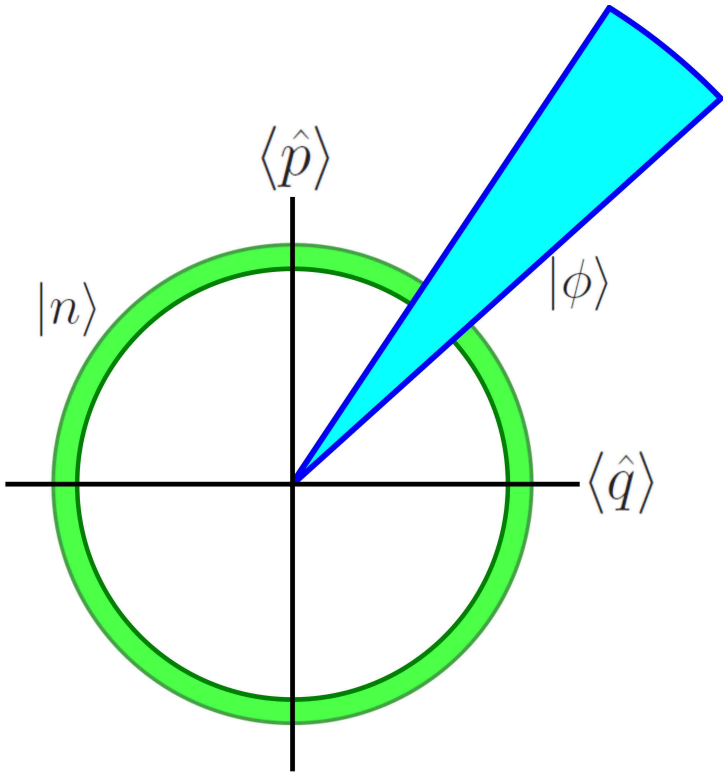

Figure 22: A quadrature diagram showing a state of definite photon number $|n\rangle$ (green), represented as a ring, and a state of definite phase $|\phi\rangle$ (blue), represented as an infinite wedge.

The definite number states are perfectly well defined as rings in quadrature space. They posses completely defined photon number, but completely undefined phase. On the other hand if we try to draw a state with completely defined phase, we end up with a wedge in quadrature space that extends out to infinity. Mathematically we would have an infinite, non-convergent sum of number states containing, in total, an infinite amount of energy. A state with infinite energy is obviously non-physical, creating an inconsistency in the derivation of Eq. (56).

This proof is admittedly slipshod. So it is fair to ask the question "Are there better, more rigorous, proofs of the Heisenberg limit?" The answer is yes, and several can be found in the paper *Fundamental Quantum Limit in Precision Phase Measurement* by Z. Y. Ou [49].

However all the proofs found there contain some other assumption or limit which renders the Heisenberg bound non-general. In fact Ou points out that the Heisenberg limit is best understood as "an approximate bound, in the limit of high photon number."

Though the Heisenberg limit is widely used as a goal post, it is not the best way to gauge sensitivity. Recent research in our group [50] has shown that the Heisenberg limit may be beaten. Furthermore there is, in fact, a setup from a paper in 1986 which could reach below the limit [51]. However that paper did not claim sub-Heisenberg scaling, this is due to either a typo, or a mathematical error.

There are better methods which can be used to gauge the sensitivity of an optical interferometer. One of these will be discussed in the next section.

3.2.3 The Minimum Detectable Phase Shift – Detection Dependent Formula

Suppose we have a device that probes the abstract phase shift by imprinting it on some measurable quantity. Mathematically this means we have some quantity that is a function of the phase $M(\phi)$. So we ask the question "Given that we are measuring M what is the smallest change we can detect in ϕ?" To answer this question start with the Taylor series expansion of a function f with one independent variable x about a point a

$$f(a+x) = f(a) + x \left.\frac{\partial f}{\partial x}\right|_{x\to a} + \frac{x^2}{2!}\left.\frac{\partial^2 f}{\partial x^2}\right|_{x\to a} + ...$$

For a measurable quantity which is a function of the phase

$$M(a+\phi) = M(a) + \phi \left.\frac{\partial M}{\partial \phi}\right|_{\phi\to a} + \frac{\phi^2}{2!}\left.\frac{\partial^2 M}{\partial \phi^2}\right|_{\phi\to a} + ...$$

Making the redefinition $\phi \to \phi - \phi_0$, where ϕ_0 is some initial phase, and choosing $a = \phi_0$

$$M(\phi) = M(\phi_0) + (\phi-\phi_0) \left.\frac{\partial M}{\partial \phi}\right|_{\phi\to\phi_0} + \frac{(\phi-\phi_0)^2}{2!}\left.\frac{\partial^2 M}{\partial \phi^2}\right|_{\phi\to\phi_0} + ...$$

Where $\partial(\phi-\phi_0) = \partial\phi$ since ϕ_0 is a constant. The smallest detectable phase shift would be equal to the smallest we could make $\phi - \phi_0$. Since we are considering this quantity to be very small, we can truncate the series after the second term and recast the above as

$$\frac{M(\phi) - M(\phi_0)}{\left.\frac{\partial M}{\partial \phi}\right|_{\phi\to\phi_0}} = \phi - \phi_0 = \Delta\phi_{\min}. \tag{57}$$

If we take ϕ_0 to be the *average* value of the phase then $M(\phi) - M(\phi_0)$ gains the interpretation of being the variance of M (as $M(\langle\phi\rangle) = \langle M(\phi)\rangle$) for a single measurement. Also

$$\left.\frac{\partial M}{\partial \phi}\right|_{\phi\to\phi_0} \to \frac{\partial\langle M\rangle}{\partial\phi},$$

where here the angle brackets mean the average value. Squaring[34] both sides of Eq. (57) then yields

$$(\Delta\phi_{\min})^2 = \frac{(M - \langle M\rangle)^2}{\left(\frac{\partial\langle M\rangle}{\partial\phi}\right)^2}. \tag{58}$$

Since we want the statistically averaged variance for a series of measurements (the standard deviation) of M take $(M - \langle M\rangle)^2$ and average it (which is the standard deviation squared)

$$\begin{aligned}
\langle (M - \langle M\rangle)^2\rangle &= \sum (M - \langle M\rangle)^2 P(M), \\
&= \sum M^2 P(M) - 2\langle M\rangle \sum M P(M) + \langle M\rangle^2 \sum P(M), \\
&= \langle M^2\rangle - \langle M\rangle^2,
\end{aligned}$$

where $P(M)$ is the probabilistic weight function. Now substituting this back into Eq. (58) and taking the square root of the expression

$$\Delta\phi_{\min} = \frac{\sqrt{\langle M^2\rangle - \langle M\rangle^2}}{\left|\frac{\partial\langle M\rangle}{\partial\phi}\right|}.$$

Now we can again put hats on things! Specifically M, making it a quantum mechanical observable. We also recognize the numerator of this expression as being the variance of an operator. So we obtain our final expression

$$\Delta\phi_{\min} = \frac{\Delta\hat{M}}{\left|\frac{\partial\langle\hat{M}\rangle}{\partial\phi}\right|}. \tag{59}$$

Recall from section 3.1.3 the simple example of a standard Mach-Zehnder Interferometer (MZI) with coherent light input, shown in Figure (19). We wish to use our new formula to calculate the sensitivity of this device to changes in the abstract phase ϕ. We need the relationship between the input modes and the output modes given by

$$\begin{aligned}
\hat{a}^\dagger_{\text{before}} &\rightarrow \frac{1}{\sqrt{2}}\left(\hat{a}^\dagger_{\text{after}} + i\hat{b}^\dagger_{\text{after}}\right), \\
\hat{b}^\dagger_{\text{before}} &\rightarrow \frac{1}{\sqrt{2}}\left(\hat{b}^\dagger_{\text{after}} + i\hat{a}^\dagger_{\text{after}}\right), \\
\hat{a}^\dagger_{\text{before}} &\rightarrow e^{i\phi}\hat{a}^\dagger_{\text{after}},
\end{aligned}$$

where the top two transformations take the operators through a 50:50 beams splitter and the bottom line represents a phase shift. This will allow us to write the operators at the

[34]It is necessary to compute the square of the variance as the average value of the variance is zero.

detection end of the device in terms of the operators at the input end. We then take the expectation values of these operators at the input end.

The most important question, with regards to our sensitivity formula, is the choice of the detection scheme $\hat{M}$. Which for a MZI is the difference of the intensities at the bright-port and the dark-port

$$\hat{M} = \hat{b}_f^\dagger \hat{b}_f - \hat{a}_f^\dagger \hat{a}_f.$$

Using this information and Eq. (59) we find for this setup $\Delta\phi_{\min} = 1/|\alpha| = 1/\sqrt{\bar{n}}$. Which is, unsurprisingly, the shot noise limit.

The equation derived in this section will constitute our primary method for calculating the sensitivity of a given interferometric scheme. It is also the most common technique in the relevant literature.

4 Interferometry with Quantum Light

4.1 Classical vs. Quantum Light: There Is No Such Thing as Classical Light – But – the Distinction Is Still Useful

"The word "classical" means only one thing in science: it's wrong!"
-J. R. Oppenheimer as paraphrased by B. R. Frieden [52]

"There is no such *expletive*-ing thing as classical mechanics!"
-Jonathan P. Dowling [53]

"We believe that the entire world is described by quantum mechanics, so you can always say that quantum mechanics is responsible for this or that. So what? Of course it would be responsible, because ultimately everything can be described by quantum mechanics. What I would like to see are things that make me say 'I would not have expected that. Wow, this is unexpected. That is a surprise.' "
-Julio Gea-Banacloche [54]

Quantum mechanics is frequently proclaimed to be the most successful physical theory, success being measured in ability to predict the behaviour of physical systems. But it is also perhaps the most frequently attacked theory in physics.[35] This is because quantum mechanics is so counter-intuitive.

Two properties of quantum mechanics are especially mind bending: superposition and entanglement. Superposition's requirement that some quantum mechanical systems be simultaneously in mutually exclusive states, until observed, is difficult to accept. Entanglement extends this bafflement by asserting that objects may be in joint superpositions. That is, not only do the objects not have definite states, but they may be "connected" in such a way that measurement of one determines the state of the other, regardless of distance.

These two departures from our classical (and every-day) view of the world have at their root something deeper. Quantum mechanics is described by a fundamentally different *statistics* than classical mechanics. Part of this could be seen in our discussion of quasi-probability distributions in section 1.3.5.

Despite the fact that quantum mechanics is fundamental, it is often-times not needed to understand how a system functions. This is because as physical systems become larger, and more interconnected, they display fewer of their "quantum" characteristics. This is best understood in the context of decoherence. Superposition and entanglement require the system in question to be suitably isolated from the outside environment; that is anything that might make a measurement of it. In this sense, most systems requiring a full quantum description are delicate and ephemeral.

One could (and many do) ask the question of *when* a quantum system becomes a classical system. The area of research which seeks to answer this query is called "quantum-to-classical transition theory" and is quite vibrant. However the process of crossing between the two realms is not the subject of this section. Instead we will focus on what the differences are

[35] I would say "in science" but sadly that designation goes to the theory of evolution.

between them. And more importantly, under what circumstances do we *need* a quantum description.

There are several indicators of "quantum-ness", one has already been discussed. That is, when the quasi-probability distributions take on negative values or become more singular than delta functions. Another was mentioned in a glancing fashion when we discussed coherent states: the behaviour of the expectation value of the electric field operator. We had mentioned that coherent states were considered quite "classical" because the electric field of a coherent state was the same as for a classical light field. What also follows for coherent states is, that if we write down a semi-classical representation of an oscillating current, the coherent state appears as the natural solution to the time evolution of the associated field.

Continuing on with our examination of coherent states, we remark that the fact that coherent states obey the shot noise limit, is also a sign of classicality. The shot noise limit was in place before it was understood as a quantum phenomenon, and though the derivation and description is easiest to understand with the quantum tool of quadrature diagrams, classical descriptions are possible.

So we have set up coherent states to be the icons of classicality. In this way we can begin to define "quantum light" as light that does *not* behave in the way coherent light does. We already have one good example, the $|1,1\rangle$ state used in the Hong-Ou-Mandel interferometer. To begin, after the beam splitter, as we have seen, the state becomes entangled as a $|2,0\rangle + |0,2\rangle$ state. A coherent state incident on a beam splitter merely becomes a simple separable state: $|\alpha\rangle|0\rangle \rightarrow |\alpha/2\rangle|\alpha/2\rangle$. Furthermore if we use the Hong-Ou-Mandel device as an interferometer to probe the abstract phase ϕ, with a detection scheme given by the operator $\hat{\Pi} = (-1)^{\hat{N}_a}$ (this is the *parity* operator, which will be extensively studied in chapter 5), we find that the minimum detectable phase shift is given by $\Delta\phi_{\min} = 1/2$. The best we can do with coherent light, (using the shot noise limit for the same number of photons) is $1/\sqrt{2}$. This is more evidence of non-classical behaviour.

Now let's return to the statement that the fundamental difference between classical and quantum mechanics is in the statistics. Take a coherent state, the probability of detecting n photons in the field is given by

$$P_n = |\langle n|\alpha\rangle|^2 = e^{-|\alpha|^2}\frac{|\alpha|^{2n}}{n!} = e^{-\bar{n}}\frac{\bar{n}^n}{n!},$$

which is a Poisson distribution. Thus, photon number distributions narrower than Poisson are considered symptoms of quantum light. Squeezed light may (depending on its parameters) have sub-Poissonian statistics. And the number state, which has a completely defined number of photons, obviously does as well.

The usefulness, and the thus the interest in, quantum light comes from its ability to violate the laws of classical mechanics. Specifically quantum light may reach far below the standard quantum limit on phase sensitivity. That will be the object of the rest of this chapter, as well as the next.

4.2 Coherent-Light Boosted, Super-Sensitive, Quantum Interferometry

This section is based on work done in collaboration with Dr. Girish Agarwal of Oklahoma State University.

We present a new scheme for quantum-optical interferometry. We call it "Coherent-Light Boosted, Super-Sensitive, Quantum Interferometry."

4.2.1 Introduction and Review

In the past few decades it has been shown that the shot-noise limit may be surpassed by taking advantage of the quantum nature of light. Viewing entanglement as a resource for sensitivity enhancement there has been much progress towards achieving the more fundamental Heisenberg limit which goes as $\Delta\phi^2 = 1/N^2$, where N is (usually) the total or average number of particles in-putted into the interferometer. There are several main thrusts in this effort: Utilizing squeezed light as one or both inputs [55, 56, 57, 58, 59, 60, 61], creating maximally path entangled number states (N00N states) inside the device [2, 62, 63, 64, 65, 66, 67, 68, 69, 70, 71, 72], use of Bose-Einstein condensates [73, 74, 75], causing the light to execute multiple passes through the phase shift [76, 77, 78, 79], and other schemes [80, 81, 82, 83, 84, 85, 86].

Though all these programs show promise, they all suffer from debilitating problems: difficulty in creating the required resource (i.e. creating high-N N00N states, large Bose-Einstein condensates, large-gain squeezed light sources, or coaxing the light into passing through the phase shift many times), exotic detection schemes (such as parity [87, 88, 89, 90, 91]), and reliance on yet to be developed technological elements.

As we shall show, our setup avoids all of these problems; whilst granting a large improvement in sensitivity. This flexibility comes from the fact that we allow for the interferometer to utilize bright coherent sources, which enhance squeezed light. We will take as an example the LIGO (Laser Interferometer Gravitational-Wave Observatory) project, and show that by using a squeezing parameter of $r = 3$ (which is not far outside the realm of what is currently available) the shot noise may be reduced by a factor of two hundred. Alternatively the coherent intensity could be reduced by a factor of forty thousand, while maintaining the original sensitivity. Thus our new scheme has the potential to both improve the most sensitive devices and to make those devices more easily accessible.

Klauder et al., [51] building on the foundational work of Eberly and Wódkiewicz [92], showed that standard Mach-Zehnder and Fabry-Perot interferometers are described by the su(2) algebra. They also showed how a device belonging to the the su(1,1) algebra would, in many ways, be superior. This type of interferometer would replace the the first coherent-input beam splitter with a vacuum input four wave mixer. The second beam splitter would also be replaced by a four wave mixer, with the result being super-sensitive scaling to changes in the abstract phase.

Recently Kolkiran and Agarwal studied-coherent-beam stimulated parametric downconversion as an input into a MZI [93]. Their work demonstrated the ability to acquire resolution enhancement at high signal values with good visibility.

The work in this paper is best regarded as the next logical step in this progression. We

modify the Klauder, et al., setup by replacing the vacuum inputs in the initial four-wave mixer with coherent states. In our treatment the four-wave mixers are expressed as optical parametric amplifiers. The – potentially very bright – coherent light in the interferometer "boosts" the squeezed light from the optical parametric amplifiers (OPAs) into the high intensity regime, while maintaining sub-SNL scaling. For some references on injecting photons from an OPA into an external non-vacuum mode see for example [94, 95, 96].

4.2.2 Characterizing the Sensitivity of Our Scheme

Take a setup as depicted in Fig. 23. An OPA is pumped by a coherent source. Assuming the pump beam is undepleted after the first OPA, it then undergoes a π-phase shift and pumps a second OPA. The first OPA is seeded with a coherent beam in each of its input modes. The phase shift to be probed is placed in the upper arm of the device and interacts with one of the output modes of the first OPA. Both output modes are then brought back together into the input modes of the second OPA. The output of the second OPA is then read out by a detector in each of the output modes.

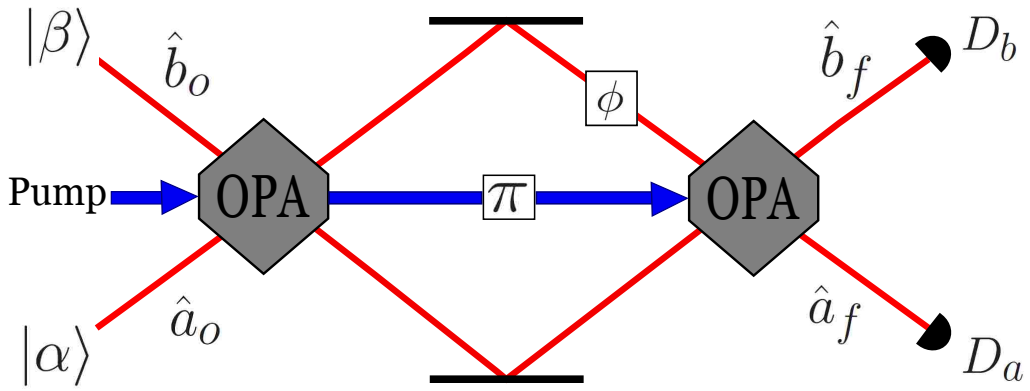

Figure 23: A strong laser beam pumps the first OPA. The beam (which is assumed to be undepleted) undergoes a π phase shift and then pumps the second OPA. The input modes of the first OPA are fed with coherent light. After the first OPA one of the outputs interacts with the phase to be probed. Both outputs are then brought back together as the inputs for the second OPA. Measurement is done on the second OPA's outputs.

This device can be modelled with the transformation between input modes and output modes given in Eq. (60). Where $\mu = \cosh r$, $\nu = \sinh r$, r is the gain of the the OPAs, and the phase of the initial pump has been set to zero. The first 4×4 matrix (from right to left) represents the first OPA, the second represents the phase shift, and the third represents the second OPA. Note that the first and third matrices are inverse transforms of each other, such that $\hat{M}_3\hat{M}_1 = \hat{I}$. Thus in the case that $\phi = 2\pi n$, $n = 0, 1, 2...$ the input equals the output.

$$\begin{bmatrix} \hat{a}_f \\ \hat{a}_f^\dagger \\ \hat{b}_f \\ \hat{b}_f^\dagger \end{bmatrix} = \begin{bmatrix} \mu & 0 & 0 & -\nu \\ 0 & \mu & -\nu & 0 \\ 0 & -\nu & \mu & 0 \\ -\nu & 0 & 0 & \mu \end{bmatrix} \begin{bmatrix} e^{i\phi} & 0 & 0 & 0 \\ 0 & e^{-i\phi} & 0 & 0 \\ 0 & 0 & 1 & 0 \\ 0 & 0 & 0 & 1 \end{bmatrix} \begin{bmatrix} \mu & 0 & 0 & \nu \\ 0 & \mu & \nu & 0 \\ 0 & \nu & \mu & 0 \\ \nu & 0 & 0 & \mu \end{bmatrix} \begin{bmatrix} \hat{a}_o \\ \hat{a}_o^\dagger \\ \hat{b}_o \\ \hat{b}_o^\dagger \end{bmatrix} \tag{60}$$

We wish to analyse the sensitivity of this setup to the phase ϕ; given a simple total intensity detection scheme represented by the operator $\hat{N}_T = \hat{a}_f^\dagger \hat{a}_f + \hat{b}_f^\dagger \hat{b}_f$. We use the standard formula for phase sensitivity 59

$$\Delta\phi^2 = \frac{\langle \hat{N}_T^2 \rangle - \langle \hat{N}_T \rangle^2}{\left(\frac{\partial \langle \hat{N}_T \rangle}{\partial \phi} \right)^2}.$$

In order to perform this calculation we require various moments. The *NCAlgebra* package [97] for Mathematica$^{\text{TM}}$ was utilized to create a program specially designed to do this. Treating the output creation and annihilation operators (functions of the input operators) as a string, the proper commutation relations are applied in a loop until the program recognizes that all operators are normally ordered. Then the input operators act on the input coherent states with easily defined rules. In this was any polynomial moment may be calculated without undue difficulty. Though the program will require more time and resources for more complicated moments. For the following results $\langle \hat{X} \rangle = \langle \alpha, \beta | \hat{X} | \alpha, \beta \rangle$,

$$\begin{aligned}
\langle \hat{a}_f^\dagger a_f \rangle &= 4|\alpha\beta| \sin\left(\frac{\phi}{2}\right) \left[\mu^3 \nu S_+ - \mu \nu^3 S_-\right] \\
&\quad -2\mu^2\nu^2[\cos\phi(1+A) - 1 - |\beta|^2] + |\alpha|^2(\mu^4 + \nu^4), \\
\langle \hat{b}_f^\dagger b_f \rangle &= 4|\alpha\beta| \sin\left(\frac{\phi}{2}\right) \left[\mu^3 \nu S_+ - \mu \nu^3 S_-\right] \\
&\quad -2\mu^2\nu^2[\cos\phi(1+A) - 1 - |\alpha|^2] + |\beta|^2(\mu^4 + \nu^4), \\
\langle \hat{a}_f^\dagger \hat{b}_f^\dagger b_f a_f \rangle &= |\alpha\beta|^2 \left(\mu^8 + \nu^8\right) + 4|\alpha\beta|\mu^7\nu\,(1+A) \sin\left(\frac{\phi}{2}\right) S_+ + 2\mu^6\nu^2 \Big\{1 + 3A + |\alpha|^4 + |\beta|^4 \\
&\quad - \left[1 + 3A + |\alpha|^4 + |\beta|^4 + 4|\alpha\beta|^2\right] \cos(\phi) + |\alpha\beta|^2 \left[2 + \cos(4\theta) + C_+ - 2C'_+\right]\Big\} \\
&\quad -4|\alpha\beta|\mu^5\nu^3 \sin\left(\frac{\phi}{2}\right) \left\{[5+3A]\,S_- - 2\,[3+A]\,S_+ + 2\,[2+A] \sin\left(2\theta + \frac{3\phi}{2}\right)\right\} \\
&\quad +2\mu^4\nu^4 \{4 - 6\cos(\phi) + 2\cos(2\phi) + A\,[6 - 10\cos(\phi) + 4\cos(2\phi)] \\
&\quad +|\alpha\beta|^2\,[7 + 4\cos(4\theta) - 2\cos(4\theta - \phi) - 8\cos(\phi) + 4\cos(2\phi) \\
&\quad -2C'_+\big] + \left[|\alpha|^4 + |\beta|^4\right][1 - 2\cos(\phi) + \cos(2\phi)]\Big\} \\
&\quad +4|\alpha\beta|\mu^3\nu^5 \sin\left(\frac{\phi}{2}\right) \left\{[5+3A]\,S_+ - 2\,[3+A]\,S_- + 2\,[2+A] \sin\left(2\theta - \frac{3\phi}{2}\right)\right\} \\
&\quad +2\mu^2\nu^6 \Big\{1 + 3A + |\alpha|^4 + |\beta|^4 - \left[1 + 3A + |\alpha|^4 + |\beta|^4 + 4|\alpha\beta|^2\right] \cos(\phi)
\end{aligned}$$

$$+|\alpha\beta|^2\left[2+\cos(4\theta)+C_- -2C'_-\right]\Big\} - 4|\alpha\beta|\mu\nu^7(1+A)\sin\left(\frac{\phi}{2}\right)S_-,$$

$$\begin{aligned}
&\langle \hat{a}_f^{\dagger 2}\hat{a}^{\dagger 2}\rangle \\
= \;& |\alpha|^4\left(\mu^8+\nu^8\right) + 8|\alpha^3\beta|\mu^7\nu\sin\left(\frac{\phi}{2}\right)S_+ + 2|\alpha|^2\mu^6\nu^2\left\{2\left[2-2\cos(\phi)-|\alpha|^2\cos(\phi)\right]\right. \\
& \left.+\,|\beta|^2\left[4+\cos(4\theta)-4\cos(\phi)+C_+-2C'_+\right]\right\} \\
& -8|\alpha\beta|\mu^5\nu^3\sin\left(\frac{\phi}{2}\right)\left\{\left[2+2|\alpha|^2+|\beta|^2\right]S_- - 2\left[2+|\beta|^2\right]S_+ + [2+A]\sin\left(2\theta+\frac{3\phi}{2}\right)\right\} \\
& +2\mu^4\nu^4\left\{6-8\cos(\phi)+2\cos(2\phi)+|\alpha|^2[4-8\cos(\phi)+4\cos(2\phi)]\right. \\
& +|\beta|^2[12-16\cos(\phi)+4\cos(2\phi)]+|\alpha|^4[2+\cos(2\phi)]+|\beta|^4[3-4\cos(\phi)+\cos(2\phi)] \\
& \left.+2|\alpha\beta|^2\left[2+2\cos(4\theta)-C'_- -4\cos(\phi)+2\cos(2\phi)-C'_+\right]\right\} \\
& +8|\alpha\beta|\mu^3\nu^5\sin\left(\frac{\phi}{2}\right)\left\{\left[2+2|\alpha|^2+|\beta|^2\right]S_+ - 2\left[2+|\beta|^2\right]S_- + [2+A]\sin\left(2\theta-\frac{3\phi}{2}\right)\right\} \\
& +2|\alpha|^2\mu^2\nu^6\left\{2\left[2-2\cos(\phi)-|\alpha|^2\cos(\phi)\right]\right. \\
& \left.+\,|\beta|^2\left[4+\cos(4\theta)-4\cos(\phi)+C_- -2C'_-\right]\right\} - 8|\alpha^3\beta|\mu\nu^7\sin\left(\frac{\phi}{2}\right)S_-,
\end{aligned}$$

$$\begin{aligned}
&\langle \hat{b}_f^{\dagger 2}\hat{b}_f^{2}\rangle \\
= \;& |\beta|^4\left(\mu^8+\nu^8\right) + 8|\alpha\beta^3|\mu^7\nu\sin\left(\frac{\phi}{2}\right)S_+ + 2|\beta|^2\mu^6\nu^2\left\{2\left[2-2\cos(\phi)-|\alpha|^2\cos(\phi)\right]\right. \\
& \left.+\,|\alpha|^2\left[4+\cos(4\theta)-4\cos(\phi)+C_+-2C'_+\right]\right\} \\
& -8|\alpha\beta|\mu^5\nu^3\sin\left(\frac{\phi}{2}\right)\left\{\left[2+2|\alpha|^2+|\beta|^2\right]S_- - 2\left[2+|\alpha|^2\right]S_+ + [2+A]\sin\left(2\theta+\frac{3\phi}{2}\right)\right\} \\
& +2\mu^4\nu^4\left\{6-8\cos(\phi)+2\cos(2\phi)+|\beta|^2[4-8\cos(\phi)+4\cos(2\phi)]\right. \\
& +|\alpha|^2[12-16\cos(\phi)+4\cos(2\phi)]+|\beta|^4[2+\cos(2\phi)]+|\alpha|^4[3-4\cos(\phi)+\cos(2\phi)] \\
& \left.+2|\alpha\beta|^2\left[2+2\cos(4\theta)-C'_- -4\cos(\phi)+2\cos(2\phi)-C'_+\right]\right\} \\
& +8|\alpha\beta|\mu^3\nu^5\sin\left(\frac{\phi}{2}\right)\left\{\left[2+2|\alpha|^2+|\beta|^2\right]S_+ - 2\left[2+|\alpha|^2\right]S_- + [2+A]\sin\left(2\theta-\frac{3\phi}{2}\right)\right\} \\
& +2|\beta|^2\mu^2\nu^6\left\{2\left[2-2\cos(\phi)-|\beta|^2\cos(\phi)\right]\right. \\
& \left.+\,|\alpha|^2\left[4+\cos(4\theta)-4\cos(\phi)+C_- -C'_-\right]\right\} - 8|\alpha\beta^3|\mu\nu^7\sin\left(\frac{\phi}{2}\right)S_-.
\end{aligned}$$

Where

$$A \;=\; |\alpha|^2+|\beta|^2,$$

$$
\begin{aligned}
S_+ &= \sin\left(2\theta + \frac{\phi}{2}\right), \\
S_- &= \sin\left(2\theta - \frac{\phi}{2}\right), \\
C_+ &= \cos(4\theta + 2\phi), \\
C_- &= \cos(4\theta - 2\phi), \\
C'_+ &= \cos(4\theta + \phi), \\
C'_- &= \cos(4\theta - \phi)
\end{aligned}
$$

and θ is the phase of the in input coherent states (which are taken to be in phase). Using these moments, after significant we obtain

$$
\Delta\phi^2 = \frac{\mu^2\nu^2\left\{B\left[1 + 4\cos(\phi) + 3\cos(2\phi) + 8\cosh(8r)\sin^4\left(\frac{\phi}{2}\right) + 8\cosh(4r)\sin^2(\phi)\right] + \Psi - 8\right\}}{256\left\{|\alpha\beta|\left[\mu^2\sin(2\theta+\phi) - \nu^2\sin(2\theta-\phi)\right] + \left[1 + |\alpha|^2 + |\beta|^2\right]\mu\nu\sin(\phi)\right\}^2},
$$

where

$$
\begin{aligned}
\Psi &= 32|\alpha\beta|^2\left\{\sin(2\theta)\sinh(2r)\left[2\cosh^2(2r)\sin(\phi)\right.\right. \\
&\quad \left. - \sin(2\phi)\sinh^2(2r)\right] + 2\cos(2\theta)\sin^2\left(\frac{\phi}{2}\right)\sinh(4r) \\
&\quad \left.\times\left[\cosh^2(2r) - \cos(\phi)\sinh^2(2r)\right]\right\},
\end{aligned}
$$

and $B = 1 + 2|\alpha|^2 + 2|\beta|^2$. We can check this formula by taking limits and comparing to known expressions. In the limit of $\alpha = \beta = \phi \to 0$ we obtain

$$
\Delta\phi^2 = \frac{1}{\sinh^2(2r)},
$$

which matches the result from Klauder, et al.

A simplification of the general expression for the phase sensitivity occurs when $\phi = 0$ and $\theta = \pi/4$

$$
\Delta\phi^2 = \frac{|\alpha|^2 + |\beta|^2}{4|\alpha\beta|^2\sinh^2(2r)} = \frac{1}{N_{\mathrm{OPA}}(N_{\mathrm{OPA}}+2)}\frac{1}{N_{\mathrm{Coh}}}, \tag{61}
$$

where the intensity N_{Coh} is the amount of coherent light at the input ($|\alpha|^2 + |\beta|^2$), and the intensity N_{OPA} is the amount of light the OPA would emit with vacuum inputs ($2\sinh^2(r)$). After the second equality we have taken $|\alpha| = |\beta|$ for the sake of simplicity. This setup multiplies the sub-Heisenberg sensitivity of the Klauder setup with the standard-quantum-limit sensitivity of a coherent light input MZI.[36] The advantage provided by the coherent-light boosting is evident, allowing sub-SNL scaling at intensities far beyond what entangled sources alone can provide.

[36]It's worthwhile to note that the equation that this expression matches in the original Klauder paper is written incorrectly. Whether this is the result of a typo or mathematical error is unknown.

Figure 24: A plot of the phase sensitivity as a function of the probe phase (ϕ) and the input phase (θ), with $r = 0.5$ and the flux of the coherent input equal to what the squeezed flux would be with vacuum inputs.

It should be noted that the result in Eq. (61), though simple, is not optimal for our scheme. The full expression shows that there is a complicated relationship between pump phase, probe phase, OPA gains, input coherent states, and the phase sensitivity. The choice of $\phi = 0, \theta = \pi/4$ was made only because it caused significant simplification. If the amplitude of the input states and the gain of the OPAs are known, then the bias and input phases may be chosen such that the phase sensitivity is maximized. If this is done some additional minor improvement can be obtained. The effect is most pronounced at low photon numbers. Take as an example Fig. 24; it is a plot of the phase sensitivity as a function of the probe phase (ϕ) and the input phase (θ), with $r = 0.5$ and the flux of the coherent input equal to what the squeezed flux would be with vacuum inputs. For each value of θ there are values of ϕ for which the smallest detectable phase shift is minimized. These effects become less pronounced as either the gain or the coherent flux are increased. For clarity, slices at constant input phase (θ) for various photon fluxes are provided in Fig. 25.

4.2.3 Examples and Comparisons

Let us take a simple numerical example. Gravitational wave detectors are essentially the largest and most sensitive interferometers to date. There are many of these interferometers around the world, the largest of which are in the LIGO project. Their interferometer arms have a circulating photon flux on the order of 10^{23}photons/sec (20kW of circulating power at a wavelength of 1064nm [98])[37]. If we we take our theoretical setup with a gain of $r = 3$ we can use Eq. (61) to calculate the coherent intensity necessary to achieve the same phase sensitivity (making the vast simplification that LIGO is a simple shot-noise-limited MZI) and arrive at $\sim 2.5 \times 10^{18}$ photons/sec, forty thousand times less than LIGO. Vacuum

[37]I would like to thank Jeff Kissel for helping with this quick calculation.

Figure 25: Slices across Fig. 24 at input phase $\theta = \pi/4$. Phase sensitivity as a function of the probe phase, with the flux of the coherent input equal to what the squeezed flux would be with vacuum inputs. The gain (r) is set to 0.5 (dashed), 1 (dotted), and 1.5 (solid).

inputs (squeezed light alone, as in the Klauder setup) would require a gain of $r \simeq 13.6$. Conversely if the coherent intensity were kept the same and the squeezed light added then the phase sensitivity would be improved by a factor of two hundred. Admittedly this is a large squeezing factor. However we would like to point out that a gain of $r = 2.25$ has been reported recently, in [99] (a gain of 4.5 in the language of that paper). So it seems likely that a gain of three will be available in the near future.

One could ask two pointed questions about our new scheme: (1) What advantage does this offer over techniques which are already planned for use in the next LIGO iteration and other next-generation, super-sensitive schemes; namely single-mode squeezed light incident into the dark input of an MZI? [100] (2) In order to create bright entangled sources – such as the OPAs in our setup – one must employ a strong coherent pump beam. Is it really practically advantageous to employ this quantum light in an interferometer, rather than simply adding this strong pump laser into the device classically. In other words, taking into account the fact that very bright lasers are quite readily available, do squeezed light setups (ours in particular) really "win out" over the brute force technique of cranking up the coherent intensity as high as it will go?

The two questions are linked. To answer the second first: Super-sensitive interferometers suffer from both shot noise (N_S) and radiation-pressure noise (N_{RP}). At lower intensities N_S dominates, however in the regime that LIGO now operates in, N_{RP} has become as important, meaning that a kind of saddle point has been reached where either increasing or decreasing the intensity will lead to increased quantum noise (via N_{RP} or N_S respectively). Therefore it is very advantageous to use squeezed light as it reduces N_S at a much faster rate than it increases N_{RP}. Furthermore, even just considering N_S, the rapid scaling of squeezed light does indeed "win". We can see this with a toy example. Suppose we have one interferometer which uses a coherent pump driven OPA to generate the squeezed light, and another which

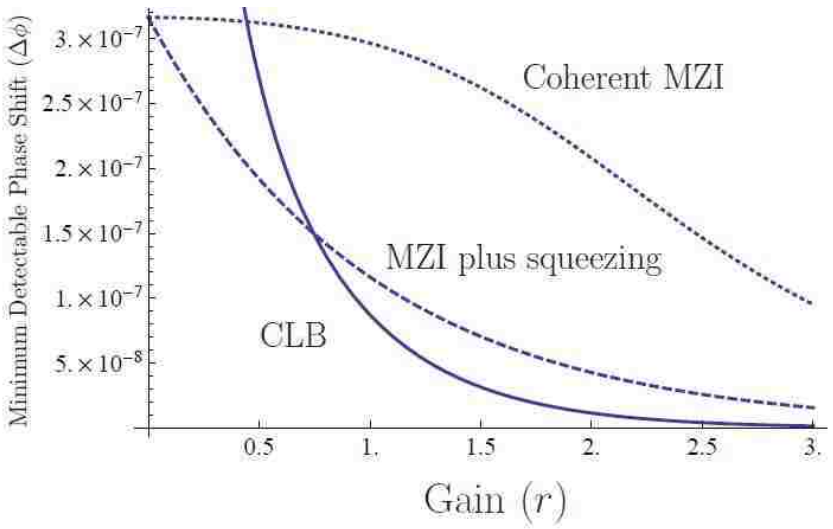

Figure 26: Comparison of three interferometer schemes. The dashed line represents an MZI with 10^{13} photons of coherent light in one input mode and squeezed light in the other. The solid line is our coherent-light boost (CLB) scheme, with 5×10^{12} photons input into each mode. The dotted line is a standard coherent-input-only MZI with additional intensity proportional to what would be needed for a pump to create the equivalent gain in the other two setups: $I_{\text{total}} = 10^{13} + 10^{12}\sinh^2(r)$.

has a classical input with that same pump *added* to the classical input beam (given that it takes approximately 10^{12} pump photons to make one pair of entangled photons [101]). This analysis is presented in Fig. (26). As can be seen, both a squeezed-light added MZI – and our coherent-light boosted setup – consistently outperform a solely coherent-input MZI for a wide range of gains.

To answer the first question, take the high gain limit of Eq. (61) which reduces to $\Delta\phi = e^{-2r}/\sqrt{2N_{\text{Coh}}}$. Compare this with a SU(2) MZI with one squeezed input (for $N_{\text{Coh}} \gg N_{\text{Squeezed}}$): $\Delta\phi = e^{-r}/\sqrt{N_{\text{Coh}}}$ (see for example [102]). Thus for large gains (a gain of $r = 2$ is sufficient for being called large) our setup is exponentially better than single mode squeezing. Again we refer to Fig. (26) for a more complete comparison.

4.2.4 Conclusion

We have presented a theoretical analysis of a new interferometric scheme that uses potentially strong coherent beams to boost the sensitivity of interferometers employing squeezed light. The result is a promising form of metrology, which achieves scaling far below the shot noise limit for bright sources. It uses only simple intensity measurement and components that are currently available. The phase sensitivity of this device scales as a coherent light input Mach-Zehnder interferometer multiplied by the sub-Heisenberg scaling of the Klauder et al. squeezed light interferometer. It does well when compared to other quantum – and even classical – schemes.

5 Parity Measurement and Homodyne Detection

5.1 Parity: The Universal Detection Scheme

"I was in Vegas last week. I was at the roulette table, having a lengthy argument about what I considered an 'odd' number."
-Steven Wright, Comedian

Parity is an odd concept. It encompasses certain ideas about the symmetry of a physical system.

It is best understood from the perspective of a parity transformation – which is, in two dimensions, a flip of the sign of one of the coordinates. In three dimensions a parity transformation is comprised of changing the sign of all three coordinates. A parity transformation in two dimensions may not be replicated by rotations, however a rotation through an extra (3rd) dimension may accomplish this. Imagine a paper cut-out of a person's hand laying on a table. Without picking it up we could never change a right hand to a left hand (or vice versa) by rotating it. But if we pick up the cut-out and rotate it through the 3rd dimension this is easily accomplished. Likewise we can not change the parity of a three dimensional object by rotating it in our physical universe, and since there is no 4th dimension to rotate it through, we can not change its parity at all.[38]

The kind of parity we will be concerned with is the parity of photon number, measured at one of the outputs of an optical interferometer. This is represented by the simple function $P = (-1)^N$. An even number of photons yields $P = 1$, while an odd number yields $P = -1$. Thus we are talking of the simple mathematical parity of a number. But why should this be a quantity of interest? And what does it say about the physical symmetry of the device?

The second question is best left to the next section, but the first can be partially answered by citing a paper by Chiruvelli and Lee: *Parity Measurements in Quantum Optical Metrology*[103]. In this paper the authors show, that for a broad class of states which are – or could be – used in optical interferometry (coherent states, number states at one or both inputs, Yurke, modified Yuen, Pezze-Smerzi, N00N, and Berry-Wiseman Optimal states), parity does as well as detection schemes designed specifically for that state. Thus parity constituents a "universal" detection scheme, one that will work for whichever input is chosen.[39] While some of these other measurement schemes exist only as abstract mathematical operators, without any known experimental interpretation, parity can be realized

[38] A *four* dimensional being could accomplish this. Though he, she, or it would be confounded by a request to invert a four dimensional object from its own plane of existence. It is interesting to mention that during the Victorian Spiritualist fad of the mid-to-late 19$^{\text{th}}$ century many self proclaimed "spirit-mediums" claimed that the fourth dimension was the realm that ghosts inhabited. These people, claiming to have contact with these ghosts, could accomplish feats of "four-dimensional magic" such as tying knots in closed loops of rope. The most famous of these charlatans was Henry Slade. Slade also happened to be the favorite medium of astronomer Johann Zöllner, who posed to Slade several challenges that only a truly four dimensional creature could accomplish, such as changing the direction a snail shell spiralled (i.e. changing its handedness). Slade was unable to do this of course, claiming the spirits were unwilling for whatever reason. He did manage – through slight of hand – some other tricks which impressed the gullible Zöllner enough for him to write a book about his "experiments": *Transcendental Physics: An Account of Experimental Investigations.*

[39] It remains to be seen whether this holds for *any* state, or merely those which have been considered so far.

with photon-number-counting detectors. Alternatively a Kerr material may be used to find the evenness or oddness of a light field [104]. But the feasibility of this scheme rests on the availability of materials with large non-linearities.

This paper also shows why parity is so useful, it is because parity – after propagated back through a beam splitter – becomes an operator that acts on all the off-diagonal terms of a density matrix, thus gathering up all possible coherence bearing terms.

An interesting possible application of the versatility of parity detection might be metrology in the presence of loss. Many of the states which show the greatest potential phase sensitivity also quickly degrade in lossy environments, limiting their usefulness. In a real world application of super-sensitive remote sensing it may, or may not, be advantageous to use delicate quantum light – depending on the conditions in the environment. One could imagine an adaptable device which could be used to send one of several different states out into the environment to perform measurement. Perhaps a N00N state [105] when conditions are good, an M&M' state [106] when conditions are fair, and a coherent state when things get bad. The receiver for such a device would not need to be different for each kind of light, but could always use parity detection, adding some robustness and ease of use.

Of particular interest is using parity detection on a two-mode squeezed-light interferometer. It has been shown that an interferometer with squeezed light input into both ports and parity detection can reach below the Heisenberg limit.[50] As such, implementing parity for squeezed light is especially promising. For the remainder of this chapter we will focus on parity detection of squeezed light. However it should be noted that the techniques we develop – with some minor modification – will be applicable to other types of light as well.

Unfortunately number-resolving detectors are difficult to make and operate, and only work at low photon numbers. Though there is significant effort and continual progress in this field [107, 108, 109, 110, 111, 112, 113, 114, 115] it would be useful to have another way of determining parity. There is hope for such an endeavour since, as it has been pointed out multiple times in the literature, photon number counting suffices for parity measurement but it provides more information than is necessary. Parity only requires that we know whether the photon number is even or odd, not exactly what it is. As will be shown – it is not necessary to measure the photon number, what we can substitute is the value of the Wigner function measured at the origin. This is an approach which is experimentally implementable.

5.2 The Relationship Between Parity and the Wigner Function

The relationship between parity and the value of the Wigner function at the origin has long been known. [116] I include a derivation of this fact by Dr. Girish Agarwal, transmitted in a personal communication, since it is particularly clear and methodical.

First, start with the characteristic function of the Wigner function $C_W = \mathrm{Tr}[\hat{\rho}\hat{D}(\lambda)]$, where $\hat{\rho}$ is the density matrix, and $\hat{D}(\lambda)$ is the displacement operator. Accordingly the Wigner function is defined in general by

$$W(\alpha, \alpha^*) = \frac{1}{\pi^2} \int d^2\lambda e^{\lambda^*\alpha - \lambda\alpha^*} C_W(\lambda),$$

which at the origin then becomes

$$W(0,0) = \frac{1}{\pi^2}\int d^2\lambda \mathrm{Tr}\left[e^{\lambda\hat{a}^\dagger - \lambda^*\hat{a}}\hat{\rho}\right].$$

Now using the Cambell-Baker-Hausdorf (CBH) theorem, $e^{\hat{A}+\hat{B}} = e^{-\frac{1}{2}[\hat{A},\hat{B}]}e^{\hat{A}}e^{\hat{B}}$ (as long as $\hat{A}$ and $\hat{B}$ commute with their commutator), we rewrite

$$W(0,0) = \frac{1}{\pi^2}\int d^2\lambda e^{-\frac{1}{2}|\lambda|^2}\langle e^{\lambda\hat{a}^\dagger}e^{-\lambda^*\hat{a}}\rangle,$$

keeping in mind that the trace over the density matrix tensored with an operator is the expectation value of that operator. Expanding out the exponentials obtains

$$\begin{aligned} W(0,0) &= \frac{1}{\pi^2}\int d^2\lambda e^{-\frac{1}{2}|\lambda|^2}\left\langle \sum_{q=0}^{\infty}\frac{(\lambda\hat{a}^\dagger)^q}{q!}\sum_{p=0}^{\infty}\frac{(-\lambda^*\hat{a})^p}{p!}\right\rangle \\ &= \frac{1}{\pi^2}\int_0^\infty\int_0^{2\pi} d|\lambda|d\theta|\lambda|e^{-\frac{1}{2}|\lambda|^2}\left\langle \sum_{p=q}\frac{(-|\lambda|^2)^p\hat{a}^{\dagger p}\hat{a}^p}{(p!)^2} + \sum_{p\neq q}\frac{(-1)^p|\lambda|^{p+q}e^{i\theta(q-p)}\hat{a}^{\dagger q}\hat{a}^p}{p!q!}\right\rangle. \end{aligned}$$

In the second line we have switched to polar coordinates ($\lambda = |\lambda|e^{i\theta}$) and rearranged the sums into terms where $p = q$ and terms where $p \neq q$. Now note that

$$\int_0^{2\pi} d\theta e^{i\theta x} = 0,$$

for all integers x. So all the terms in the second sum integrate to zero and we have, after some rearranging,

$$W(0,0) = \frac{1}{\pi^2}\sum_p\int_0^\infty\int_0^{2\pi} d|\lambda|d\theta|\lambda|e^{-\frac{1}{2}|\lambda|^2}(-|\lambda|^2)^p\left\langle\frac{\hat{a}^{\dagger p}\hat{a}^p}{(p!)^2}\right\rangle.$$

The integral over $|\lambda|$ is not trivial but it can be changed to a known form with some substitution, the integral over θ is straightforward, leaving

$$\begin{aligned} W(0,0) &= \frac{1}{\pi}\sum_p\frac{(-1)^p 2^{p+1}}{p!}\left\langle\frac{\hat{a}^{\dagger p}\hat{a}^p}{(p!)^2}\right\rangle \\ &= \frac{2}{\pi}\sum_{n=0}^{\infty}C_n\langle n|\sum_{p=0}^{n}\frac{(-2)^p}{p!}\hat{a}^{\dagger p}\hat{a}^p|n\rangle, \end{aligned}$$

where in the second line the expectation value is taken to be explicitly in the number basis (note that the sum over p can now only extend to n). The operators acting on the right number state produce

$$W(0,0) = \frac{2}{\pi}\sum_{n=0}^{\infty} C_n \sum_{p=0}^{n} \left(\begin{array}{c} n \\ p \end{array} \right) (1)^n (-2)^p,$$

where all the factorials have been written as n-choose-p. Also note that we have multiplied by one. The sum over p is now clearly the binomial expansion of $(1-2)^n$. And so all that remains is

$$W(0,0) = \frac{2}{\pi}\sum_{n=0}^{\infty} C_n (-1)^n = \frac{2}{\pi}\left\langle (-1)^{\hat{n}} \right\rangle. \tag{62}$$

The expectation value of the parity operator times a constant. Q.E.D.

We are now in a position to answer the question posed in the previous section: "What does parity have to say about the physical symmetry of the device?" We can see now that parity is not related to a physical symmetry of the object in question, but to the Wigner function (a quasi-probability distribution) which describes the statistics of the light field, and the inversion of its centre point through the plane.

5.3 Practical Measurement of Parity Using Homodyne

Now that it has been established how the parity operator is related to the Wigner function at the origin, we can now begin to look at how to measure it in a practical experiment.

Wigner functions of an unknown quantum state are typically constructed by performing optical quantum state tomography. [117] This process is similar in concept to the CT (computerized tomography) scans used in hospitals and in certain realms of research. The way CT scans work is by first taking a two dimensional X-ray image of an object by rotating the X-ray emitter and imager through a single plane. This constitutes one "slice" of the total picture. Many of these slices are built up and are then used to reconstruct a three dimensional internal image of the desired person or object. The process of creating the whole 3-D picture from the many 2-D images is known as tomography.

Optical quantum state tomography is in many ways analogous to this procedure (and in some cases even makes use of the same software). The difference is that instead of physical dimensions we have the abstract vector space in which the Wigner function exists. Homodyne measurements[40] are used to measure the the expectation values of the creation and annihilation operators at different bias phases (each phase constituting a "slice"). The full Wigner function can then be built up from these "images". This would be sufficient to discover the value at the origin and thus the parity, but it is overkill. We only need the value at one point.

Let us consider a specific class of Wigner functions: the Gaussian states. These states are so called because their descriptions as Wigner functions are Gaussian in shape. This includes a very broad category of states, including the coherent states and, conveniently, the squeezed states. It has been shown [118] that Gaussian Wigner functions are given by

[40] An explanation of this concept will be provided shortly

$$W(\alpha,\alpha^*) = \frac{1}{\pi(\tau^2-4|\mu|^2)} e^{-\frac{\mu(\alpha-\alpha_o)^2+\mu^*(\alpha-\alpha_o)^{*2}+\tau|\alpha-\alpha_o|^2}{\tau^2-4|\mu|^2}}$$
$$W(0,0) = \frac{1}{\pi(\tau^2-4|\mu|^2)} e^{-\frac{\mu\alpha_o^2+\mu^*\alpha_o^{*2}+\tau|\alpha_o|^2}{\tau^2-4|\mu|^2}}$$

where $\langle\hat{a}\rangle = \alpha_o$, $\langle\hat{a}^{\dagger 2}\rangle - \langle\hat{a}^\dagger\rangle^2 = -2\mu$, and $\langle\hat{a}^\dagger\hat{a}+\frac{1}{2}\rangle - \langle\hat{a}^\dagger\rangle\langle\hat{a}\rangle = \tau$. So we need to find α_o, μ, τ, and their complex conjugates. Since squeezing the vacuum state does not change the expectation values of its quadratures $\alpha_o = 0$. And we are left with

$$W(0,0) = \frac{1}{\pi(\tau^2-4|\mu|^2)}. \tag{63}$$

So now we need only find $\langle\hat{a}^\dagger\hat{a}\rangle$. As well as $\langle\hat{a}^{\dagger 2}\rangle$ and/or its complex conjugate. The first is simply the intensity of the light, this is easy to obtain. However the second expectation value is of a non-Hermitian operator[41]. Thus it can not be measured directly. However the technique of homodyning may be employed to determine it indirectly.

To begin let's take the "standard" example of homodyne measurement. The problem that homodyne techniques address is how to measure an, usually inaccessible, quadrature of the light field. The unknown light beam (represented by the state vector $|?\rangle$), on which measurements are to be performed, is mixed on a beam splitter with a strong coherent beam of known intensity and phase ($|\beta\rangle$), called a local oscillator. Photo-detectors are then placed at the output ports. See Fig. 27.

For the case of a 50-50 beam splitter we utilize the standard transformations $\hat{c} \to (\hat{a} + i\hat{b})/\sqrt{2}$ and $\hat{d} \to (\hat{b} + i\hat{a})/\sqrt{2}$. The intensity difference at the detectors in terms of the input operators is then given by

$$\hat{N}_D = \hat{c}^\dagger\hat{c} - \hat{d}^\dagger\hat{d} = -i(\hat{a}^\dagger\hat{b} - \hat{b}^\dagger\hat{a}). \tag{64}$$

The expectation value of Eq. (64), taken at the input is

$$\langle?|\langle\beta|\hat{N}_D|\beta\rangle|?\rangle = -i|\beta|\left(\langle\hat{a}^\dagger\rangle e^{i\phi} - \langle\hat{a}\rangle e^{-i\phi}\right),$$

where ϕ is the known phase of the local oscillator. Let's call this expectation value $Y(\phi)$. Now we see that we can measure either quadrature of the unknown light field by making measurements at two different phases of the local oscillator

$$\langle\hat{a}^\dagger\rangle = \frac{Y\left(\frac{\pi}{2}\right) + iY(0)}{2|\beta|}$$
$$\langle\hat{a}\rangle = \frac{Y\left(\frac{\pi}{2}\right) - iY(0)}{2|\beta|}$$

[41] Hermitian operators satisfy $\hat{H}^\dagger = \hat{H}$. For an operator to be an observable it must be Hermitian (it's expectation value must be real).

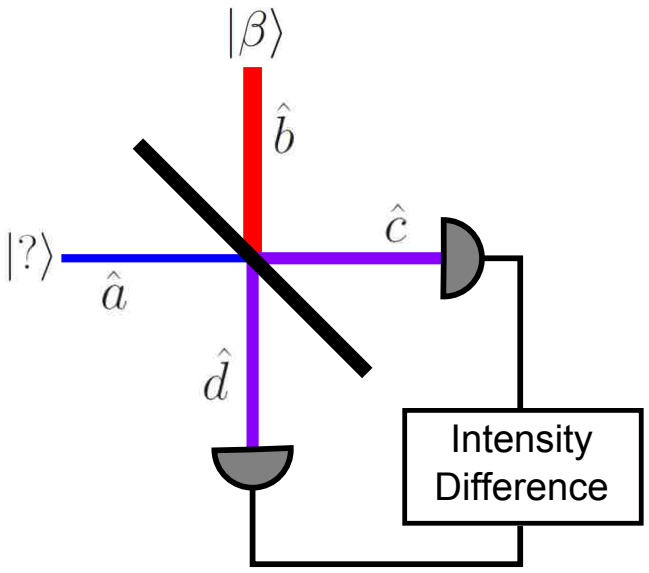

Figure 27: An unknown light beam ($|?\rangle$) is mixed on a beam splitter with a strong coherent beam of known intensity and phase ($|\beta\rangle$), called a local oscillator. Photo-detectors are then placed at the output ports. These are connected to a post-processing unit which carries out a difference count. Thus the quadratures of the unknown light may be measured.

Now we return to our related problem of measuring the second order moments of squeezed light in order to obtain the Wigner function at the origin – and thus parity. We will need the second order moment $\langle \hat{a}^2 \rangle$ and its complex conjugate. To do this take the setup in Fig. 28, a strong pump beam is sent in from the left. Some of the beam is peeled of for later use as two equal intensity local oscillators. The beam then goes through a frequency doubler before pumping an OPA. Thus the squeezed light and the reference beams are of the same frequency, and are phase locked. The squeezed light then proceeds through a standard MZI interacting with the phase to be measured. On output each mode is mixed separately on a beam splitter with one of the local oscillators. After this four detectors make intensity measurements on the final outputs which are fed into a post processor which controls the bias phases placed on the local oscillators according to a prescription which will be discussed shortly. This scheme is designed to measure the second order quadrature on the lower output port of the MZI.

First note that $\langle \hat{a}^2 \rangle$ becomes $1/2\left(\langle \hat{z}_1^2 \rangle - \langle \hat{z}_2^2 \rangle + 2i\langle \hat{z}_1 \hat{z}_2 \rangle\right)$ when propagated back through the last beam splitter. Now we "guess" the moment $\hat{d}_1^\dagger \hat{d}_1 \hat{c}_1^\dagger \hat{c}_1 + \hat{d}_2^\dagger \hat{d}_2 \hat{c}_2^\dagger \hat{c}_2$, which represents the intensity-intensity correlations between the bottom two detectors plus the intensity-intensity correlations between the top two detectors. Back propagating this to the z modes yields

$$\begin{aligned} X(|\beta|, \theta_1, \theta_2) &\equiv \langle ?|\langle \beta_1|\langle \beta_2| \left(\hat{d}_1^\dagger \hat{d}_1 \hat{c}_1^\dagger \hat{c}_1 + \hat{d}_2^\dagger \hat{d}_2 \hat{c}_2^\dagger \hat{c}_2 \right) |\beta_2\rangle |\beta_1\rangle |?\rangle \\ &= \frac{1}{4} \Big\langle 2\hat{z}_1^\dagger \hat{z}_1 \hat{z}_2^\dagger \hat{z}_2 + \frac{1}{2}\hat{z}_1^{\dagger 2}\hat{z}_1^2 + \frac{1}{2}\hat{z}_2^{\dagger 2}\hat{z}_2^2 - \frac{1}{2}\hat{z}_1^{\dagger 2}\hat{z}_2^2 - \frac{1}{2}\hat{z}_2^{\dagger 2}\hat{z}_1^2 \\ &\quad + \frac{\hat{b}_1^2 - \hat{b}_2^2}{2}\left(\hat{z}_1^{\dagger 2} - \hat{z}_2^{\dagger 2}\right) - i\left(\hat{b}_1^2 + \hat{b}_2^2\right)\hat{z}_1^\dagger \hat{z}_2^\dagger \end{aligned}$$

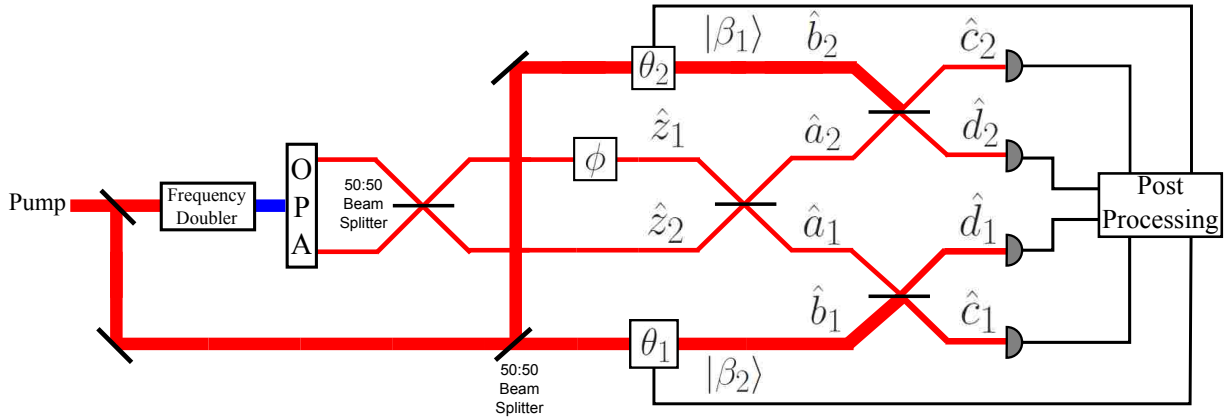

Figure 28: The setup we will discuss: a strong pump beam is sent in from the left. Some of the beam is peeled of for later use as two equal intensity local oscillators. The beam then goes through a frequency doubler before pumping an OPA. Thus the squeezed light and the reference beams are of the same frequency, and are phase locked. The squeezed light then proceeds through a standard MZI interacting with the phase to be measured. On output each mode is mixed separately on a beam splitter with one of the local oscillators. After this four detectors make intensity measurements on the final outputs which are fed into a post processor which controls the bias phases placed on the local oscillators.

$$+\frac{\hat{b}_1^{\dagger 2}-\hat{b}_2^{\dagger 2}}{2}\left(\hat{z}_1^2-\hat{z}_2^2\right)+i\left(\hat{b}_1^{\dagger 2}+\hat{b}_2^{\dagger 2}\right)\hat{z}_1\hat{z}_2 + \hat{b}_1^{\dagger 2}\hat{b}_1^2+\hat{b}_2^{\dagger 2}\hat{b}_2^2\Big\rangle, \tag{65}$$

where $X(|\beta|,\theta_1,\theta_2)$ has been defined, and is a function of the intensities and phases of the local oscillators (where the intensities have been taken to be equivalent). Also, $|?\rangle$ represents the unknown state in the a modes. The middle two lines of the above contain the information we need to obtain $1/2\left(\langle\hat{z}_1^2\rangle-\langle\hat{z}_2^2\rangle\ +2i\langle\hat{z}_1\hat{z}_2\rangle\right)$ and thus – indirectly – $\langle\hat{a}^2\rangle$. The bottom line is simply the intensity squared of the upper and lower mixing (homodyne) modes. However the top line (from here on labelled Z^4) is less tractable, it introduces an unknown quantity to the homodyne equation. It must be eliminated. consider an X measurement (again the intensity-intensity correlations between the bottom two detectors plus the intensity-intensity correlations between the top two detectors) where $\theta_2=\theta_1+\pi/2$ and we get

$$X\left(|\beta|,\theta_1,\theta_1+\frac{\pi}{2}\right)=Z^4+2|\beta|^4+|\beta|^2\left[e^{2i\theta_1}\left\langle\hat{z}_1^{\dagger 2}-\hat{z}_2^{\dagger 2}\right\rangle+e^{-2i\theta_1}\left\langle\hat{z}_1^2-\hat{z}_2^2\right\rangle\right]. \tag{66}$$

Also, we will need a measurement where both phases are set equal and offset by $\pi/2$

$$X\left(|\beta|,\theta_1+\frac{\pi}{2},\theta_1+\frac{\pi}{2}\right)=Z^4+2|\beta|^4+2i|\beta|^2\left[e^{2i\theta_1}\left\langle\hat{z}_1^{\dagger}\hat{z}_2^{\dagger}\right\rangle-e^{-2i\theta_1}\left\langle\hat{z}_1\hat{z}_2\right\rangle\right].$$

Now we need to define a new measurement

$$
\begin{aligned}
X'(|\beta|,\theta_1) &\equiv X\left(|\beta|,\theta_1,\theta_1+\frac{\pi}{2}\right)-X\left(|\beta|,\theta_1+\frac{\pi}{2},\theta_1+\frac{\pi}{2}\right)\\
&= |\beta|^2 e^{2i\theta_1}\left[\left\langle\hat{z}_1^{\dagger 2}\right\rangle-\left\langle\hat{z}_2^{\dagger 2}\right\rangle-2i\left\langle\hat{z}_1^{\dagger}\hat{z}_2^{\dagger}\right\rangle\right]\\
&\quad +|\beta|^2 e^{-2i\theta_1}\left[\left\langle\hat{z}_1^{2}\right\rangle-\left\langle\hat{z}_2^{2}\right\rangle+2i\left\langle\hat{z}_1\hat{z}_2\right\rangle\right]\\
&= |\beta|^2\left[e^{2i\theta_1}\langle\hat{a}_1^{\dagger 2}\rangle+e^{-2i\theta_1}\langle\hat{a}_1^{2}\rangle\right].
\end{aligned}
$$

Where in the last line we have propagated the operators back forward through the beam splitter to arrive at the desired moments. What remains is fairly straightforward. In order to measure one or the other quadrature take X' at two phases and combine:

$$\langle\hat{a}_1^{\dagger 2}\rangle=\frac{X'\left(|\beta|,\frac{\pi}{4}\right)+iX'(|\beta|,0)}{2i|\beta|^2} \tag{67}$$

$$\langle\hat{a}_1^{2}\rangle=\frac{iX'(|\beta|,0)-X'\left(|\beta|,\frac{\pi}{4}\right)}{2i|\beta|^2}. \tag{68}$$

So we have arrived at the prescription needed to measure the second order quadrature moments, and thus the value of the Wigner function at the origin, and thus parity. Let's take minute to recap and discuss what must be physically done to implement Eqs. (67,68). Measure the intensity-intensity correlations between the two bottom detectors and add this to the same for the top two detectors. This must be done first while the bottom homodyne phase (θ_1) is set to zero and the top homodyne phase (θ_2) is set to $\pi/2$, then again with $\theta_1=\pi/2$, and with θ_2 still set to $\pi/2$. Then a measurement with $\theta_1=\pi/4$ and $\theta_2=3\pi/4$, and finally a measurement with $\theta_1=3\pi/4$ and θ_2 again still set to $3\pi/4$. So parity requires four measurements at two settings of θ_2 and four settings of θ_1.

To conclude we have devised a method by which the very desirable parity measurement may be performed on Gaussian states. We have shown in detail how to set up a parity detector for the specific case of squeezed light using double homodyning, thus realizing the possibility of practical sub-Heisenberg phase estimation in a Mach-Zehnder Interferometer.

6 Conclusions

We have theoretically investigated, in detail, three potentially useful physical systems, after first developing the theoretical framework necessary for studying them. Specifically we have studied the absorption properties of maximally path entangled number (N00N) states, coherent-light boosted super-sensitive quantum interferometry, and the use of a double homodyning technique to perform parity detection on a two-more squeezed vacuum interferometer.

In our study of multiphoton absorption we found that, as expected, the absorption properties of ideal N00N states were poor when compared to other states of light, but still fared better than Fock states. However we found that for the case of realistic 2002 states, generated from spontaneous parametric down conversion, the high degree of temporal correlation resulting from the spectral entanglement created a large advantage in two-photon absorption. Though we studied only the $N = 2$ N00N state in realistic detail, our research gives hope to the idea that when efficient sources of larger N00N states are available, the N-photon absorption properties are likely to be good as well. It is our hope that this will stimulate and encourage further research into the field of quantum lithography.

Next we developed a new scheme for quantum interferometry, dubbed Coherent-Light Boosted Interferometry. Two, potentially very strong, coherent states are fed into an optical parametric amplifier (OPA), which itself is pumped with a strong coherent field; the output then interacts with an abstract phase and is fed into a second OPA. The final output is then registered with intensity measuring photo-detectors. We show that this scheme is very competitive with both classical and quantum interferometric schemes, and has several advantages: Its detection scheme, total intensity measurement, is simple. It can operate at high-photon fluxes, and requires no unknown technological elements.

Finally, we developed a practical detection scheme which indirectly obtains parity for a two-mode squeezed vacuum (TMSV) input interferometer. This may make possible a sub-Heisenberg interferometer in the near future. The scheme operates by mixing the output states of the TMSV Mach-Zehnder interferometer, with strong local oscillators and performing intensity correlation measurements at certain bias phases.

These systems we have studied provide numerous opportunities for expansion. The Quantum Well is far from dry.[42] It remains to be seen whether the total intensity detection scheme for the coherent-light boosted setup is optimal. Determining this will require a study of the Fisher information of the system, and a detailed understanding of the role of the reference beam. Also, there are several potential applications of the parity detection scheme apart from the interferometer presented. With some adjustments to the measuring process, it may be possible to extend the parity detection to number detection, for small photon numbers of specific states of light. This could have further potential application to metrology, and possibly quantum computing.

[42] This is my last pun. (And this my last footnote. *And this my last parenthetical statement *And so on...**)

References

[1] C. H. Bennett, F. Bessette, G. Brassard, L. Salvail, and J. Smolin, Journal of Cryptology **5**, 3 (1992).

[2] Agedi N. Boto, Pieter Kok, Daniel S. Abrams, Samuel L. Braunstein, Colin P. Williams, and Jonathan P. Dowling, Phys. Rev. Lett. **85**, 2733 (2000).

[3] R. A. Shelby, D. R. Smith, S. Schultz, D. R. Smith, S. Shultz, Science **292**, 5514 (2001).

[4] M. A. Nielsen, I. L. Chuang *Quantum Computation and Quantum Information*, (Cambridge University Press, MA, 2001).

[5] James Clerk Maxwell, Philosophical Transactions of the Royal Society of London **155**, 459 (1865).

[6] H. R. Hertz, Annalen der Physik, **267**, 983-1000 (1887).

[7] Max Planck, Annalen der Physik, **4**, 553 (1901).

[8] Phillip Lenard, *Über Kathodenstrahlen*, (1906).

[9] Albert Einstein, Annalen der Physik **17**, 132 (1905).

[10] Louis de Broglie, *Recherches sur la thorie des quanta*, Doctoral Thesis, Paris (1924).

[11] E. Yablonovitch and R. B. Vrijen, Opt. Eng. **38**, 334 (1999).

[12] C. F. Wildfeuer, and J. P. Dowling, Phys. Rev. A, **76**, 052101 (2007).

[13] Roy J. Glauber, Phys. Rev. **130**, 2529 (1963).

[14] Mankei Tsang, Phys. Rev A **75**, 043813 (2007).

[15] Robert W. Boyd, Sean J. Bently, J. Mod. Optic. **53**, 713 (2006).

[16] Hwang Lee, Pieter Kok, Jonathan P. Dowling, arXiv:quant-ph/0306113v1 (2008).

[17] Vittorio Giovannetti, Seth Lloyd, and Lorenzo Maccone, Phys. Rev. Lett. **96**, 010401 (2006).

[18] J. Gea-Banacloche, Phys. Rev. Lett. **62**, 1603 (1989).

[19] Juha Javanainen, and Phillip L. Gould, Phys. Rev. A **41**, 5088 (1990).

[20] N. Ph. Georgiades, E.S. Polzik, K. Edamatsu, and H.J. Kimble, Phys. Rev. Lett. **75**, 3426 (1995).

[21] J. J. Sakurai, *Modern Quantum Mechanics p.333*, (Addison-Wesley, Reading, MA, 1994).

[22] G. S. Agarwal, Phys. Rev. A **1**, 1445 (1970).

[23] S.E. Harris, Phys. Rev. Lett. **98**, 063602 (2007).

[24] Shengwang Du, Jianming Wen, Chinmay Belthangady, Phys. Rev. A **79**, 043811 (2009).

[25] Dmitry V. Strekalov, Matthew C. Stowe, Maria V. Chekhova and Jonathan P. Dowling, J. Mod. Optic. **49**, 2349 (2002).

[26] Barak Dayan, Avi Peer, Asher A. Friesem, and Yaron Silberberg, Phys. Rev. Lett. **93**, 023005 (2004).

[27] Adel Joobeur, Bahaa E. A. Saleh, Todd S. Larchuk, and Malvin C. Teich, Phys. Rev. A **53**, 4360 (1996).

[28] M. Hendrych, Xiaojuan Shi, A. Valencia, Juan P. Torres, Phys. Rev. A **29**, 023817 (2009).

[29] Barak Dayan, Phys. Rev. A **76**, 043813 (2007).

[30] Kevin A. O'Donnell and Alfred B. U'Ren, Phys. Rev. Lett. **103**, 123602 (2009).

[31] Morton H. Rubin, David N. Klyshko, Y. H. Shih, and A. V. Sergienko, Phys. Rev. A **50**, 5122 (1994).

[32] C. K. Hong, Z. Y. Ou, and L. Mandel, Phys. Rev. Lett. **59**, 2044 (1987).

[33] D.S. Elliott, M.W. Hamilton, K. Arnett, and S.J. Smith, Phys. Rev. A **32**, 887 (1985).

[34] Ce Chen, D.S. Elliott, and M.W. Hamilton, Phys. Rev. A **68**, 3531 (1992).

[35] B. R. Mollow, Phys. Rev. **175**, 1555 (1968).

[36] Timothy E. Keller and Morton H. Rubin, Phys. Rev. A **56**, 1534 (1997).

[37] Yoon-Ho Kim, Vincenzo Berardi, Maria V. Chekhova, Augusto Garuccio, and Yanhua Shih, Phys. Rev. A **62**, 043820 (2000).

[38] Yoon-Ho Kim, Two-Photon Quantum Entanglement, (Thesis Dissertation, University of Maryland, 2001).

[39] Yanhua Shih, Rep. Prog. Phys. **66**, 1009 (2003).

[40] D. N. Nikogosyan, Applied Physics A **52**, 359 (1991).

[41] Christian Kurtsiefer, Markus Oberparleiter, and Harald Weinfurter, Phys. Rev. A **64**, 023802 (2001).

[42] Hong-Bing Fei, Bradley M. Jost, Sandu Popescu, Bahaa E.A. Saleh, and Malvin C. Teich, Phys. Rev. Lett. **78**, 1679 (1997).

[43] Michael R. Harpham, Özgün Süzer, Chang-Qi Ma, Peter Bäuerle, and Theodore Goodson III J. Am. Chem. Soc. **131**, 973 (2009).

[44] Dong-Ik Lee, and Theodore Goodson III, J. Phys. Chem. B **110**, 25582 (2006).

[45] H. Fizeau, Comptes Rendus, **33**, 349 (1851).

[46] C. J. Davidson, and L. H. Germer, Phys. Rev. **30**, 705 (1927).

[47] O. Nariz, M. Arndt, and A. Zeilinger, Am. J. Phys. **71**, 319 (2002).

[48] P. A. M. Dirac, Proc. R. Soc. Lond. A, **114**, 243 (1927).

[49] Z. Y. Ou, Phys. Rev. A, **55**, 2598 (1997).

[50] Petr M. Anisimov, Gretchen M. Raterman, Aravind Chiruvelli, William N. Plick, Sean D. Huver, Hwang Lee, Jonathan P. Dowling, arXiv:0910.5942v1 (2009). To appear in Phys. Rev. Lett.

[51] Bernard Yurke, Samuel L. McCall, and John R. Klauder, Phys. Rev. A **33**, 4033 (1985).

[52] B. R. Frieden, *Probability, Statistical Optics, and Data Testing* (Berlin: Springer, p.363, 1991).

[53] J. P. Dowling, personal communication.

[54] J. Gea-Banacloche, Fluctuation and Noise Letters, **8**, C5 (2008).

[55] Carlton M. Caves, Phys. Rev. D **23**, 1693 (1980).

[56] Min Xiao, Ling-An Wu, H. J. Kimble, Phys. Rev. Lett. **59**, 278 (1987).

[57] P. Grangier, R.E. Slusher, B. Yurke, and A. LaPorta, Phys. Rev. Lett. **59**, 2153 (1987).

[58] Alfredo Luis, Phys. Lett. A **354**, 71 (2006).

[59] Aziz Kolkiran and G. S. Agarwal, Opt. Exp. **15**, 6798 (2007).

[60] Fabio Sciarrino, Chiara Vitelli, Francesco De Martini, Ryan Glasser, Hugo Cable, and Jonathan P. Dowling, Phys. Rev. A **77**, 012324 (2008).

[61] Takafumi Ono, and Holger F. Hofmann, (2009), arXiv:0910.3727v1 [quant-ph].

[62] Girish S. Agarwal, Robert W. Boyd, Elna M. Nagasako, and Sean J. Bentley, Phys. Rev. Lett. **89**, 1389 (2001).

[63] Philip Walther, Jian-Wei Pan, Markus Aspelmeyer, Rupert Ursin, Sara Gasparoni, and Anton Zeilinger, Nature **429**, 158 (2004).

[64] M. W. Mitchell, J. S. Lundeen, and A. M. Steinberg, Nature **429**, 161 (2004).

[65] Tomohisa Nagata, et al., Science **316**, 726 (2007).

[66] Holger F. Hofmann, and Takafumi Ono, Phys. Rev. A **76**, 031806 (2007).

[67] K. J. Resch, K. L. Pregnell, R. Prevedel, A. Gilchrist, G. J. Pryde, J. L. OBrien, and A. G. White, Phys. Rev. Lett. **98**, 223601 (2007).

[68] Jonathan P. Dowling, Cont. Phys. **49**, 125 (2008).

[69] Yang Gao and Hwang Lee, J. Mod. Opt. **55**, 3319 (2008).

[70] Sean D. Huver, Christoph F. Wildfeuer, and Jonathan P. Dowling, Phys. Rev. A **78**, 063828 (2008).

[71] Ryan T. Glasser, Hugo Cable, and Jonathan P. Dowling, Phys. Rev. A **78**, 012339 (2008).

[72] Chiara Vitelli, Nicol Spagnolo, Fabio Sciarrino, and Francesco De Martini, J. Opt. Soc. Am. B **26**, 892 (2009).

[73] Sergio Boixo, Animesh Datta, Steven T. Flammia, Anil Shaji, Emilio Bagan, and Carlton M. Caves, Phys. Rev. A **77**, 012317 (2008).

[74] J. Estève, C. Gross, A. Weller1, S. Giovanazzi1, and M. K. Oberthaler, Nature **455**, 1216 (2008).

[75] Sergio Boixo, Animesh Datta, Matthew J. Davis, Anil Shaji, Alexandre B. Tacla, and Carlton M. Caves, Phys. Rev. A **80**, 032103 (2009).

[76] B. L. Higgins, D. W. Berry, S. D. Bartlett, M. W. Mitchell, H. M. Wiseman, and G. J. Pryde, New J. Phys. **11**, 073023 (2009).

[77] B. L. Higgins, D. W. Berry, S. D. Bartlett, H. M. Wiseman, and G. J. Pryde, Nature **450**, 393 (2007).

[78] Jonathan P. Dowling, Nature **450**, 362 (2007).

[79] Jeremy L. OBrien, Science **318**, 1393 (2007).

[80] Masahiro Kitagawa, and Masahito Ueda, Phys. Rev. A **47**, 5138 (1992).

[81] M. J. Holland, and K. Burnett, Phys. Rev. Lett. **71**, 1355 (1993).

[82] Artur Widera, Olaf Mandel, Markus Greiner, Susanne Kreim, Theodor W. Hänsch, and Immanuel Bloch, Phys. Rev. Lett. **92**, 160406 (2004).

[83] Taesoo Kim, Jacob Dunningham, and Keith Burnett, Phys. Rev. Lett. **72**, 055801 (2005).

[84] J. Dunningham, and T. Kim, J. Mod. Opt. **53**, 557 (2006).

[85] Chaohong Lee, Phys. Rev. Lett. **97**, 150402 (2006).

[86] Taesoo Kim, and Heonoh Kim, J. Opt. Soc. Am. B **26**, 671 (2009).

[87] J. J. Bollinger, W. M. Itano, D. J. Wineland, and D. J. Heinzen, Phys. Rev. A **54**, R4649 (1996).

[88] C. C. Gerry, Phys. Rev. A **61**, 043811 (2000).

[89] C. C. Gerry and R. A. Campos, Phys. Rev. A **64**, 063814 (2001).

[90] A. Chiruvelli and H. Lee, (2009), arXiv:0901.4395v1 [quant-ph].

[91] Y. Gao, C. F. Wildfeuer, P. M. Anisimov, H. Lee, and J. P. Dowling, (2009), arXiv:0907.2382v2 [quant-ph].

[92] K. Wódkiewicz and J. H. Eberly, J. Opt. Soc. Am. B **2**, 458 (1985).

[93] Aziz Kolkiran and G. S. Agarwal, Opt. Exp. **16**, 6479 (2008).

[94] Alessandro Zavatta, Silvia Viciani, and Marco Bellini, Science **306**, 660 (2004).

[95] Alessandro Zavatta, Silvia Viciani, and Marco Bellini, Phys. Rev. A **72**, 023820 (2005).

[96] Valentina Parigi, Alessandro Zavatta, Myungshik Kim, and Marco Bellini, Science **317**, 1890 (2007).

[97] Available at http://math.ucsd.edu/ ncalg/.

[98] B. Abbott, et al., Rep. Prog. Phys. **72**, 076901 (2009).

[99] Ivan N. Agafonov, Maria V. Chekhova, and Gerd Leuchs, (2010), arXiv:0910.4831v3 [quant-ph].

[100] Goda et al., Nature Physics **4**, 472 (2008).

[101] Christian Kurtsiefer, Markus Oberparleiter, and Harald Weinfurter, Phys. Rev. A 64, 023802 (2001).

[102] H. J. Kimble, Yuri Levin, Andrey B. Matsko, Kip S. Thorne, and Sergey P. Vyatchanin, Phys. Rev. D **65**, 022002 (2001).

[103] Aravind Chiruvelli and Hwang Lee, arXiv:0901.4395v2 (2009).

[104] Christopher C. Gerry, A. Benmoussa, and R. A. Campos, Phys. Rev. A 72, 053818 (2005).

[105] Jonathan P. Dowling, Cont. Phys. 49, 125 (2008).

[106] Sean D. Huver, Christoph F. Wildfeuer, and Jonathan P. Dowling, Phys. Rev. A 78, 063828 (2008).

[107] R. A. Campos, C. C. Gerry, and A. Benmoussa, Phys. Rev. A 68, 023810 (2003).

[108] H. A. Bachor and T. C. Ralph, A Guide to Experiments in Quantum Optics, (Wiley-VCH 2004).

[109] D. Achilles et al., J. Mod. Opt. 51, 9-10, 1499 (2004).

[110] H. Lee et al., J. Mod. Opt. 51, 9-10, 1517 (2004).

[111] M. Ware et al., J. Mod. Opt. 51, 9-10, 1549 (2004).

[112] D. Rosenberg et al., Phys. Rev. A 71, 061803(R), (2005).

[113] A. E. Lita, A. J. Miller, S. W. Nam, Opt. Exp. 16, 3032(2008).

[114] I. Afek, A. Natan, O. Ambar, and Y. Silberg, Phys. Rev. A, 79, 043830 (2009).

[115] Christoph F. Wildfeuer, Aaron J. Pearlman, Jun Chen, Jingyun Fan, Alan Migdall, and Jonathan P. Dowling, Phys. Rev. A 80, 043822 (2009).

[116] Antoine Royer, Phys. Rev. A 15, 449 (1977).

[117] D. T. Smithey, M. Beck, M.G. Raymer, and A. Faridani, Phys. Rev. Lett. 70, 1244 (1993).

[118] G. S. Agarwal, J. Mod. Opt. 34, 909 (1987).

Vita

William Nicholas Plick was born to Victoria, and William Robert Plick in April 1982, in Vineland, New Jersey, in accordance with eldritch prophecie. He attended Sacred Heart Middle School in Vineland, and St. Augustine College Preparatory school in Richland, New Jersey. He then attended Connecticut College in New London Connecticut, Old London being unsuitable. After graduation he taught English as a second language in Yamagata-City, Japan. After that he enrolled in the doctoral program at LSU and has been there since 2005. His research interests include quantum optics, light-matter interactions, and the foundations of quantum mechanics. He hopes to graduate in May of 2010 and has accepted a post-doctoral research position at the Institute for Quantum Optics and Quantum Information in Vienna, Austria. He enjoys cooking, snowboarding, travelling, hiking, reading science fiction and history, antiquated and obscure language, getting lost in new places, and is knowledgeable about tea. He has a poor sense of time and direction and is prone to distractions and tangents. He has an exploitable weakness for beer, spicy food, and dark chocolate. He does not eat fruit and has a very impressive collection of beer bottle-caps.